

University of Southampton Research Repository

Copyright © and Moral Rights for this thesis and, where applicable, any accompanying data are retained by the author and/or other copyright owners. A copy can be downloaded for personal non-commercial research or study, without prior permission or charge. This thesis and the accompanying data cannot be reproduced or quoted extensively from without first obtaining permission in writing from the copyright holder/s. The content of the thesis and accompanying research data (where applicable) must not be changed in any way or sold commercially in any format or medium without the formal permission of the copyright holder/s.

When referring to this thesis and any accompanying data, full bibliographic details must be given, e.g.

Thesis: Author (Year of Submission) "Full thesis title", University of Southampton, name of the University Faculty or School or Department, PhD Thesis, pagination.

Data: Author (Year) Title. URI [dataset]

University of Southampton

Faculty of Environmental and Life Sciences

School of Ocean and Earth Science

Reconstructing the Ocean Floor Shape in Turbidite Basins using Seismic Interpretations and Forward Modelling

By

Donald Neil Christie BSc. MSc.

ORCID ID: 0000-0002-6800-8047

Thesis for the degree of Doctor of Philosophy

December 2021

University of Southampton

Abstract

Faculty of Environmental and Life Sciences

School of Ocean and Earth Science

Doctor of Philosophy

Reconstructing the Ocean Floor Shape in Turbidite Basins using Seismic
Interpretations and Forward Modelling

by

Donald Neil Christie

Deep-water depositional systems in different tectonic regimes display markedly different tectonostratigraphic evolution. The objective of this PhD was to develop a stratigraphic forward modelling program which deconvolves the controlling factors on basin fill architecture, in order to understand the dynamic interaction between structural deformation and sediment supply, using real, mapped structural geometries and stratigraphic package thicknesses. Understanding the interaction between structural deformation and sediment supply is important on active continental slopes. This interaction controls the vertical and lateral distribution of reservoir and seal lithologies, and their relation to growing structures. Subsurface prediction of trap and seal effectiveness is a vital component of CO₂ sequestration or hydrocarbon exploration projects.

Onlapse-2D is a geometric-based stratigraphic forward modelling program that simulates the tectonostratigraphic evolution of mini-basins using only commonly available reflection seismic, age-dated horizon interpretations and well data, if available (not required). The resulting models efficiently simulate the stratal architecture and palaeobathymetry of the mini-basin through time. *Onlapse-2D* produces geologically realistic cross-sections of a range of idealized mini-basins and simulates the evolution of a mini-basin using real data in the Gulf of Mexico.

Through the modelling, I show that the development of offlap and onlap stratal terminations in structurally active mini-basins may be linked to sediment supply in some cases. However, in others the link between onlap and offlap may be weak or non-existent. Therefore, there is no requirement for the development of onlap or offlap to have a hard-wired link to extrinsic processes, such as relative sea-level change.

Simulating the tectonostratigraphic evolution of the Late Miocene within three mini-basins in the Sureste Basin of Mexico allowed me to test and develop the capacity of *Onlapse-2D*. This case study integrated high resolution age-dated horizons and well data with 3D-seismic horizon interpretations, and the model results revealed three phases of structural activity, which controlled the stratigraphic development in the Late Miocene. These comprise two distinct pulses of contraction-related folding, and the long-term effects of salt-withdrawal and diapirism. This case study highlights the capacity of *Onlapse-2D* to aid in hydrocarbon exploration, by predicting reservoir presence away from well control and by identifying candidate stratigraphic traps.

Table of Contents

Table of Contents	ii
Table of Tables	ix
Table of Figures	xi
List of Accompanying Materials	xxv
Research Thesis: Declaration of Authorship	xxvii
Acknowledgements	1
Chapter 1 Introduction.....	2
1.1 Understanding the tectonostratigraphic history of Basins.....	2
1.1.1 Background Information	2
1.1.2 Observational Methods	2
1.1.3 The Importance of Topography	3
1.1.4 Stratal Terminations and their importance	4
1.2 Methods of Modelling	6
1.2.1 Introduction to Modelling.....	6
1.2.2 Process Based Modelling	6
1.2.3 Geometric Based Modelling	7
1.2.4 Previous Modelling Work	7
1.3 Aims:	8
1.3.1 Establishing Constraints.....	9
1.4 PhD Synopsis:.....	10
1.4.1 Chapter 2: <i>Onlap</i> – 2D – A new geometric tool to model tectonostratigraphic evolution of deep water basins.	10
1.4.2 Chapter 3: Conditions favouring onlap and offlap: why are onlaps common, and offlaps rare?	10
1.4.3 Chapter 4: Forward Modelling for Structural Stratigraphic Analysis, Offshore Sureste Basin, Mexico	10
1.4.4 Chapter 5: Conclusions and Future Directions	11
1.5 Statement of Contributions of Authors	11

1.5.1	Chapter 2: <i>Onlapse – 2D</i> – A new geometric tool to model tectonostratigraphic evolution of deep water basins.....	11
1.5.2	Chapter 3: Conditions favouring onlap and offlap: why are onlaps common, and offlaps rare?	11
1.5.3	Chapter 4: Forward Modelling for Structural Stratigraphic Analysis, Offshore Sureste Basin, Mexico	12
	Chapter 2 <i>Onlapse-2D</i>: A new geometric tool to model tectonostratigraphic evolution of deep-water basins.....	13
2.1	Abstract	13
2.2	Introduction.....	14
2.2.1	Aims	15
2.2.2	Current Approaches to Stratigraphic Forward Modelling	16
2.2.3	Philosophy of <i>Onlapse-2D</i>	18
2.3	Methods	21
2.3.1	What is <i>Onlapse-2D</i> ?	21
2.3.2	Basic Logic	22
2.3.3	Definition of Input Parameters	23
2.3.3.1	Initial Basin Structure (Figure 2.3a).....	23
2.3.3.2	Rate of Rise of the Structural Profile (Figure 2.3b)	23
2.3.3.3	Rate of Rise of the Clastic Limiting Surface (Figure 2.3c).....	25
2.3.3.4	Background Sedimentation Rate (Figure 2.3d)	26
2.3.4	Workflow	27
2.4	Results	31
2.4.1	Hypothetical Basins	31
2.4.1.1	Symmetrical Basin (Figure 2.7).....	32
2.4.1.2	Asymmetrical Basin (Figure 2.8).....	32
2.4.1.3	Regional Tilt (Figure 2.9).....	32
2.4.1.4	Complex Basin – Turtle Anticline (Figure 2.10)	33
2.4.2	Case Study	42
2.4.2.1	SymB1 Basin – Central Gulf of Mexico (Figure 2.11).....	42

Table of Contents

2.5	Discussion.....	49
2.5.1	Discussion of Symb1 Results.....	49
2.5.2	Assumptions, Uncertainty, Useful anomalies, and Informative Discrepancies	52
2.5.2.1	Assumptions and Uncertainty.....	52
2.5.2.2	Useful anomalies and Informative Discrepancies.....	52
2.6	Conclusions	54
2.7	Appendix	55
Chapter 3 Conditions favouring Onlap and Offlap: Why are onlaps common, and offlaps rare?		57
3.1	Abstract:.....	57
3.2	Introduction:	58
3.2.1	Why are Onlap and Offlap important in deep-water stratigraphy?.....	58
3.2.2	What are Onlap and Offlap?	59
3.2.3	Why does Onlap dominate over Offlap?	60
3.2.4	Aims	62
3.3	Method	64
3.3.1	What is <i>Onlapse-2D</i> ?.....	64
3.3.2	Initial Basin set up:.....	64
3.3.3	What we varied:.....	65
3.4	Results:.....	66
3.4.1	Model Observations:.....	66
3.4.2	Prevalence of onlap, offlap, and static pinchout:.....	68
3.4.2.1	Analysis by population size:	68
3.4.2.2	Analysis by Area:	75
3.4.2.3	Does changing the rate of rise of the Clastic Limiting Surface or Structural Growth Profile effect the development of offlap?	76
3.4.2.4	Analysis by Numbers:.....	77
3.4.3	Sensitivity of model results to temporal and spatial resolutions:.....	77
3.5	Discussion:	81

3.6	Conclusions.....	84
3.7	Appendix Information	85
Chapter 4 Forward Stratigraphic Modelling with <i>Onlapse-2D</i> for Reservoir Prediction:		
	Offshore Sureste Basin, Mexico	87
4.1	Abstract:	87
4.2	Introduction:.....	88
4.2.1	Geological History of the Sureste Basin, Southern Mexico	88
4.2.1.1	Opening of the Gulf	88
4.2.1.2	Deposition of the Salt Basin and Oceanic Spreading	88
4.2.1.3	Post-Rift Mesozoic.....	89
4.2.1.4	Mexican Fold-and-Thrust Belt development	89
4.2.1.5	Miocene Tectonics and Stratigraphy.....	90
4.2.1.6	Post Miocene Tectonics to Present Day.....	92
4.2.2	Aims of the Project	92
4.2.3	Data Used	93
4.3	Method:.....	93
4.3.1	What is <i>Onlapse-2D</i> ?	93
4.3.2	Study Area and Line Locations	93
4.3.3	Boundary Conditions and Input Parameters.....	94
4.3.3.1	Initial Basin Structure (Figure 4.4a).....	94
4.3.3.2	Rate of Rise of the Structural Growth Profile (Figure 4.4b)	94
4.3.3.3	Rate of Rise of the Clastic Limiting Surface (Figure 4.4c).....	95
4.3.3.4	Background Sedimentation Rate (Figure 4.4d)	95
4.3.3.5	A Note on Gravity Flow Deposit Packages	96
4.3.3.6	A Note on Compaction	96
4.3.4	Workflow	97
4.4	Results	98
4.4.1	Line 1	98
4.4.2	Line 2	102
4.5	Discussion	106

Table of Contents

4.5.1	Structural Evolution of Line 1 and Line 2	106
4.5.2	Predicting Reservoir Properties with <i>Onlapse-2D</i>	113
4.5.3	What is the significance of the different background sedimentation rates?	115
4.5.4	Possible Carbonate Sediment Gravity Flows	117
4.5.5	Informative Discrepancies	117
4.5.5.1	Informative Discrepancy in Line 1	118
4.5.5.2	Informative Discrepancy in Line 2	121
4.6	Conclusion	122
4.7	Appendix Information	123
Chapter 5	Conclusions	125
5.1	Main Findings	125
5.2	Chapter 2	125
5.3	Chapter 3	126
5.4	Chapter 4	126
5.5	Future Work	127
Appendix A	Chapter 2: A new geometric tool to model tectonostratigraphic evolution of deep-water basins	129
A.1	Inputs for Hypothetical Basins:	129
A.1.1	Symmetrical Basin	129
A.1.2	Asymmetrical Basin	130
A.1.3	Tilted Strata	132
A.1.4	Turtle Anticline	133
A.2	Inputs for Symb1	134
A.2.1	Run 26	134
A.2.2	Run 39	136
Appendix B	Chapter 3: Conditions favouring Onlap and Offlap: Why are onlaps common, and offlaps rare?	139
B.1	Input Parameters for Basins	139
B.2	Horizontal Resolution Increase Inputs	144
B.3	Time-Step Increase Inputs	145

B.3.1 Total Number of Beds Raw Numbers.....	147
Appendix C Chapter 4 : Forward Stratigraphic Modelling with <i>Onlapse-2D</i> for Reservoir Prediction: Offshore Sureste Basin, Mexico	150
C.1 Input Parameters Line 1	150
C.2 Input Parameters Line 2	155
Bibliography	161

Table of Tables

Table 1	This table is an illustrative example, tied to Figure 2.6. The “Derived Thickness from Seismic” is compared against the “Modelled Thickness – Total”. If the difference is outside a set window of tolerance, in this example it is 25m, then alterations are made to the physical inputs. The red cell at Basin Position 480 shows where the difference is beyond the tolerance. A negative difference shows where the modelled thickness for Zone N is higher, and a positive difference is where it is lower.30
Table 2	Shows the results of modelling 180 different combinations of clastic limiting surface rise and structural growth profiles. The colour of the cells represent either the lack of (red) or relative amount of offlapping surfaces (orange – green) modelled to develop. Percentages in those cells represent the total percentage of clastic beds that terminate in an offlapping manner. While a red cell indicates that no offlap is found, it does not necessarily mean that only onlap stratal terminations are produced, as static pinchout terminations may also develop.70
Table 3	Shows the results of modelling 180 different combinations of clastic limiting surface rise and structural growth profiles. The percentages in each cell represent the number of beds that terminate in an onlapping manner.72
Table 4	Shows the ratio of Onlap:Offlap in terms of number of beds from 180 different combinations of clastic limiting surface rise and structural growth profiles. .74
Table 5	Total number of Gravity Flow deposits148
Table 6	Total Number of Gravity Flow Deposits that terminate in Offlap148
Table 7	Total number of Gravity Flow Deposits that terminate in Static Pinchout ...149
Table 8	Total number of Gravity Flow Deposits that terminate in Onlap149
Table 9	Total Number of Gravity Flow Deposits, and number that end in Onlap, Offlap, and Static Pinchout150
Table 10	Total number of Gravity flow Deposits, and number that end in Onlap, Offlap, and Static Pinchout150

Table of Figures

Figure 1.1	Onlapping interval where each successive onlap surface progresses up-dip towards the edge of the basin while the offlapping interval shows each progressive onlap progressing down-dip away from the basin flank.....5
Figure 2.1	a) Cartoon cross-section of a continental slope, highlighting a salt-withdrawal mini-basin (b). While not exhaustive the sections serve to illustrate the point that the range of extrinsic processes that may occur on the continental shelf is large, which would need to be modelled if a process-based simulation of the tectonostratigraphic evolution of the salt-withdrawal mini-basin was to be attempted. The alternative minimal approach, in which deposition within an isolated area of interest (b) is considered to be locally determined by a clastic limiting surface (dotted line) beyond which deposition does not occur, itself controlled by the larger-scale factors.....19
Figure 2.2	a) Termination styles found within an idealized seismic sequence that were based on the types of stratal terminations defined: redrawn illustration from Mitchum et al (1977). B) Stratigraphic conditions necessary for the development of discrete onlapping surfaces redrawn from Cartwright et al (1993). Onlap develops onto a discrete surface i) only if there is no up-slope accumulation during onlap ii) if sediment accumulation takes place up-dip of the limit of onlap then onlap will occur on successively younger surfaces in an up-slope direction iii - iv). This may lead to the misinterpretation of the more complex onlap as a single onlap surface if the seismic resolution is low (red dotted apparent onlap surface line). C) Onlapping interval where each successive onlap surface progresses up-dip towards the edge of the basin while the offlapping interval shows each progressive onlap progressing down-dip away from the basin flank.....21
Figure 2.3	A) The Initial Basin Structure at Time-Step 0, E) illustrates how we derive this from seismic data. B) Dotted line represents the Structural Growth Profile, with red arrows indicating the rate of rise being applied to the Basin Structure (dark grey structure). The Structural Growth Rate Profile consists of multiple profiles, in this example it is a single profile. C) Blue dotted line is the Clastic Limiting Surface, if there is available accommodation space below then gravity flow deposit packages are deposited, if not then no deposition occurs. D) A uniform

Table of Figures

	thickness of background sediment is deposited along the cross-section, through pelagic and hemi-pelagic settling. E) The Initial Basin Structure at Time-Step 0 is derived by mapping the first continuous seismic reflector (red) and measuring the thickness of the isopach below it. Inspection of the subsequent and underlying, strata to identify patterns of onlap and geometry allow us to infer how much topography existed at Time-Step 0 and how much topography may have been created by subsequent structure growth.....	24
Figure 2.4	Illustrative examples of some geological reasons for the position of the Clastic Limiting Surface (green line), within the Line of Section and why it may rise or fall with time. A) In some periods of time the Clastic Limiting Surface may be below the sea-floor because sediment input is limited, so no Gravity Flow Deposits are deposited within the line of section. B) In other periods of time, the Clastic Limiting Surface may be rise above the sea-floor because of high sediment input into the basin. C) The Clastic Limiting Surface is controlled by a spill point in this example, even though sediment input is high. The spill point is outside the plane of section. D) The position of the Clastic Limiting Surface in this example is above the sea-floor because for this period of time sediment input has reached an equilibrium surface.....	26
Figure 2.5	1: Time Step 0 shows the Initial Basin Structure with height in meters on the Y axis and Basin Position on the X axis. 2: Onlapse – 2D applies a structural growth rate to the initial basin structure, then Onlapse – 2D applies a rise to the clastic limiting surface and if there is accommodation available gravity flow deposit packages are preserved. After this, Onlapse – 2D applies a uniform thickness of pelagic/hemipelagic sediment across the cross section. This process is repeated as many times as needed to produce a final cross section 3	28
Figure 2.6	Illustrative example of subsurface information (A) can be compared against the modelled modelled output (B). Do the observed stratal terminations seen in A, develop in B? Does the stacked turbidites seen in Well-X correspond to gravity flow deposits in the modelled output? Do the thickness measurements in A correspond to those in B?	31
Figure 2.7	Inputs used to model the evolution of a simple symmetrical basin. A) 3D representation of the Structural Growth Profile; X axis represents position in space, Y axis represents the position in time, Z axis represents the growth that the structure grows in meters per time step. B) The rate of rise of the Clastic	

	Limiting Surface shown is binary, either at a constate rate of rise of 13m or 0m per Time Step. C) Background Sedimentation Rate is kept temporally and spatially uniform. D) The red box highlights the trajectory of the onlapping surfaces and highlights a lack of offlapping surfaces.35
Figure 2.8	Basin simulation of an Asymmetrical Basin. A) A simple asymmetrical Structural Growth Profile is combined with a rate of rise of the Clastic Limiting Surface (B) that is sinusoidal, along with a temporally and spatially uniform Background Sedimentation Rate (C) these inputs combine to produce the basin simulation shown in D) Three main units of gravity flow deposit packages occur. Each contains onlapping and offlapping packages that are highlighted by the red box37
Figure 2.9	A) The Structural Growth Rate simulates tilting to the right-hand side of the cross section, B) along with a binary rate of rise of the Clastic Limiting Surface, and C) a Background Sedimentation Rate that is kept spatially and temporally uniform. These combine to produce D) two distinct units of progressively onlapping updip gravity flow deposit packages.39
Figure 2.10	A) The Structural Growth Rate Profile is a combination of two distinct Structural Growth Profiles, which simulates the processes of salt withdrawal (a single depocenter), welding, and then flank subsidence (simulated by the development of two depocenters to the left and right of the original depocenter in the middle). B) The rate of rise of the Clastic Limiting Surface is variable through time but shows that sediment was continually deposited within the system. C) Background Sedimentation Rate is kept temporally and spatially uniform. D) The process of welding has raised the depocenter in the lower part of the interval into an anticlinal structure while the flank subsidence has allowed for the formation of two new depocenters41
Figure 2.11	A) Near symmetrical apparently simple salt-withdrawal mini-basin from the Gulf of Mexico. B) Interpreted horizons on Seismic cross-section on the right hand side, along with the name of the zones that the mini-basin was split into.....42
Figure 2.12	A) Simple, constant Structural Growth Rate Profile; B) the Clastic Limiting Surface that varies in the rate of rise and the length of the rise with periods of hiatus, and a Background Sedimentation Rate (C) that was spatially and temporally uniform combine to produce this Basin Simulation of Symb1 (D). The

Table of Figures

	period of Hiatus at the start of the simulation produces ~32m of background sediment, while the brief period of rapid deposition that consists of a single Time Step produces a thick laterally extensive gravity flow deposit that is most likely a Mass Transport Complex.....	45
Figure 2.13	Comparison of the model produced by Onlapse-2D (A) and the seismic data set (B). Comparing the zones in the Onlapse-2D model with the seismic we found the depocenter was generally under-thickened in Zones 5 and 6 while the flanks were over thickened. Within Zone 1, the modelled output was predicting gravity flow deposit packages that were more laterally restricted than seen in the subsurface data. The red box in A) highlights an area where we were unable to use changes to the rate of rise of the Clastic Limiting Surface to correct the anomaly that had formed. Red circles indicate where Onlapse-2D models the thickness of the Gravity Flow Deposits 125 – 150m thinner than seismic data shows. The green circle represents a good match between the model and data. Seismic facies character of shows that “Probable” MTC is very likely an actual MTC	46
Figure 2.14	Inputs used to simulate a more accurate basin evolution of SymB1 with a closer match to the seismic data. A) The addition of a second, subtly different structural profile that allowed for an increase in accommodation during the deposition of gravity flow deposits in Zone 6 (red box Insert). B) Changes in the rate of rise of the Clastic Limiting Surface allowed us to model the lateral extent and thicknesses seen in Zones 3 and 4 much more accurately as well as produce a closer match to the thickness and lateral extent of the MTC seen in the seismic data. Cf figures 2.9 & 2.10	48
Figure 2.15	Two methods used to hone the final output in Onlapse-2D. A) Thickness of each zone is considered separately, e.g. Zone 1 within the seismic is compared to Zone 1 within the model. B) Second method that involves taking into account the total thickness of the sediment deposited in the model. The thickness of each zone contains the thickness of the zone(s) before it in a cumulative manner, e.g. Zone 2 has the thickness of Zone 1 added to it.	51
Figure 2.16	Interpreted seismic section of a Salt-Detached Ramp Syncline Basin, modified from (Pichel, et al., 2018) showing many features that Onlapse-2D would be unable to model. The large horizontal component of structural movement	

	(white arrow) and major erosion unconformity would preclude this type of basin from being accurately modelled.....	54
Figure 3.1	Onlapping interval where each successive stratal termination progresses up-dip towards the basin edge. The offlapping interval shows each progressive stratal termination progressing down-dip away from the basin edge.	59
Figure 3.2	a) typical deep-water mini-basin demonstrating the apparent domination of onlap stratal terminations over offlap. b) uninterpreted seismic of Figure 3.2a	62
Figure 3.3	Example of basin simulation, corresponding to model G8. Fig. 3a, input parameters used for this model, 1 Time-Step equals 10ky; Fig 3b, output simulation. Onlap is able to form when both the rate of rise of the Clastic Limiting Surface and the Structural Growth Profile are increasing and decreasing. Offlap forms only when the rate of rise of the Clastic Limiting Surface is decreasing.....	63
Figure 3.4	Example of basin simulation, corresponding to model F6. Fig 3.4a, input parameters used for this model; Fig 3.4b, output simulation. See text for discussion of highlighted points.	67
Figure 3.5	Example of basin simulation, corresponding to model I3. Fig 5.5a, input parameters used for this model; Fig 5.5b, output simulation. See text for discussion of highlighted points.	68
Figure 3.6	Histogram of the ratio of the number of intervals displaying offlap/onlap in the 180 base case simulation models	75
Figure 3.7	<i>Comparison of the proportion of offlapping gravity flow deposit packages by number against the proportion by cross-sectional area.....</i>	76
Figure 3.8	The effect of changing spatial resolution of the same 10-clastic-layer geometry by a factor of x2 (Figure 3.8b) and x4 (Figure 3.8c) on the proportion of apparent onlap, offlap and static pinchout. Figure 3.8a represents the base case. The pie-charts show the apparent proportions of layer terminations of different types; on = onlap, off = offlap, static = static pinchout.....	78
Figure 3.9	The effect of changing model resolution on the apparent proportion of onlap/offlap/static pinchout, determined by population size (number of layers).	

Table of Figures

	Blue diamond = base case; green stars = temporal resolution increase by factor of 2; orange squares = spatial resolution increased by a factor of 2.	79
Figure 3.10	The effect of changing model resolution on the apparent volumetric proportion of layers showing onlap/offlap/static pinchout, (area of layers). Blue diamond = base case; green stars = temporal resolution increase by factor of 2; orange squares = spatial resolution increased by a factor of 2.....	80
Figure 3.11	Schematic illustration of variation through time of a controlling factor (structural growth rate or CLS rise rate) that is asymmetric (3.11a) or symmetric (3.11b)	82
Figure 3.12	Construction used to illustrate the thicknesses of stratigraphy exhibiting onlap vs. offlap. Graphical analysis of a model similar to simulation run E2 (constant rate of structural growth, sinusoidal variation of rate of rise of CLS). For simplicity of construction, this analysis does not include any component of background sedimentation. a, rate of processes through time, red curve = CLS, green line = rate of structural uplift of edge of mini-basin, blue line = rate of uplift in the deepest part of the mini-basin; b, chronology of periods of onlap, offlap and non-deposition; c, graphical plot in elevation vs. time used to construct stratigraphic thicknesses. Colour key as in b; d, stratigraphic.....	83
Figure 3.13	The orange line represents the Clastic Limiting Surface for the current Time-Step. The Offlap Limit line highlighting (black dotted line) highlights that the available accommodation for offlap is considerably lower than the available accommodation for Onlap.	84
Figure 4.1	Outline of the Sureste Basin in Southern Mexico, the study area is located in the offshore section of the basin. Red shapes represent salt bodies.	89
Figure 4.2	Location of Well A superimposed over a relative depth map of the 12.2Ma horizon interpretation, and the two modelled cross-sections Line 1 and Line 2. Colours represent relative depth, where Red contours are the highest, and purple contours represent the relatively deepest sections of the study area. Frame of reference has been rotated to preserve confidentiality.	91
Figure 4.3	Geoseismic cross section of a Sand Injectite complex found to the south-west of High-1. Injectites observed to penetrate from Middle Miocene horizon (12.2Ma) into Upper Miocene stratigraphy, forming dyke and sill complex. Question marks show areas where presence of injectites is be inferred, such as the 10.5Ma	

	horizon jack-up structure. Chronostratigraphic chart show timing of injectites observed around High-1 from Middle Miocene before observations cease in the Upper Tortonian. After an absence of fluid flow structures, in the Upper Tortonian to Messinian pock marks are observed.92
Figure 4.4	<p>a) The Initial Basin Structure at Time-Step 0, Figure 4.5 illustrates how we derive this from seismic data. b) Dotted line represents the Structural Growth Profile, with red arrows indicating the rate of rise being applied to the Basin Structure (dark grey structure). The Structural Growth Rate Profile consist of multiple profiles, in this example it is a single profile. c) Blue dotted line is the Clastic Limiting Surface, if there is available accommodation space below then gravity flow deposit packages are deposited, if not then no deposition occurs. d) A uniform thickness of background sediment is deposited along the cross-section, through pelagic and hemi-pelagic settling.96</p>
Figure 4.5	<p>The Initial Basin Structure at Time-Step 0 is derived by mapping the first continuous seismic reflector (red) and measuring the thickness of the isopach below it. Inspection of the subsequent and underlying, strata to identify patterns of onlap and geometry allow us to infer how much topography existed at Time-Step 0 and how much topography may have been created by subsequent structure growth.....97</p>
Figure 4.6	<p>a) Line 1 geoseismic cross section, with major onlapping reflectors highlighted in red. Major horizons are age-dated with biostratigraphy from Well-A. Modelling was completed from 12.2Ma until present-day, with 12.2 Ma– 5.3 Ma being the focus, while 5.3Ma until Present day being modelled to a lower resolution. b) Onlapse-2D final simulation, overall there was a good match between the simulation and the geoseismic.99</p>
Figure 4.7	<p>I Inputs used to model the evolution of Line 1. a) 3D Representation of the Structural Growth Profile, X axis represents position in space, Y Axis represents position in Time, Z axis represents the growth that the structure grows in meters per time step. b) The rate of rise of the clastic limiting surface; showing the sporadic nature and short lived time in which sediment gravity flows occur in the cross-section. c) Background Sedimentation Rate; derived from data from Well A. X Axis represents position in Space along the cross section, Y axis represents position in Time, and Z axis represents amount of background sediment deposited in meters. d) Final simulation for Line 1.101</p>

Table of Figures

Figure 4.8	<p>a) a) Geoseismic cross-section of Line 2. Line 2 crosses both High-1 and High-2, with High-2 containing salt. Wedging geometry seen in geoseismic cross-section is above our area of interest, but is still modelled at a lower resolution. b) Onlap-2D final simulation, overall within the section of interest there is a good match between model and the geoseismic. The model is able to match the general form of the basin as well, and major onlapping reflectors seen in 8a, occur in the modelled simulation..... 103</p>
Figure 4.9	<p>Inputs used to model the evolution of Line 2. a) 3D representation of the Structural Growth Profile, a much more complicated structural growth history is visible. A combination of 2 Structural Growth Profiles, one represent salt tectonics and the other focusing on growth of the Fold. b) The rate of rise of the Clastic Limiting Surface shows a more sustained input of gravity driven currents to achieve a good match compared to the more sporadic input in Line 1. c) Background Sedimentation Rate used in Line 1 is used in Line 2. d) Final simulation for Line 2. Insert section highlights thin gravity flow deposits, with red arrow showing the direction of onlap onto the basin flank..... 105</p>
Figure 4.10	<p>3D representation of the rate of rise of the Structural Growth Profile through time. X –axis represents position in time, Y – axis represents basin position along Line 2, Z – axis showing the rate of rise in meters per Time-Step. Diagram shows the combination of two Structural Growth Profiles through time. Profile 1 was consistent with compressional folding over High-1, Profile 2 is focused on salt diapirism and withdrawal at High-2. Fold growth (Profile-1) dominates in two distinct phases, phase one occurs from 12.2Ma till ceasing at 9.0Ma, at this point Profile 2 (salt growth) dominates until 7.8Ma, at which point compressional folding begins again. Profile 1 continues to dominate until the middle Pliocene when fold growth tapers off. At this point, salt tectonics dominates, represented by Profile 2..... 108</p>
Figure 4.11	<p>Schematic drawing of the structural components of study area. Red dotted line represents phase 1 fold axes that trend roughly east-west. Brown dotted line represents the phase-2 folding axes which trends southwest-northeast. Phase 1 shortening direction is towards the southwest, phase 2 shortening direction is northwest. Line 1 does not intersect the fold axis of phase 2 folding, while Line 2 intersects both phase 1 and 2. 109</p>

Figure 4.12	Tectono-Chronostratigraphic chart of Line 2. Representations of the two structural growth profiles superimposed upon a chronostratigraphic chart of Line 2. Chronostratigraphic chart shows the distribution and thickness of gravity flow deposits. Width of profiles represent relative strength, Salt Growth (Profile 2) continues throughout time while the Fold Growth (Profile 1) has two distinct phases, and can be seen to decrease rapidly in the Pliocene. Well-A shows multiple condensed sections in which no gravity flow deposits are intercepted. Section labelled not condensed is where Onlapse-2D had to introduce a small but continuous rise to the Clastic Limiting Surface, this deposited thin gravity flow deposits that onlap onto flanks of High-1.112
Figure 4.13	Time-Step 44 (10.0Ma) of Line 2, showing the predicted presence of sediment gravity flows in the Mini-basin-1. Thick sediment gravity flows modelled in Zone 1 onlap onto the high flanks, topped by a thick laterally extensive seal of draping mudstone. Thin unit penetrated by Well-A in Zone 2 would likely have a thicker, lateral equivalent found within the basin which is what the Onlapse-2D model has simulated to develop.....114
Figure 4.14	3D representation of Background Sedimentation Rate as it evolves through time. Derived from well data from Well A. X axis represents position in Time, showing both Time-Step and where in the chronostratigraphic column each event is. Y axis represents position along the cross-section. Z axis represents the rate of Background Sedimentation in meters.116
Figure 4.15	Basin simulation of Top Zone 4 of Line 1. A good match was achieved between the Onlapse-2D model and subsurface data in Zone – 3 & 4 in Mini-basin-1 and High-1. Red hashes show in Mini-basin 2 where for Zone 3 & 4 a significant mismatch occurred. Insert shows what Onlapse-2D simulated to develop, within Zone 3, an increasing amount of over-thickening is shown, and while for Zone 4 the over-thickening is more constrained to the centre of Mini-basin 2.119
Figure 4.16	Geoseismic cross section focused on Mini-basin-2. Map insert shows location where geoseismic is taken from. Red arrows highlight that between 10.0Ma – 9.5Ma & 9.5Ma – 9.0Ma, seismic reflectors are eroded into by major horizons .This provides evidence that the mismatch between simulation and subsurface data occurs because there has been erosion within Mini-basin 2.120

Table of Figures

Figure 4.17	a) Schematic diagram of mismatch between the Onlapse-2D simulation and seismic data, with significant over-thickness within Mini-basin 4. Red horizon represents the original simulated boundary between Zone 4 & 5. Green horizon represents boundary between Zone 4 & 5 with positive depositional topography taken from seismic data. b) Schematic diagram of Onlapse-2D in final simulation, red horizon represents Onlapse-2D simulated horizon, which now matches the boundary seen in seismic in Mini-basin. From the difference between red and green horizon on High-1 we can infer the amount of positive depositional topography that is present.....	122
Figure 5.1	Bounding conditions for Symmetrical Basin.....	129
Figure 5.2	Initial Basin Height and Position in Matrix, along with Absolute Structural Growth Rate and their position.....	129
Figure 5.3	Structural Growth Amplification Rate initial inputs	129
Figure 5.4	Initial Clastic Limiting Surface and Positions in Matrix, along with the growth per time step and its position in matrix.....	130
Figure 5.5	Clastic Limiting Surface Amplification Rate Input parameters.....	130
Figure 5.6	Background Sediment input parameters	130
Figure 5.7	Initial Basin bounding conditions	130
Figure 5.8	Initial Basin Height and Position in matrix	131
Figure 5.9	Structural Growth input parameters.....	131
Figure 5.10	Clastic Limiting Surface input parameters	131
Figure 5.11	Background Sediment input parameters	131
Figure 5.12	Bounding conditions.....	132
Figure 5.13	Input conditions for initial basin structure.....	132
Figure 5.14	Structural growth input parameters	132
Figure 5.15	Clastic Limiting Surface input parameters	132
Figure 5.16	Background Sediment input parameters	133

Figure 5.17	Bounding Conditions used	133
Figure 5.18	Initial Basin Structure conditions.....	133
Figure 5.19	Structural Growth Profile and Rate input parameters for Profile 1 and Profile 2	133
Figure 5.20	Input Parameters for Clastic Limiting Surface Profile and Rise as well as initial starting positions	134
Figure 5.21	Input parameters for Background Sedimentation.....	134
Figure 5.22	Bounding Conditions for Run 26 of Symb1.....	134
Figure 5.23	Input parameters for Initial Basin Structure.....	135
Figure 5.24	Input parameters for Structural Growth Profile and Rate	135
Figure 5.25	Input parameters for initial starting height of Clastic Limiting Surface and Growth per Time-Step	135
Figure 5.26	Input parameters for Clastic Limiting Surface Rise Amplification rate.....	136
Figure 5.27	Input parameters for Background Sedimentation Rate	136
Figure 5.28	Bounding Conditions for Run 39 of Symb1.....	136
Figure 5.29	Input parameters for Initial Basin Height	137
Figure 5.30	Input parameters for Structural Growth Profile 1 and 2	137
Figure 5.31	Input parameters for Strucutral Growth Profile 1 and 2 amplitudes	137
Figure 5.32	Input parameters for Clastic Limiting Surface profile and initial height.....	137
Figure 5.33	Input parameters for Clastic Limiting Surface rate of rise (amplitude)	138
Figure 5.34	Input parameters for Background Sedimentation rate	138
Figure 5.35	Input parameters for Initial Basin Structure and Bounding conditions.....	139
Figure 5.36	Input parameters for Background Sedimentation Rate	139
Figure 5.37	Input parameters for Structural Growth Rate Amplitude	140
Figure 5.38	Input parameters for Structural Growth Profile.....	141

Table of Figures

Figure 5.39	Input parameters for Clastic Limiting Surface Profile Rise.....	142
Figure 5.40	Input parameters for Clastic Limiting Surface Profile Rise continued.....	143
Figure 5.41	Input parameters for Low, Medium, High Clastic Limiting Surface Profiles .	143
Figure 5.42	Input parameters for Initial Basin Structure and Bounding Conditions.....	144
Figure 5.43	Input Parameters for Structural Growth Profile HR increase	144
Figure 5.44	Input parameters for Initial Basin Structure and Bounding Conditions.....	145
Figure 5.45	Input parameters for Clastic Limiting Surface Profile Rise.....	146
Figure 5.46	Input parameters for Clastic Limiting Surface Profile Rise continued.....	147
Figure 5.47	Input Parameters for Clastic Limiting Surface Profile	147
Figure 5.48	Bounding Conditions	150
Figure 5.49	Input parameters for Initial Basin Structure	151
Figure 5.50	Input parameters for Structural Growth Profile and Rise.....	151
Figure 5.51	Input parameters for Clastic Limiting Surface.....	151
Figure 5.52	Input parameters for Clastic Limiting Surface continued.....	152
Figure 5.53	Input parameters for Clastic Limiting Surface continued.....	153
Figure 5.54	Input parameters for Clastic Limiting Surface continued.....	154
Figure 5.55	Input parameters for Background Sedimentation	155
Figure 5.56	Bounding Conditions Line 2.....	155
Figure 5.57	Input Parameters for Initial Basin Structure	155
Figure 5.58	Input parameters for Line 2 Structural Growth Profile amplitudes	155
Figure 5.59	Input parameters for Line 2 Structural Growth Profiles	156
Figure 5.60	Input parameters for Clastic Limiting Surface Profile rate of rise.....	157
Figure 5.61	Input parameters for Clastic Limiting Surface Profile rate of rise continued	158
Figure 5.62	Input parameters for Clastic Limiting Surface Profile rate of rise continued	159

Figure 5.63	Input parameters for Background Sedimentation Rate	160
-------------	--	-----

List of Accompanying Materials

Supplementary Material A – Chapter 2 SymB1

Supplementary Material B – Chapter 3

Supplementary Material C – Chapter 4

Research Thesis: Declaration of Authorship

Print name: Donald Neil Christie

Title of thesis: Reconstructing the Ocean Floor Shape in Turbidite Basins using Seismic Interpretations and Forward Modelling

I declare that this thesis and the work presented in it are my own and has been generated by me as the result of my own original research.

I confirm that:

1. This work was done wholly or mainly while in candidature for a research degree at this University;
2. Where any part of this thesis has previously been submitted for a degree or any other qualification at this University or any other institution, this has been clearly stated;
3. Where I have consulted the published work of others, this is always clearly attributed;
4. Where I have quoted from the work of others, the source is always given. With the exception of such quotations, this thesis is entirely my own work;
5. I have acknowledged all main sources of help;
6. Where the thesis is based on work done by myself jointly with others, I have made clear exactly what was done by others and what I have contributed myself;
7. None of this work has been published before submission

Signature: Date:03/12/21

Acknowledgements

I would like to express my deepest appreciation to my PhD supervisors, Frank Peel, Esther Sumner, Gillian Apps, and Stan Stanbrook for all of the hard work and assistance they provided from the outset of this PhD. Their immense knowledge, experience, and guided me throughout this processes and I will always be grateful. I look forward to continuing down this path and hopefully working with them all soon!

I would like to show gratitude to the NERC-CDT for providing the funding for this PhD and running the fantastic conferences, field-trips, and workshops that allowed me to enjoy a breadth of experiences most PhD students can only dream of. As well as allowing me to meet and become friends a host of fantastic people that I will never forget.

I gratefully acknowledge the assistance of all the staff and my friends at the University of Southampton who have supported me throughout this journey. I would like to personally thank Justin Dix who went above and beyond to ensure that I was given the same opportunity to extend my PhD as was offered to other students.

I would like to extend my thanks to Mike Hudec and the rest of the staff at the Applied Geodynamics Laboratory in the University of Texas at Austin. Thank you for not only inviting me to Austin, but for giving me the opportunity to learn and work with a fantastic group of people.

I am grateful to Murphy Exploration and Production for providing the data and the opportunity to use this research on amazing data. I'd also like to give my thanks to the staff who provided me technical support and advice.

To those of you I consider my oldest and closet friends, I owe you a debt I can never repay. The unprecedented love and support from London, Oxford, Brisbane, and Stavanger kept my head above the water. Each one of you knows how much you have supported me and how much you mean to me. Without any of you I would not be where I am today. Thank you.

To Gemma & Pico, I will be forever grateful for the love and support you gave me from the beginning. Thank you for being a part of this journey and for making this time a little bit easier, and for eagerly listening to the many rants and raves.

Finally, I'd like to thank my Mum, Dad, and sister. You were always behind me despite the distance. Thank you for always being there.

Chapter 1 Introduction

1.1 Understanding the tectonostratigraphic history of Basins

1.1.1 Background Information

Deep-water sedimentary systems are found throughout the globe and are important depositional sinks of sediments shed from the continental shelf and slope (Dade & Huppert, 1994) (Wynn, et al., 2002) (Talling, et al., 2007); they help form important hydrocarbon plays and offer potential storage of CO₂ (Pettingill & Weimer, 2002) (Szulczewski, et al., 2013). In both active and so-called “passive” regimes, these deep-water depositional systems will encounter a wide variety of sea-floor topography. Sediment gravity flows are the primary agent for the transfer of sediment from shelf to the deep-sea, with turbidity currents arguably being the most volumetrically important of these (Talling, 2014). These sediment gravity flows will likely encounter varying topography as they travel through the continental slope. The effects of sea-floor topography on sediment gravity flows and their deposits is well documented (Prather, et al., 1998), (Kneller & McCaffrey, 1999), (Kneller, 2003), (Amy, et al., 2004), (Bakke, et al., 2013), (Sylvester, et al., 2015). The intra-basinal topography encountered by sediment gravity flows includes pre-existing topography resulting from tectonic deformation (Kilhams, et al., 2012), syn-depositional faulting (Haughton, 2000), (Hodgson & Haughton, 2004), salt withdrawal and diapirism (Prather, 2003), (Peel, 2014), (Jackson & Hudec, 2017), and gravity sliding/gliding (Jackson & Hudec, 2017).

Each individual basin on the continental slope has its own unique structural and stratigraphic history. Therefore, deconvolving the interaction between structural deformation and sedimentation is fundamental to understanding the geology of continental slopes. Structural deformation and sediment supply control important aspects of hydrocarbon plays, such as reservoir geometry and distribution, seal distribution and presence, and stratigraphic traps (Prather, 2003) (Hawie, et al., 2018) (Stirling, et al., 2018) (Amy, 2019); it is therefore vital to understand how structural deformation and sedimentation have evolved through time. Therefore, modelling the interplay between structural deformation and sedimentation could help provide valuable insight into the likelihood of reservoir presence, seal presence and effectiveness which can then be integrated with observational data.

1.1.2 Observational Methods

To explore for hydrocarbons, or previously uncharged structures for CO₂ storage, it is necessary to make predictions of the subsurface geometry and lithology. When well imaged by high-quality

seismic reflection data this can be done by primarily observational methods, e.g. horizon mapping, interpretation, and attribute extraction from the seismic data. However, observation-based prediction is not always possible in areas where imaging quality is compromised by overlying salt (Leveille, et al., 2011), volcanism (Behera, 2006) (Sanford, et al., 2018), or where state-of-the-art data is not available. In these areas, stratigraphic forward modelling can help constrain interpretations, and provide insights to evaluate alternative depositional and structural histories (Peel, 2014) (Falivene, et al., 2014) (Huang, et al., 2015) (Gervais, et al., 2018).

1.1.3 The Importance of Topography

Turbidity currents are the principle mechanism by which clastic sediments are transported and deposited in deep-water sedimentary systems (Amy, et al., 2004) (Twichell, et al., 2005) (Talling, et al., 2007) , and their deposits, turbidites are the most prolific reservoirs for hydrocarbons in deep-water sedimentary systems (Prather, 2003) (Amy, et al., 2004) (Mayall, et al., 2006). Topography is a primary controlling factor on the behaviour of sediment gravity flows and the distribution and character of their deposits (Prather, 2003) (Kneller, 2003) (Bakke, et al., 2013) (Jackson, et al., 2008). Even subtle topography (e.g. a decrease in sea-floor gradient of 0.05° to 0.01°) can have a radical effect on depositional geometry and character (Talling, et al., 2007), and thus exert influence on the distribution and presence of potential reservoir rocks. This makes understanding how topography and turbidity currents interact important to understand.

Turbidity currents are particle laden, seafloor sediment gravity currents. The term turbidity current encompasses a range of flow types from low density flows in which turbulence is the dominant particle support mechanism (Meiburg & Kneller, 2010) , to high density turbidity currents in which grain interactions are important (Lowe, 1982). When turbidity currents encounter topography spatial variations are produced within the flow, such as changes in velocity or direction of flow. These spatial variations work in conjunction with the grain-size distribution within the flow to determine where the sediment load is deposited. Encountering topography will also effect the suspended-load fallout rate, thus topography influences the distribution and depositional facies of potential reservoir rock (Kneller, et al., 1991), (Kneller & Branney, 1995), (Kneller & McCaffrey, 1999).

Conventional models suggest that sediment gravity flows in unconfined settings on basin floors produce lobes and that these lobes typically have fairly predictable facies and thickness transitions (Baas, 2004) (Spychala, et al., 2017). However, recent studies challenge the notion of just how predictable unconfined lobes really are (Kane, et al., 2017). It is also well established, as described above, that topography influences the distribution and depositional facies of sediment

gravity flows. For example, a sediment gravity flow that runs axially along a confined basin floor may produce longer and narrower deposits with a greater thickness of sediment deposited than those in an unconfined setting (Cunha, et al., 2017). This depositional pattern shift means that favourable reservoir facies and stratal terminations are also shifted.

1.1.4 Stratal Terminations and their importance

Stratal terminations are one of the fundamental components of the stratal stacking patterns that make up conventional sequence stratigraphy (Catuneanu, 2019). The origin of large scale stratal patterns and terminations has been extensively investigated within the confines of conventional sequence stratigraphy throughout the last several decades (e.g. (Vail, et al., 1977), (Helland-Hansen & Hampson, 2009)). Emphasis has been placed on how changes in relative sea-level and sediment supply interact to produce a variety of clinoform geometries and stratal termination patterns in shallow water shelf edge settings. As noted by Prather et al (1998), the stratal geometries seen within deep-water sedimentary systems such as *Onlap* and *Offlap* are the result of the interplay between deep-water depositional processes and the evolution of accommodation on the continental slope. However, the stratigraphy of deep-water sedimentary settings is only indirectly affected by changes in relative sea-level with the clinoform geometries seen in shallow-water sedimentary systems essentially absent (Sylvester, et al., 2015) (Catuneanu, 2020). Many authors have linked the development of onlap and offlap in deep-water basins to changes in relative sea-level (e.g. (Christie-Blick, 1991), (Pomar & Ward, 1994), (Catuneanu, 2006) (Catuneanu, et al., 2009), (Catuneanu, et al., 2011) (Zhang, et al., 2018)) despite sea level only having an indirect impact on sedimentation in deep water and the fact that there are multiple allogenic and autogenic factors that influence their development (Kneller, 2003) (Brunt, et al., 2004) (Carvajal, et al., 2009) (Dixon, et al., 2012) (Bourget, et al., 2014) (Liu, et al., 2016) (Harris, et al., 2018). In this thesis, which is concerned with deep-water sedimentary systems, there is no assumed nor required link between the development of the stratal terminations of *Onlap* and *Offlap* and relative sea-level change. In this thesis, *Onlap* is defined as the lateral termination of a package of sediment gravity flow deposits against a surface of greater inclination. An onlapping interval, is one in which the stratal termination point of each successive onlap progresses up-dip on the basin flank (Figure 1.1). An offlapping interval is one in which the stratal termination point progresses down-dip into the basin centre (Figure 1.1).

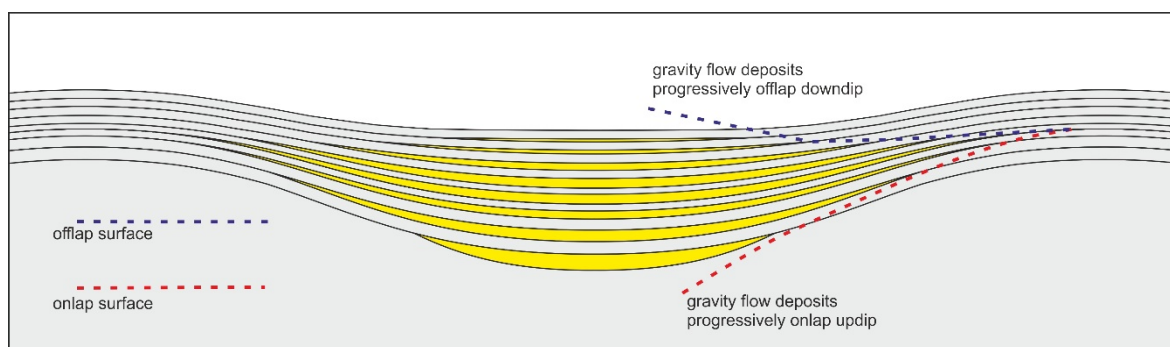


Figure 1.1 Onlapping interval where each successive onlap surface progresses up-dip towards the edge of the basin while the offlapping interval shows each progressive onlap progressing down-dip away from the basin flank.

As noted by Sylvester et al (2015), within deep-water mini-basins the development of the stratal geometries that make up the sequence boundaries is in general a much simpler process than in shallow-water settings. Aside from the notable exception of Sylvester et al (2015), there has been little quantitative analysis of the processes that generate these important surfaces in deep-water stratigraphy. Fundamental questions remain: are deep-water onlap and offlap surfaces diagnostically related to sea level changes, or can they be generated entirely by other, more local processes? Why is it that deep-water onlapping surfaces are a commonly observed feature but offlapping surfaces appear to be much less common?

The majority of our knowledge about the intricacies of turbidity currents and their deposits comes from the study of ancient deposits (e.g. (Bouma, 2004), (Talling, 2014), (Soutter, et al., 2019)), flume tank experiments (e.g. (Ross, et al., 2002), (Cartigny, et al., 2013)), or numerical modelling (e.g. (Syvitski, et al., 2007), (Teles, et al., 2016), (Wang, et al., 2017)), only a limited number of studies have directly monitored turbidity currents (e.g. (Xu, 2011), (Symons, et al., 2017), (Hage, et al., 2018), (Paull, et al., 2018), (Hage, et al., 2019)). These direct monitoring studies show differences between reality and the assumptions that we make when producing numerical and flume tank modelling. For example, direct measurements show more concentrated rather than dilute flows are observed. However, direct measurements of turbidity currents are almost always in canyons (e.g. (Symons, et al., 2017)), channels (e.g. (Hage, et al., 2018)), or delta fronts (e.g. (Hage, et al., 2019)). These direct measurements highlight the issue that many of the assumptions we make about turbidity currents that directly affect reservoir distribution and properties remain to be tested in the real world.

In areas of poor subsurface imaging, it can be challenging to make the necessary observations needed to unravel the tectonostratigraphic evolution of the basin, let alone decipher the characteristics of individual sediment gravity flows. This highlights the need for a robust method to help constrain interpretations and provide insight into the tectonostratigraphic evolution of

basins before considering the characteristics of individual flows. Stratigraphic Forward Modelling is one such method.

1.2 Methods of Modelling

1.2.1 Introduction to Modelling

Stratigraphic Forward Modelling is the use of mathematical formulae and algorithms to create synthetic stratigraphy, with the aim of understanding and predicting dynamic sedimentary systems (Burgess, 2012) (Huang, et al., 2015). Natural systems are complex and dynamic, and consequently are difficult to model. Stratigraphic Forward Modelling can be broadly split into two end member methods, *Process Based Modelling* and *Geometric Based Modelling*, each with its own advantages and disadvantages (Paola, 2000) (Burgess, 2012) (Huang, et al., 2015).

1.2.2 Process Based Modelling

Process based modelling aims to model the stratigraphic record from the properties and dynamics of individual flows; identifying input points at the basin margin and predicting where sediment will be deposited and what calibre of sediment will be deposited along the transport path (Burgess, 2012). Both diffusion models (e.g (Hutton & Syvitski, 2008)) and hydraulic models (e.g (Basani, et al., 2014)) come under the umbrella of Process based modelling.

Process based modelling can create informative simulations for generic stratigraphy (e.g (Hawie, et al., 2018) (Burgess, et al., 2019)) which may be appropriate for modelling at a variety of scales. This includes simulation of reservoir-scale details over multiple flow attempts (e.g (Huang, et al., 2015)), and looking at sediment architecture and facies distribution of sub marine fans systems and turbidite complexes. They are also successfully used as analytical studies of geological principles, e.g. the formation of stratal geometries in sequence stratigraphy, or the influence of relative sea-level change in deep marine basins (Hawie, et al., 2018) (Harris, et al., 2018) (Burgess, et al., 2019).

A disadvantage of process based stratigraphic forward models is that they are computationally intensive and take a great deal of time to run. For example, numerical models that solve the full 3-D Navier-Stokes equations that represent the fundamental physics of fluid flow take the most computational power and time to run (Huang, et al., 2015). Even models that deal with simplified sets of equations such as diffusion-based models or depth-average models take a considerable

amount of computing time and power (Paola, 2000) (Huang, et al., 2015). Process based modelling also requires the user to define the values of parameters for which there may be limited real world data, e.g. precise point of sediment input, average flow concentration, flow thickness, and sea-floor shape at time of deposition. These factors may also be different for each individual flow modelled.

1.2.3 Geometric Based Modelling

Geometric models, do not consider the dynamics of sediment transport. Instead they use a simple set of rules to model the overall thickness and stratal geometry of discrete stratigraphic intervals rather than the individual depositional events within the intervals. Typically geometric models are rigid lid and average deposition is over a geological period of time (Paola, 2000) (Burgess, 2012). Rigid lid models are where the top of the deposit has a predefined geometry (Paola, 2000).

Geometric models capture only the essential behaviour of a system and can approximate complicated processes found in many sedimentary systems without the need for complex equations, which makes them computationally quick to run (Burgess, 2012). In this context, essential behaviour refers to the fundamental geological controls that effect the development of sedimentary systems, primarily the sediment input into the basin and the space available for sediment to fill (accommodation). In the past geometric models have been used to create basin-fill stratigraphic patterns of idealized basins with simple subsidence histories (e.g. (Sylvester, et al., 2015)).

However, geometric based models can only produce approximations of real-world basin geometries, and it can often be difficult to demonstrate just how realistic and predictive these models are (Burgess, 2012).

1.2.4 Previous Modelling Work

Stratigraphic forward modelling is used in a wide range of depositional systems, from terrestrial, shallow-marine, to deep-marine and at a variety of scales. It is used to create synthetic stratigraphy based on simulated stratigraphic and tectonic processes. However, much more attention is generally given to stratigraphic processes such as sediment supply variations than tectonic processes such as subsidence and uplift. Generally, stratigraphic forward modelling has been conducted on either stable surfaces (e.g. (Imran, et al., 2001), (Jerolmack & Paola, 2007), (Burgess, et al., 2019)) or through simple subsidence and uplift (e.g. (Ritchie, et al., 2004), (Granjeon, 2014), (Sylvester, et al., 2015), (Harris, et al., 2018)).

Chapter 1

There are notable examples in which more complex tectonics have been integrated into stratigraphic forward modelling. For example, Clevis et al (2004) simulated the effect of low angle thrust faults on fluvial sands, Barrett et al (2018) introduced both spatial and temporally variable tectonic components into a 3D sequence stratigraphic forward model in shallow marine settings, and Howlett et al (2019) modelled the interaction of turbidity currents against deep-water fold and thrust belts by integrating complex structural movement of the seafloor.

While not an exhaustive list, the studies here serve to illustrate that while there have been notable attempts to integrate structural components to stratigraphic forward modelling, generally speaking structural movement is confined to simple subsidence. Furthermore, with the exceptions of Sylvester et al (2015) and Howlett et al (2019) there has been little focus using numerical modelling on the interaction between structure and sedimentation within deep-water sedimentary systems.

1.3 Aims:

The aim of this thesis is to develop a stratigraphic forward modelling program to aid in the exploration of hydrocarbons in structurally controlled deep-water sedimentary successions that occur in areas of poor data quality and quantity. The model will generate realizations of the final stratal architecture, and the palaeotopography of the basin through time.

Aim 1: Develop an analytical tool that can simulate the tectonostratigraphic evolution of deep-water basins from real, readily available subsurface information (interpreted seismic horizons, well data etc.) to create geologically realistic simulations easily, rapidly, with minimal computational time, and with minimal input parameters.

Aim 2: Utilize the stratigraphic forward modelling program to better understand fundamental concepts (e.g. the prevalence of onlap and offlap) and their controlling processes by modelling stratal geometries.

Aim 3: Demonstrate the utility of the stratigraphic forward in the exploration of hydrocarbons.

In order to fulfil the above aims I have chosen to develop a Geometric Stratigraphic Forward Modelling program. Both Geometric and Process based methods can be effective, however each is suited for different situations. A Geometric based system was chosen because unlike a Process based model, it does not rely on a large number of assumptions and variables and it due to this it is computational simple and quick to run. Process based modelling is better suited to simulating

stratigraphy in areas of good subsurface illumination where the large number of variables needed to produce an accurate model can be well constrained.

1.3.1 Establishing Constraints

Is well known that there is a large variety of ancient deep-water sedimentary systems found globally and in a wide variety of tectonic environments (Stow & Mayall, 2008). While the aim of this PhD research is to develop a stratigraphic forward model for use in as many structural active deep-water sedimentary systems as possible, it is still however important to establish constraints to narrow down where, at least initially, *Onlapse-2D* can be effectively utilized.

Onlapse-2D is intended to be utilized in deep-water sedimentary basins which have either in the past been structurally active, or are currently structurally active. At least initially, *Onlapse-2D* is intended to model deep-water systems at a mini-basin scale, which can range from kilometres to 10s of kilometres in size. However, because of the simplicity of the rules that *Onlapse-2D* follows there are no theoretical limits to the spatial scaling of *Onlapse-2D*. This means, it could be utilized on much smaller spatial scales, for example simulating a 100m+ section of a basin, or it could be used at a larger scale.

Developing a new stratigraphic forward model is not a simple task and it is vital to ensure that when testing and refining the model an appropriate study area is chosen. The Gulf of Mexico was chosen as the initial area to test and refine the model. The gulf exhibits not only a wide array of mini-basin morphologies and histories, but due to its long history as an area of interest of hydrocarbon exploration there is wide coverage of good quality seismic and access to publicly released well data.

Much of the modelling in this thesis takes place in mini-basins, and according to Jackson & Hudec (2017), a mini-basin is as its name suggests, a small basin, or depression (up to 10's of km in width and length). Its key feature being that a mini-basin subsides into relatively thick salt.

Stereotypically, a mini-basin can be seen as disc shaped and positioned in a vast wide expanse of salt. While originally restricted to the continental slope of the northern Gulf of Mexico, the term has proved so useful that it has spread beyond the borders of the Gulf of Mexico and salt tectonics itself. Because of this, in this thesis the term "mini-basin" is used in a broader sense than the definition as suggested by Jackson & Hudec (2017). Here it refers to any small basin (10's of kilometres in length and width) that is or has been structurally controlled.

1.4 PhD Synopsis:

1.4.1 Chapter 2: *Onlapse* – 2D – A new geometric tool to model tectonostratigraphic evolution of deep water basins.

In this chapter we focus on the Philosophy of *Onlapse-2D*, and why we chose to develop it as a Geometric based modelling program. I define the basic logic behind *Onlapse-2D*, define the input parameters, and demonstrate the workflow. I also show our initial results by simulating the tectonostratigraphic evolution of 4 different geologically realistic hypothetical mini-basins. I also demonstrate that *Onlapse-2D* is able to go one step further than other Geometric based models by simulating a real mini-basin from the Gulf of Mexico. I also evaluate the limitations of the model and its use as an analytical tool to aid in the exploration of Hydrocarbons.

This chapter was submitted for publication in Basin Research and the manuscript is currently being revised according to reviewer comments.

1.4.2 Chapter 3: Conditions favouring onlap and offlap: why are onlaps common, and offlaps rare?

Chapter 3 focuses on using *Onlapse-2D* to better understand fundamental stratigraphic concepts. Here I attempt to understand why deep-water mini-basins show abundant onlap terminations but offlap terminations are relatively rare in deep-water stratigraphy. This is done using a sensitivity study where I forward modelled 180 simulations of structurally active mini-basins with different histories of structural growth and sediment supply. This chapter also demonstrates that *Onlapse-2D* can produce geologically realistic models and that the imbalance between offlap and onlap is similar to what we see in nature. The analysis suggests that development of onlap-biased stratigraphy may be the natural consequence of basin-fill processes in structurally active basins and there is not always a requirement for the observed patterns to have any hard-wired link to extrinsic processes such as relative sea-level change.

1.4.3 Chapter 4: Forward Modelling for Structural Stratigraphic Analysis, Offshore Sureste Basin, Mexico

Chapter 4 focuses on the idea of using *Onlapse-2D* to improve the understanding of the tectonostratigraphic evolution of the study area in the offshore Sureste Basin in southern Mexico. We demonstrate how *Onlapse-2D* integrates subsurface data by using age-dated horizons tied to a well that is intersected by two modelled cross-sections. This chapter highlights *Onlapse-2D*'s use as both an analytical tool that can simulate the tectonostratigraphic evolution of a deep-water

system but also highlights its ability to aid in the exploration of hydrocarbons. This is done by showing how *Onlapse-2D* is able to tease out complex tectonic histories and can be used to predict reservoir properties.

1.4.4 Chapter 5: Conclusions and Future Directions

We present our conclusions on the project here, highlighting that we have developed an analytical tool that can simulate the tectonostratigraphic evolution of real world mini-basins. Also showing that it can be used to perform sensitivity studies and be used as an aid in the exploration of hydrocarbons. Our future plans are focused on further testing and integration of new features including compaction and transition into three dimensions.

1.5 Statement of Contributions of Authors

1.5.1 Chapter 2: *Onlapse – 2D* – A new geometric tool to model tectonostratigraphic evolution of deep water basins.

The original idea and prototype for *Onlapse* was conceived by Frank Peel and Gillian Apps. The development, testing, and optimization of this prototype into its current form as *Onlapse-2D* was performed by Donald Christie. Esther Sumner and Frank Peel supervised. The initial testing and analysis of hypothetical basin simulations was performed by Donald Christie. Interpretation of seismic horizons was performed by Donald Christie. Modelling and analysis of SymB1 basin was performed by Donald Christie, Frank Peel assisted in analysis. Frank Peel, Gillian Apps, and Esther Sumner supervised. Donald Christie wrote the manuscript and all authors provided critical feedback to shape manuscript as well as further research and analysis.

1.5.2 Chapter 3: Conditions favouring onlap and offlap: why are onlaps common, and offlaps rare?

Original idea for study proposed by Donald Christie, all authors contributed supervised this chapter and suggesting directions of this chapter. Donald Christie performed all numerical modelling and sensitivity analysis. Frank Peel and Gillian Apps provided assistance in analysis. Donald Christie wrote the manuscript, and all authors provided critical feedback to help shape manuscript.

1.5.3 Chapter 4: Forward Modelling for Structural Stratigraphic Analysis, Offshore Sureste Basin, Mexico

Original idea for study proposed by Stan Stanbrook. Scope and aims were designed by Donald Christie, Stan Stanbrook, and Frank Peel. Access to subsurface data was organized by Stan Stanbrook. Original interpretations provided in chapter were completed by Stan Stanbrook and other Murphy Oil staff. Numerical modelling, interpretation of model, and analysis was performed by Donald Christie. Frank Peel, Gillian Apps, and Stanbrook contributed to analysis, and supervised. Donald Christie wrote the manuscript, and all authors provided critical feedback to help shape the manuscript. This chapter has been submitted and accepted to *Frontiers in Earth Science* under the title *“Forward Modelling for Structural Stratigraphic Analysis, Offshore Sureste Basin, Mexico”*

Chapter 2 ***Onlapse-2D: A new geometric tool to model tectonostratigraphic evolution of deep-water basins***

Donald N. Christie¹, Frank J. Peel², Esther Sumner¹, Gillian Apps², David “Stan” Stanbrook³

¹ Ocean and Earth Science, University of Southampton, Southampton, United Kingdom

² Bureau of Economic Geology, Jackson School of Geosciences, The University of Texas at Austin, University Station, Austin, Texas, United States

³ Murphy Exploration & Production Company, 9805 Katy Freeway Suite G-200, Houston, Texas, United States

Submitted to Basin Research: - Undergoing revision based on reviewer comments

2.1 Abstract

Deep-water depositional systems in active tectonic regimes display markedly different tectonostratigraphic evolutions than in passive regimes. Deconvolving basin fill architecture in order to understand structural deformation and sediment supply, and their interactions, is fundamental in understanding the geology of active continental slopes. Specifically, understanding the interaction between structural deformation and sediment supply is important because it controls key elements of hydrocarbon plays such as reservoir and seal presence. However, traditional methods of structural stratigraphic analysis rely on high-quality seismic reflection data, and most commonly use modelling software that relies on parameters that cannot be easily quantified from commonly available data.

We present a simple analytical tool (*Onlapse-2D*) that can be of service in any tectonically active basin dominated by vertical uplift and subsidence, for example continental slope systems underlain by salt, and it is of particular value in areas without high-quality seismic data. *Onlapse-2D* creates a geometric model of the tectonostratigraphic evolution of a mini-basin using commonly available horizon interpretations, and the resulting model simulates the stratal architecture and palaeobathymetry of the mini-basin through time. *Onlapse-2D* uses four physical

inputs: initial basin structure; background sedimentation rate; structural growth profile rate; and a variable rate of rise of a clastic limiting surface. Multiple simulations can be generated quickly, with minimal computing power, making *Onlapse-2D* invaluable for rapidly investigating the impact of alternative structural stratigraphic models.

We demonstrate that *Onlapse-2D* produces geologically realistic cross-sections of a range of idealized basin types. Further, we use subsurface data to simulate the evolution of a near-symmetrical mini-basin from the Gulf of Mexico. Using only four physical inputs, *Onlapse-2D* provides realistic simulations of the tectonostratigraphic evolution of both the idealized, and real-world mini-basins. Minor discrepancies between the model and real-world mini-basin helped reveal how regional effects, extrinsic to the basin of interest, impacted the basin evolution.

2.2 Introduction

Models for interpreting the evolution and architecture of basins on continental margins have existed for the last half century (e.g. Mitchum, Vail, & Sangree (1977)). Classic sequence stratigraphy models consider the construction of a depositional architecture, primarily controlled by variations in sea level and sediment supply, on a more or less static substrate (Catuneanu, et al., 2011). However, recent studies recognize that environmental signals, such as those generated by changes in relative sea level, can become shredded, destroyed, and modified by processes along the sediment routing system and within the sediment accumulation zones (e.g. (Jerolmack & Paola, 2010), (Romans, et al., 2016), (Hawie, et al., 2018), (Harris, et al., 2018), (Sharman, et al., 2019), (Burgess, et al., 2019), (Tofelde, et al., 2021). In both active and so-called “passive” regimes, deep-water depositional systems will encounter a wide variety of sea-floor topography. Sediment gravity flows are the primary agent for the transfer of sediment from shelf to the deep-sea, with turbidity currents arguably being the most volumetrically important of these (Talling, 2014). These sediment gravity flows will likely encounter varying topography as they travel through the continental slope. The effects of sea-floor topography on sediment gravity flows and their deposits is well documented (Prather, et al., 1998), (Kneller & McCaffrey, 1999), (Kneller, 2003), (Amy, et al., 2004), (Bakke, et al., 2013), (Sylvester, et al., 2015). The intra-basinal topography encountered by sediment gravity flows includes pre-existing topography resulting from tectonic deformation (Kilhams, et al., 2012), syn-depositional faulting (Haughton, 2000), (Hodgson & Haughton, 2004), salt withdrawal and diapirism (Prather, 2003), (Peel, 2014), (Jackson & Hudec, 2017), and gravity sliding/gliding (Jackson & Hudec, 2017).

Each individual basin on the continental slope has its own unique structural and stratigraphic history. Consequently deconvolving the interaction between structural deformation and

sedimentation is fundamental to understanding the geology of continental slopes. Both structural deformation and sediment supply control important aspects of hydrocarbon plays, such as reservoir geometry and distribution, seal distribution and presence, and stratigraphic traps (Prather, 2003) (Hawie, et al., 2018) (Stirling, et al., 2018) (Amy, 2019); it is therefore vital to understand how structural deformation and sedimentation have evolved through time. Therefore, modelling the interplay between structural deformation and sedimentation could help provide valuable insight into the likelihood of reservoir presence, seal presence and effectiveness which can then be integrated with observational data.

To explore for hydrocarbons, it is necessary to quantify reservoir, seal and source rock presence, risk and parameter uncertainty used for hydrocarbon volumetric calculations as well as lithologic prognoses ahead of the drill bit (Magoon & Dow, 1994), (Allen & Allen, 2013). Where the subsurface is well-imaged by high quality seismic reflection data, such predictions may be based primarily on observation (interpretation, mapping, and attribute extractions of the seismic data) (Allen & Allen, 2013). However, observation-based prediction may not be possible in areas of poor data quality, for example in structurally complex areas, especially where imaging is compromised by overlying salt or volcanics, or where state-of-the-art data is unavailable. In these regions, stratigraphic forward modelling can help to constrain the seismic interpretation, and can provide insights that allow the interpreter to evaluate alternative models, run sensitivity analyses, and quantify the range of critical factors.

Some methods of stratigraphic forward modelling involve complex numerical simulation of depositional processes, which are computationally intense, and sensitive to a wide range of controlling variables. In this paper we present a pragmatic, reduced complexity method for forward modelling in structurally active basins, which is computationally rapid and dependent on a small number of controlling factors.

2.2.1 Aims

To address the problem of poor subsurface data quality (e.g. low resolution seismic images, lack of wells etc.), we have constructed “*Onlapse-2D*”, an analytical tool to aid in the exploration of hydrocarbons in deep-water sedimentary successions that occur in areas with poor data quality and density. This MATLAB-based software creates a geometric model of the structural and stratigraphic evolution of a basin from real, readily available information (e.g. interpreted seismic horizons, well data), generating realizations of the final stratal architecture, and the palaeotopography of the basin floor through time.

Our objective is to create stratal simulations easily, rapidly, and with minimal computational time. It is possible to create an optimized model that fits the model output to the observed data by iteratively comparing the simulations with the observations, and then adjusting the model input parameters systematically to reduce mismatch. This provides value by:

- Providing insights into the evolution of the basin and the processes that govern structural and stratigraphic changes.
- Creating a stratal model that can be interrogated to obtain a valid (if not necessarily unique) interpretation of poorly-imaged regions.
- Creating a valid model of the basin topography and its evolution through time which may be used to refine depositional models
- Identifying problematic stratigraphic intervals where it is difficult to create a satisfactory model. In such intervals the user may find that the existing seismic interpretation is questionable, or that additional geological processes may be involved that are not explicitly modelled in *Onlapse-2D*.

We aim to use *Onlapse-2D* to produce geologically realistic simulations of deep-water basin stratigraphy; in this study, we focus on salt withdrawal mini-basins, but the method is applicable to other basin types. To do this we investigate: 1) whether a simple geometric model can replicate a range of hypothetical geologically realistic basins (symmetrical, asymmetrical, tilted basin, and a turtle anticline basin); 2) whether *Onlapse-2D* can simulate the complex structural and stratigraphic architecture of a real world salt withdrawal mini-basin; and 3) because *Onlapse-2D* is a deliberately simple model, we also consider the limitations of our model and how consideration of these limitations can reveal further information about the geological development of a basin.

2.2.2 Current Approaches to Stratigraphic Forward Modelling

There are two main methods for Stratigraphic Forward Modelling: 1) process-based modelling; and 2) geometric modelling. Below we discuss the appropriateness of these two methods for dealing with datasets at different spatial and temporal resolutions.

Process-based modelling aims to model the stratigraphic record from the properties and dynamics of individual flows; identifying input points at the basin margin and predicting where sediment will be deposited and what calibre of sediment will be deposited in different positions along the transport paths (Burgess, 2012); (Teles, et al., 2016). Construction of process-based models requires the user to define the values of parameters for which there may be limited constraint from real world data, such as the precise point of sediment input, average flow concentration, flow thickness, and geometry of the seafloor slope at time of deposition (Paola,

2000); (Waltham, et al., 2008); these controlling factors are likely to be different for each flow event.

Process-based models can create informative simulations of generic stratigraphy; in some cases the approach may be appropriate for the modelling of real world stratigraphy (e.g. simulation of reservoir-scale details of a few flow events). However, their use for replicating real-world stratigraphy comprising a large number of event deposits is limited by the requirement to quantify multiple flow parameters for each event, in addition to slope gradient and palaeocurrent direction. (Burgess, et al., 2019); (Hawie, et al., 2018).

Process based models are also computationally intensive to run, with numerical models that solve the full 3-D Navier-Stokes equations that represent the fundamental physics of fluid flow taking the most computational power and time to produce. Even models that deal with a simplified set of equations, such as depth-averaged models, take a considerable amount of computing time and power (Burgess, 2012).

To create a full process-based simulation of the evolution of a structurally active salt withdrawal mini-basin on the continental slope not only requires a computationally intensive numerical-model to model the gravity-driven currents. It would also require quantified parameters for the structural processes such as salt withdrawal and syn-sedimentary deformation, which would also add significant computational complexity.

In contrast, geometric models do not consider the dynamics of sediment transport, instead they use a relatively simple set of rules to model the overall deposition thicknesses and stratal architecture of discrete stratigraphic intervals, rather than the individual depositional events within those intervals (Rivenaes, 1992) (Paola, 2000). Geometric models only capture the essential behaviours of the system and can approximate complicated processes found in many sedimentary systems without the need for complex equations, making them computationally quick to run (Burgess, 2012). Geometric models typically work by averaging deposition over a geological period of time (Paola, 2000). Past studies have used geometric models to create basin-fill stratigraphic patterns in idealized basins with simple subsidence histories Sylvester et al, (2015). However, many geometric models produce only approximations of real-world basin architectures (Paola, 2000), and it can be difficult to demonstrate how realistic and predictive these models are (Burgess, 2012) .

While used in a wide range of depositional environments generally speaking, stratigraphic forward modelling has been conducted on either stable surfaces (e.g. (Imran, et al., 2001), (Jerolmack & Paola, 2007), (Burgess, et al., 2019)) or incorporates structural movement using

simple subsidence and uplift (e.g. (Ritchie, et al., 2004), (Granjeon, 2014), (Sylvester, et al., 2015), (Harris, et al., 2018)). There are however notable examples in which more complex structural movement has been integrated into stratigraphic forward modelling (e.g. (Clevis, et al., 2004), (Barrett, et al., 2018), (Howlett, et al., 2019)).

2.2.3 Philosophy of *Onlapse-2D*

Previous studies that have attempted to simulate structurally active deep-water basins have generally use one of two approaches. Approach one produces generic models using simple rules for sediment deposition and structural movement within idealized basins (e.g. Sylvester, et al. (2015)). These are rapidly generated and give useful insights into the general processes of basin evolution, but typically do not seek to replicate real world examples. Or they apply a more complex algorithm to simulate the flow of individual or a number of turbidity currents to produce synthetic stratigraphy (e.g. (Burgess, et al. 2019) while structural movement is usually only modelled through simple subsidence, with the exception of Howlett, et al. (2019) who includes more structural movement.

In this study we take a different approach. *Onlapse-2D* is computationally fast geometric based modelling package that uses a small number of physical inputs to simulate the interaction between complex structural movement and sedimentation to produce geologically realistic simulations. It uses simple rules to match subsurface data from real world examples, and iterates towards a best-fit solution through hundreds of simulation runs.

We define “geologically realistic simulations” as those that show plausible relationships and geometries within the basin-fill architecture. Plausible relationships and geometries refer to those that fall within on the range of geometries observed in real-world mini-basins based on seismic, outcrop, or well data.

We recognize that in the real world, deposition within a particular region of interest on the continental slope (Figure 2.1b) while controlled by two factors (sediment input and amount of available accommodation) a host of geological factors outside the local region that can impact both of these factors (Figure 2.1a). For example, regional tectonics, sedimentary transport dynamics, shelf morphology, and climate can influence the rate of delivery of clastic sediments into the deep-water (Kneller, 2003) (Brunt, et al., 2004) (Carvajal, et al., 2009) (Dixon, et al., 2012) (Bourget, et al., 2014) (Liu, et al., 2016) (Harris, et al., 2018). A complete simulation of deposition on the continental slope would require a source-to-sink model in which each of these extrinsic components is quantified and modelled. This could include processes within the mantle (dynamic uplift) and crust (including tectonics, crustal flexure, isostasy, etc.); the nature of the sediment

provenance area, dynamics of the fluvial transport system, deposition on the shelf and slope updip of the study area, etc.

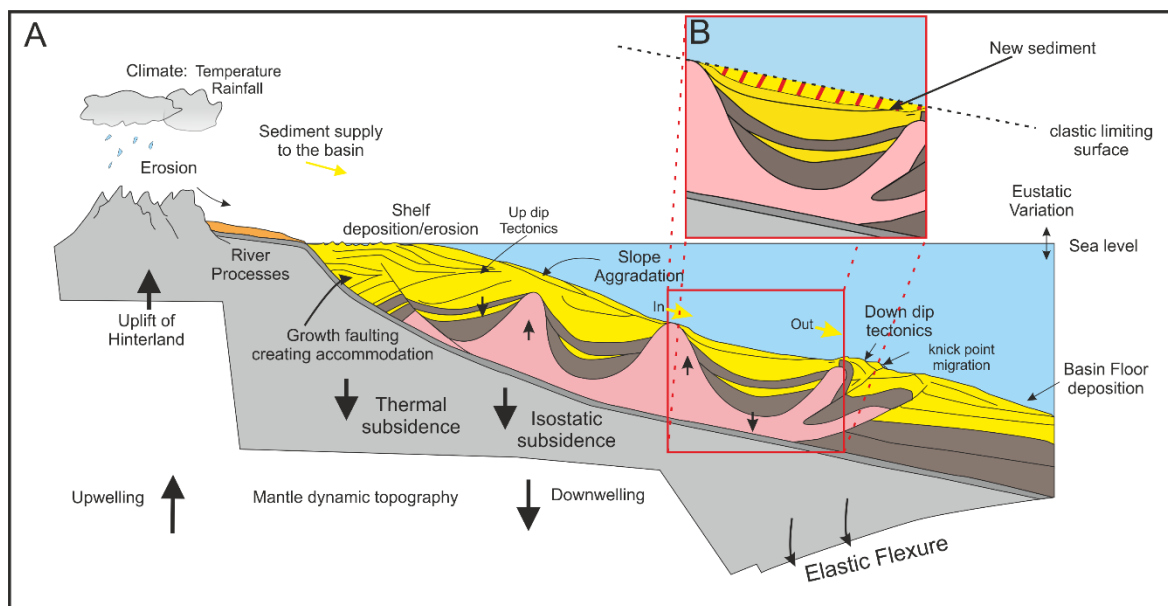


Figure 2.1 a) Cartoon cross-section of a continental slope, highlighting a salt-withdrawal mini-basin (b). While not exhaustive the sections serve to illustrate the point that the range of extrinsic processes that may occur on the continental shelf is large, which would need to be modelled if a process-based simulation of the tectonostratigraphic evolution of the salt-withdrawal mini-basin was to be attempted. The alternative minimal approach, in which deposition within an isolated area of interest (b) is considered to be locally determined by a clastic limiting surface (dotted line) beyond which deposition does not occur, itself controlled by the larger-scale factors

However within a restricted area of interest (the “box” of figure 2.1b), the effects of all these extrinsic processes can be combined into a much smaller set of factors that set the boundary conditions at the edges of the box, such as clastic sediment flux in/out, seafloor elevation at the entry- and exit-point, basal uplift/subsidence, and fallout from the water column (pelagic/hemipelagic). If we are primarily concerned with knowing the amount of clastic sediment that is deposited within the box rather than the process of deposition, or the amount that bypasses (passes through the box without depositing), this can be simplified still further. The minimal approach used here defines a limiting surface within the box, which moves with time. If there is space between this limiting surface and the sea floor, it is filled with clastic sediment; where the limiting surface lies at or below the sea bed, no clastic sediment is deposited. Movement of this clastic limiting surface through time is, in the real world, the product of a myriad of geological processes as described above. If the area of interest is smaller than the scale of the depositional system the clastic limiting surface may provide a useful first-pass approximation requiring no detailed knowledge of the extrinsic inputs. This approach forms the basis of *Onlapse-2D*.

Two fundamental geometric relationships found within mini-basins are *onlap* and *offlap*; these concepts were first introduced and debated in the 1940's in three papers by Melton (1947), Lovely (1948), and Swain (1949). The concept of an onlapping surface has been further developed since, notably by Mitchum (1977) and Mitchum et al. (1977) where onlap and offlapping surfaces are defined by the relationships of individual beds to a single discrete surface onto which beds terminate (Figure 2.2a). Taking this further, (Cartwright, et al., 1993) suggested that for onlap to develop there must be a slope with a greater inclination than 1° so that a pinchout occurs and that there must be no coeval deposition upslope from the point of onlap (Figure 2.2b). While this strict definition of Cartwright *et al.* (1993) may be appropriate in some settings, observations of deep-water stratigraphy made by the authors demonstrate that onlap can occur on slopes less than 1 degree, while Stanbrook (2003) and Smith & Joseph (2004) show that a sequence of sediment gravity flows may accumulate down dip while draping sediments are deposited updip.

The majority of existing publications relate the development of stratal geometries such as onlap and offlap to changes in relative sea-level (Christie-Blick, 1991), Pomer & Ward (1994), (Catuneanu, 2006), (Catuneanu, et al., 2009), (Zhang, et al., 2018). This has validity for coastal and shallow marine sedimentary successions because this relationship is based predominantly on these shallow parts of the sediment systems tract. In deep-water sedimentary systems there are multiple allogenic and autogenic factors that influence their development, including local and regional tectonic, sedimentary transport dynamics, shelf morphology and climate. These factors can negate, enhance, or destroy the effect of relative sea-level change on the rate of delivery of clastics into deep-water (Kneller, 2003) (Brunt, et al., 2004) (Carvajal, et al., 2009) (Dixon, et al., 2012) (Bourget, et al., 2014) (Liu, et al., 2016) (Harris, et al., 2018). This suggests that the development of stratal geometries such as onlap and offlap within deep-water systems may be controlled by other local factors, aside from relative sea-level changes.

In this study, which is entirely concerned with onlap in deep-water we do not assume or require a direct link between onlap and the water depth or sea surface level. For clarity, in *Onlapse-2D*, we define onlap as the lateral termination of a package of gravity flow deposits against a surface of greater inclination. An onlapping interval is one in which the onlap point of each successive deposit progresses up-dip up the basin flank (Figure 2.2c). An offlapping interval is one in which the onlap point of each successive deposit progresses down-dip away from the basin flank (Figure 2.2c).

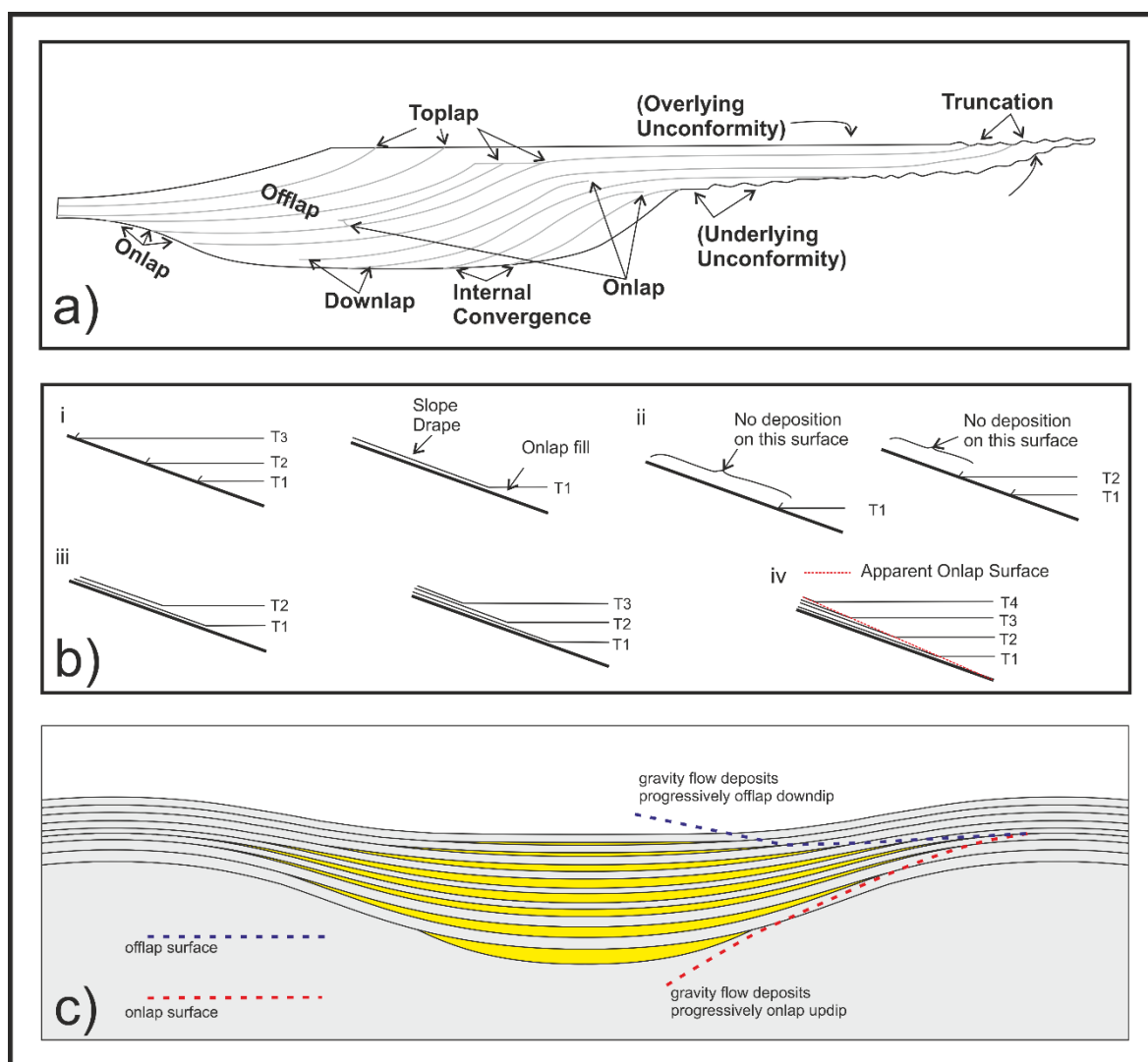


Figure 2.2 a) Termination styles found within an idealized seismic sequence that were based on the types of stratal terminations defined: redrawn illustration from Mitchum et al (1977). B) Stratigraphic conditions necessary for the development of discrete onlapping surfaces redrawn from Cartwright et al (1993). Onlap develops onto a discrete surface i) only if there is no up-slope accumulation during onlap ii) if sediment accumulation takes place up-dip of the limit of onlap then onlap will occur on successively younger surfaces in an up-slope direction iii - iv). This may lead to the misinterpretation of the more complex onlap as a single onlap surface if the seismic resolution is low (red dotted apparent onlap surface line). C) Onlapping interval where each successive onlap surface progresses up-dip towards the edge of the basin while the offlapping interval shows each progressive onlap progressing down-dip away from the basin flank.

2.3 Methods

2.3.1 What is *Onlapse-2D*?

Onlapse-2D is a simple tool that provides a structured way to investigate the structural and stratigraphic evolution of a deep-water basin with limited data and/or data quality. *Onlapse-2D* is

a two-dimensional model, i.e. the input data are two-dimensional cross sections. The simplicity of *Onlapse-2D* enables a large number of simulations to be rapidly generated so that the parameters controlling basin evolution can easily be tested.

The bounding conditions that *Onlapse-2D* uses to constrain and define the spatial and temporal limits of the modelling are:

- Total Cross Section Width (m)
- Horizontal Resolution (m), the horizontal distance that each cell in the model represents
- Total Simulation Time (years; generally millions of years for the stratigraphic interval of interest)
- Time per Time Step (years; commonly tens to hundreds of thousands of years per time step)

The total cross sectional width is derived from seismic data and the total simulation time is derived from biostratigraphic control, from wells either in the mini-basin of interest, or from wells in the region via mapped seismic horizons. While there is no theoretical limits to the spatial and temporal scales of deep-water sedimentary systems that could be modelled by *Onlapse-2D* (aside than those imposed by computing power). *Onlapse-2D* is intended to be utilized at the mini-basin scale (kilometres to 10s of kilometres) over a geological period of time (hundreds of thousands of years to millions of years).

2.3.2 Basic Logic

Onlapse-2D follows a straightforward logic, dividing the geological activity in a deep-water mini-basin into three fundamental components: structural activity; background sedimentation (both hemipelagic and pelagic); and clastic deposition from a range of sediment gravity flow types (e.g. turbidity currents, debris flows, mass transport etc.). The interval of interest is selected and divided into an appropriate number of time steps, each in the order of thousands of years. The model has an initial basin bathymetry that is generated from the lowest mapped surface of interest in the mini-basin. For each time step of the model, the three geological components are applied to the model in order. 1) A laterally variable amount of structural relief which creates a modified subsurface structure and deformed bathymetry. 2) Background sediment is draped over that new topography. 3) Sediment gravity flow deposits are added to fill accommodation as defined by the user (see below).

Repeated application of this three-step process results in the final structure and stratal patterns in the basin. Each layer within the model represents the total deposition in that time step, and will represent deposition from multiple sediment gravity flows.

2.3.3 Definition of Input Parameters

2.3.3.1 Initial Basin Structure (Figure 2.3a)

The Initial Basin Structure is generated directly from the lowest mapped horizon of interest and refers to the initial sea floor bathymetry of a basin at the start of a simulation (Figure 2.3a). It is the height in meters from the lowest point in the model to any point of that initial topographic surface along the modelled profile. This important surface requires geological thought: inspection of the seismic line that is the basis for the 2D section reveals the structures active during the interval of interest, and may require flattening of the seismic horizon (Figure 2.3e). For the first model run, a relatively simple initial bathymetry is recommended; the initial relief is inferred from the lowermost stratal terminations onto that bounding surface. The initial basin relief can be amended in subsequent runs if necessary.

2.3.3.2 Rate of Rise of the Structural Profile (Figure 2.3b)

The rate of rise of the Structural Growth Profile is calculated by combining two separate user defined curves, The Structural Growth Profile and the Structural Growth Rate. The Structural Growth Profile is a curve that defines the shape of the growing structure, e.g. the shape of the subsiding basin, a growing fold, a rising salt diapir, etc. and it remains constant through time. The Structural Growth Rate is a user defined curve that defines the amount of growth applied to the Structural Growth Profile. It is spatially uniform but varies through time. For each time step, these two curves are combined by multiplication to calculate the vertical distance that each point in the 2D profile moves for each time step. This is the *Rate of Rise of the Structural Growth Profile*, and it is the amount of rise in mm/yr converted to m/Time-Step that is applied to the basin structure through vertical shear.

In nature, structures may grow by a variety of processes (such as extensional faulting, contractional faulting, buckle folding, salt diapirism/withdrawal, etc.) and while all of these involve vertical motion, many also involve a component of lateral movement (Fossen, 2010). *Onlapse-2D* is not intended to provide a precise simulation of multiple types of deformation. We are principally concerned with processes that deform the sea floor, in particular vertical displacements, and therefore, *Onlapse-2D* accounts for only the vertical component of structural growth. For the purposes of stratal simulation, this is generally an adequate approximation of many structural processes where horizontal displacement is minimized and the steepness of the angles is kept relatively low; e.g. salt withdrawal, gentle buckle folding (Peel, 2014). We believe this method provides a suitable approximation, which is fit for purpose to model most aspects of salt tectonics and gentle buckle folding, for example. However, we recognize that the approach

has its limitations for modelling other processes, in particular fault-bend folding resulting from movement over low-angle faults, and we would not recommend using *Onlapse-2D* in these settings.

The geological structure of a mini-basin is commonly created by a combination of processes, e.g. folding plus salt withdrawal plus basin tilting, and that these processes may operate at different rates throughout the evolution of the section. In order to simulate this, several different shape profiles may be used in the same model, one for each structural process, each with its own individual growth rate curve.

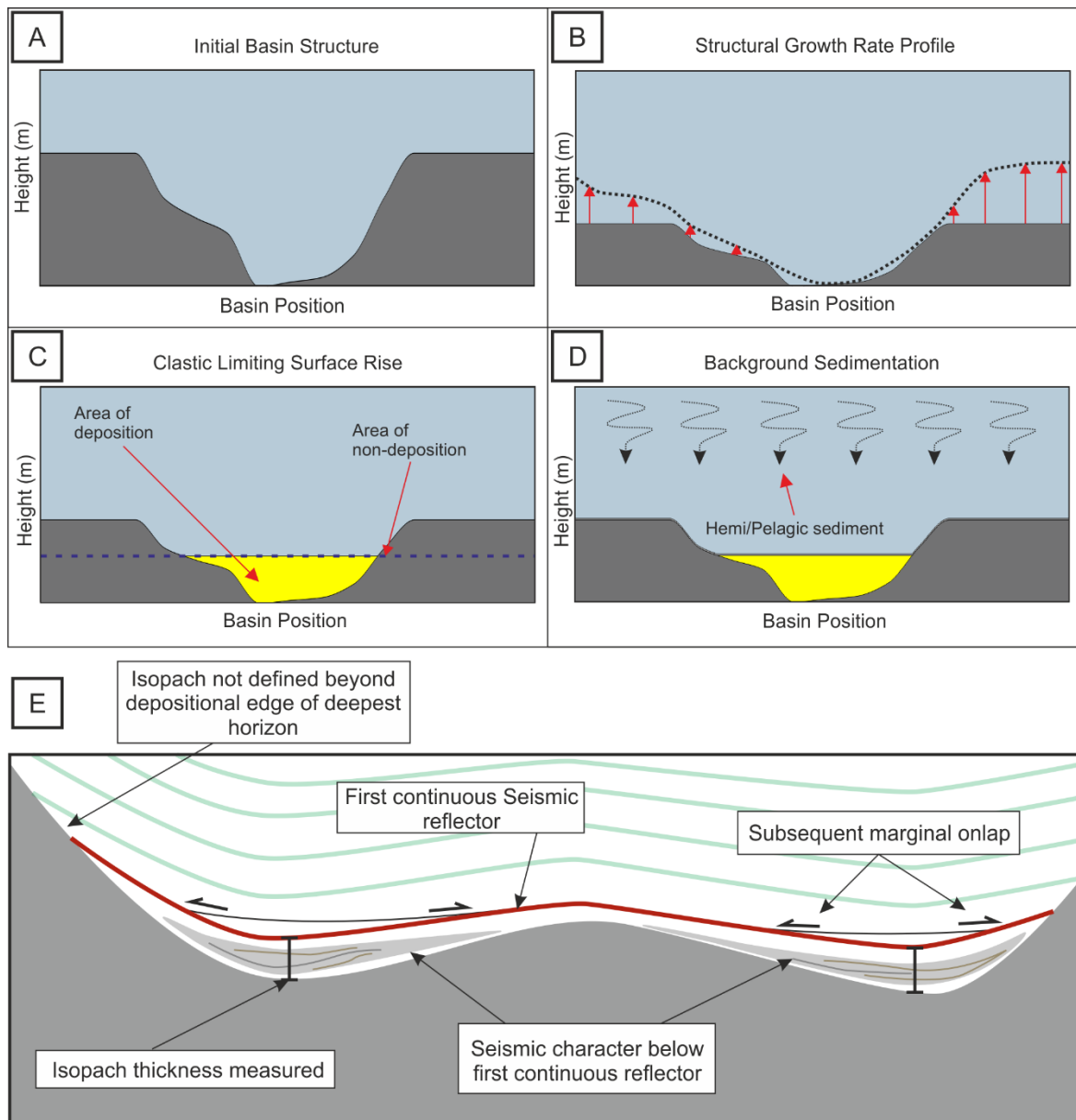


Figure 2.3 A) The Initial Basin Structure at Time-Step 0, E) illustrates how we derive this from seismic data. B) Dotted line represents the Structural Growth Profile, with red arrows indicating the rate of rise being applied to the Basin Structure (dark grey structure). The Structural Growth Rate Profile consist of multiple profiles, in this example it is a single profile. C) Blue dotted line is the Clastic Limiting Surface, if there is available accommodation space below then gravity flow deposit packages are deposited, if not

then no deposition occurs. D) A uniform thickness of background sediment is deposited along the cross-section, through pelagic and hemi-pelagic settling. E) The Initial Basin Structure at Time-Step 0 is derived by mapping the first continuous seismic reflector (red) and measuring the thickness of the isopach below it. Inspection of the subsequent and underlying strata to identify patterns of onlap and geometry allow us to infer how much topography existed at Time-Step 0 and how much topography may have been created by subsequent structure growth

2.3.3.3 Rate of Rise of the Clastic Limiting Surface (Figure 2.3c)

The Rate of Rise of the Clastic Limiting Surface is the amount of rise in mm/yr converted to m/Time-Step that is applied to the Clastic Limiting Surface. The Clastic Limiting Surface is used to determine whether new gravity flow sediment is deposited at a given position on a cross-section. It is a line that delineates above which, no sediment gravity flow deposits are preserved, and below which if there is accommodation, they are preserved and given the name *Gravity Flow Deposit Packages*. This is a user-defined horizontal level that can rise or fall with time. The Clastic Limiting Surface provides a straightforward means of determining the amount of sediment being captured by a basin over time.

Onlapse-2D does not require knowledge of larger scale variables or inputs (Figure 2.1). The user needs not make assumptions on how or why sediment flows into the modelled section just that sediment does, and has been captured within the mini-basin. The user instead controls only the amount of sediment captured within the mini-basin at any one time using the Clastic Limiting Surface. The Clastic Limiting Surface is not necessarily equivalent to a base-level, equilibrium surface, or even a spill point (because the user may not know that level for the basin on the chosen cross-section), but they can influence why the surface rises or falls (Figure 2.4). There are multiple geological factors that influence the movement of the Clastic Limiting Surface (Figure 2.4), which are not explicitly defined by *Onlapse-2D*, all it takes into account is that because there are gravity flows found, the Clastic Limiting Surface was above the sea-floor. While in nature, changes in the rate of sediment supply to deep-water systems is attributed to a variety of external geological factors (e.g. relative sea-level fall, climate, shelf geomorphology etc. (Carvajal, et al., 2009) (Covault & Graham, 2010) (Liu, et al., 2016)), these factors are rarely well understood and constrained, and quantification is difficult.

The Rate of Rise of the Clastic Limiting Surface is determined by local subsurface data only (e.g. reflection seismic and well data, especially biostratigraphic data that contains information on the rate of sediment accumulation in the basin through time). It is a user-defined surface that is specific to the mini-basin being modelled. It does not require knowledge of larger scale variables,

nor does it require the user to know where the basin was relative to the sediment fairway, or whether the mini-basin was close to the regional slope gradient or structurally perched above the regional slope. However, prior knowledge of this information can help constrain the rate of rise applied to the Clastic Limiting Surface and regional literature can that discusses average sedimentation rates (e.g. Carvajal et al (2009)).

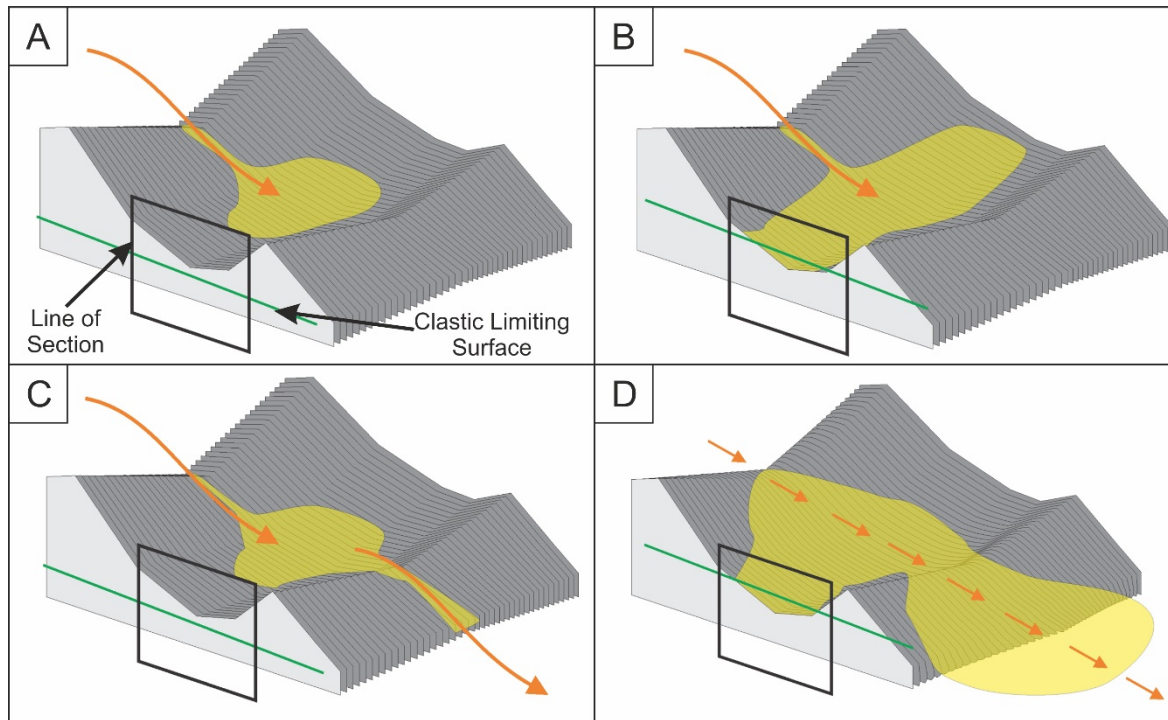


Figure 2.4 Illustrative examples of some geological reasons for the position of the Clastic Limiting Surface (green line), within the Line of Section and why it may rise or fall with time. A) In some periods of time the Clastic Limiting Surface may be below the sea-floor because sediment input is limited, so no Gravity Flow Deposits are deposited within the line of section. B) In other periods of time, the Clastic Limiting Surface may be rise above the sea-floor because of high sediment input into the basin. C) The Clastic Limiting Surface is controlled by a spill point in this example, even though sediment input is high. The spill point is outside the plane of section. D) The position of the Clastic Limiting Surface in this example is above the sea-floor because for this period of time sediment input has reached an equilibrium surface.

2.3.3.4 Background Sedimentation Rate (Figure 2.3d)

This is the amount of sediment in mm/year that is deposited uniformly across the modelled mini-basin, draping both highs and lows, through pelagic and hemipelagic settling. This represents any sediment that falls through the water column, such as pelagic organic remains, fallout from dilute sediment clouds, wind-blown dust, volcanic ash fall, meteoric dust, etc. The Background Sedimentation Rate is calculated from well control in the area of interest, using condensed intervals (periods of time with very little clastic input) and is either constant through time or changes over a longer time scale (multiple time steps).

2.3.4 Workflow

The procedure of generating stratigraphy using *Onlapse-2D* is: 1) generate an Initial Basin Structure; then for each time step of the model; 2) apply the Structural Growth Profile rise to the model; 3) apply a rise to the Clastic Limiting Surface, and if there is accommodation preserve gravity flow deposit packages up to the Clastic Limiting Surface; and then 4) draping a uniform thickness of background sediment throughout the cross section (Figure 2.5). Steps 2-4 are repeated for each iteration of the model.

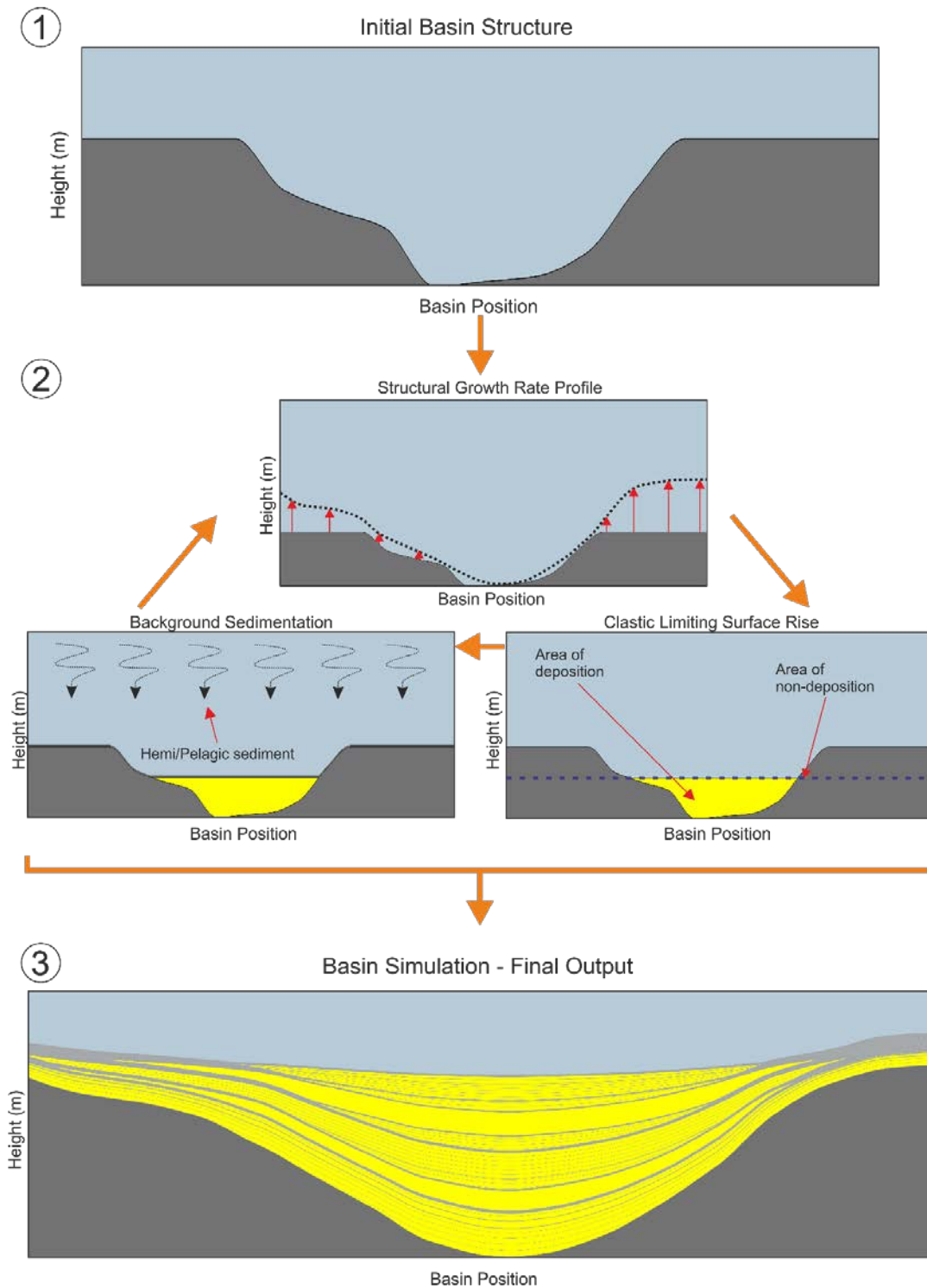


Figure 2.5 1: Time Step 0 shows the Initial Basin Structure with height in meters on the Y axis and Basin Position on the X axis. 2: Onlapse – 2D applies a structural growth rate to the initial basin structure, then Onlapse – 2D applies a rise to the clastic limiting surface and if there is accommodation available gravity flow deposit packages are preserved. After this, Onlapse – 2D applies a uniform thickness of pelagic/hemipelagic sediment across the cross section. This process is repeated as many times as needed to produce a final cross section 3

Once the simulation is complete, we consider whether the modelled stratigraphy is geologically plausible. Does the stratigraphy fall within the range of forms seen in real basins? Are the

relationships between sediment packages geologically plausible? If the model is deemed unrealistic then the input variables (e.g. Clastic Limiting Surface or Structural Growth Rate Profile) are altered, with the aim of producing a realistic geological cross section.

After each iteration of the simulation, we compare the generated stratigraphy to the subsurface data to consider if the stratigraphy generated is consistent with it and what, if any, differences can be found. First we measure the thickness of modelled intervals at key points along the cross-section. Key points are equally spaced points along the cross-section, for example every 2000m, but also include important features of interest such as the tops of anticlines, the deepest points of synclines, or wells. This is compared to the same interval isopachs on the seismic section that is the basis for the modelled 2D profile. Table 1 shows an example of how the subsurface data is quantitatively measured against the modelled *Onlapse-2D* output. Second, we inspect the match between the stratal relationships generated in the model and those observed on the seismic line; for example, where there are onlaps on the seismic line, there should be onlaps on the model. Third, we consider the seismic facies of each zone, and lithology if a well penetration is present (Figure 2.6). While *Onlapse-2D* does not explicitly define the lithology, the seismic facies, or mappable architectural elements within an interval, are good indicators of the type of gravity flow deposits and a proxy for the relatively speed at which the package was deposited. Intervals with active siliciclastic systems should match the zones in the *Onlapse-2D* model with high values for the Clastic Limiting Surface (more deposition per unit time). Spikes in the rate of Clastic Limiting Surface rise (i.e. zones deposited at the fastest rate) commonly correspond on seismic data to distinctive thick laterally extensive discontinuous, chaotic seismic facies interpreted as probable mass transport complexes, however they can also represent a mega-turbidite deposit.

Zone N

Distance along Cross-section (m)	0	2000	4000	6000	8000	10000	12000	14000	15500
<i>Basin Position</i>	1	80	160	240	320	400	480	560	631
<i>Derived Thickness from Seismic</i>	20	30	25	160	235	160	60	20	20
<i>Modelled Thickness - GFD</i>	0	0	0	121	195	166	58	0	0
<i>Modelled Thickness - Total</i>	32.81	32.81	32.81	153.81	227.81	198.81	90.81	32.81	32.81
<i>Difference (Seis/Model) (m)</i>	-12.81	-2.81	-7.81	6.19	7.19	-38.81	-30.81	-12.81	-12.81

Table 1 This table is an illustrative example, tied to Figure 2.6. The “Derived Thickness from Seismic” is compared against the “Modelled Thickness – Total”. If the difference is outside a set window of tolerance, in this example it is 25m, then alterations are made to the physical inputs. The red cell at Basin Position 480 shows where the difference is beyond the tolerance. A negative difference shows where the modelled thickness for Zone N is higher, and a positive difference is where it is lower.

If a good match is not achieved, then the input variables (e.g. Clastic Limiting Surface, Structural Growth Profile, and Initial Basin Structure) are altered until the modelled stratigraphy fits within an acceptable range. For example, alteration of the input variables can include increasing or decreasing the rates of rise of the Clastic Limiting Surface or the Structural Growth Profile, adding additional Structural Growth Profiles, changing the shape of the Initial Basin Structure.

If these changes do not iterate towards a good fit to the available data, there are two possibilities. In some cases, the difference may be resolved by introducing additional elements to the *Onlapse-2D* model, such as an additional component of the structure, and iterating towards a best-fit solution. In other cases, the discrepancy may be caused by some process that cannot yet be simulated in the *Onlapse-2D* method, as this method does not attempt to model erosion, or construction of positive depositional forms such as channel-levee systems or relief produced on some ponded fans ($\sim 0.5^\circ$). Examples of both of these discrepancies will be addressed later in the paper.

Iterating towards a match with the available data is an important aspect in constructing a model with *Onlapse-2D*. As *Onlapse-2D* is a geometric model, it is computationally quick; for example, the calculation of outputs for a 101x1200 cell matrix that contains 122400 cells takes 1/10th of a second to complete.

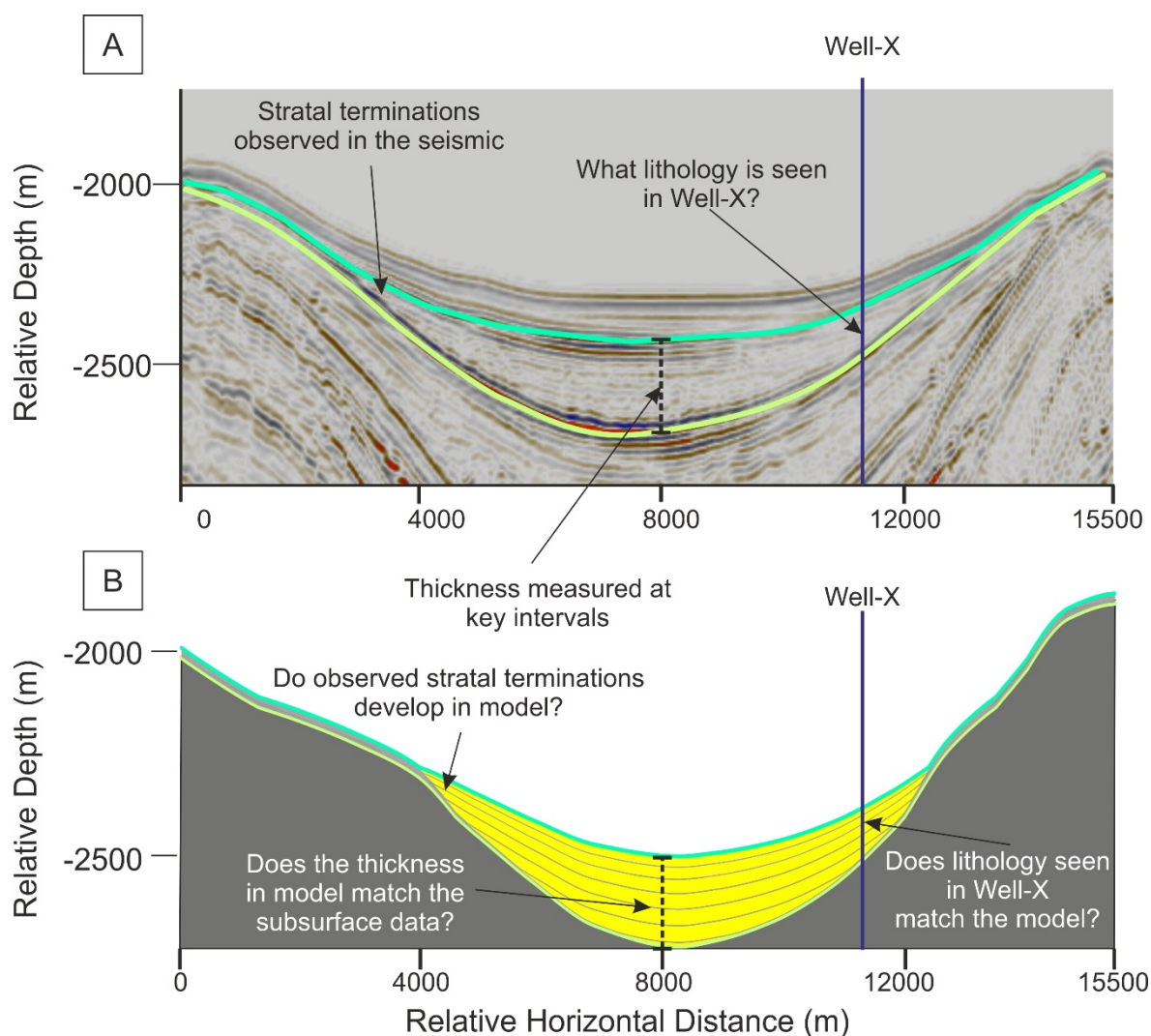


Figure 2.6 Illustrative example of subsurface information (A) can be compared against the modelled modelled output (B). Do the observed stratal terminations seen in A, develop in B? Does the stacked turbidites seen in Well-X correspond to gravity flow deposits in the modelled output? Do the thickness measurements in A correspond to those in B?

2.4 Results

2.4.1 Hypothetical Basins

To test if *Onlapse-2D* was able to produce geologically realistic basins we chose to model four different mini-basin types, a symmetrical basin (Figure 2.7), an asymmetrical basin (Figure 2.8), a tilted basin (Figure 2.9), and a turtle anticline mini-basin (Figure 2.10). The purpose of these simulations is to demonstrate that the model can reproduce the general form of these basin types, matching the overall shapes, the overall distribution of clastic sediments, and overall patterns of thickening/thinning and onlap/offlap seen in nature. In these models, we have kept the degree of stratigraphic complexity to a minimum by applying a very simple form of Clastic

Limiting Surface development. We will show in a later section that more realistic and more complex stratal geometries can be achieved using a more complex Clastic Limiting Surface.

2.4.1.1 Symmetrical Basin (Figure 2.7)

This is a simple symmetrical salt-withdrawal mini-basin. We applied a single Structural Growth Rate Profile to a simple, flat Initial Basin Structure. The Clastic Limiting Surface growth per Time-Step was applied in a binary manner with either a constant rate of rise per Time-Step or with a rate of rise of zero. The change between the two states was geologically instantaneously to simulate an avulsing sediment input. Application of these conditions generated a symmetrical mini-basin with three intervals of gravity flow deposit packages separated by thicknesses of background sediment. Each of the gravity flow packages shows onlapping intervals but no offlapping intervals. All three gravity flow deposit packages are thickest within the deepest point of the basin, within the depocenter the overall thickness for each package within the intervals remains static.

2.4.1.2 Asymmetrical Basin (Figure 2.8)

In this simple asymmetrical salt-withdrawal mini-basin, we applied a single, asymmetrical Structural Growth Rate Profile to an asymmetrical Initial Basin Structure. The rate of rise of the Clastic Limiting Surface was sinusoidal in nature, to simulate a constant increase then decrease in sediment input. This combination of inputs and initial starting conditions produces three intervals of gravity flow deposit packages that contain both onlapping and offlapping successions. The number of packages with onlapping surfaces in each interval is greater than that of those with offlapping surfaces. The gravity flow deposit packages that pinch out with onlapping surfaces are also thicker than those that terminate in an offlapping succession. This combination of onlapping and offlapping succession in each interval produces an overall upwards thickening then thinning of the packages within the intervals.

2.4.1.3 Regional Tilt (Figure 2.9)

Onlapse-2D is not only restricted to modelling the entirety of a basin, it can be used to model “partial” cross-sections such as in Figure 2.9. Regional and local tilting is important in many tectonic regimes such as compressional systems which can cause a regional tilt to be applied to a system through time. A single Structural Growth Rate Profile that simulates tilting to one side of the cross section was applied to an Initial Basin Structure with no topography. The Clastic Limiting Surface growth profile was applied in the binary method to show two distinct periods of sediment input that occur over the same number of time steps. Applications of these conditions ultimately

leads to a tilted basin with two intervals of gravity flow deposit packages that both progressively onlap updip.

2.4.1.4 Complex Basin – Turtle Anticline (Figure 2.10)

Turtle anticlines, first described in northern Germany by Trusheim (1960), are an important class of salt withdrawal basin in which the core of the mini-basin has experienced structural inversion. Turtle anticlines are of particular interest because the part of the basin that was deepest at the time of early salt withdrawal, and which therefore may contain the best reservoir section, is raised up into an anticlinal closure. This anticlinal closure creates favourable conditions for giant hydrocarbon accumulations such as Girassol, Dalia, Plutonio, and Zinco in Angola, Thunder Horse, Pluto, and Mensa in the US Gulf of Mexico (Warren, 2006).

In nature, turtle anticlines form in two stages. In the first stage, a salt-withdrawal mini-basin develops by subsiding into salt. The rate of subsidence is greatest in the middle of the basin where the sediment load is the greatest, and subsidence is slower around the flanks of the basin, where the load is smaller. In this first stage, clastic sediments tend to be thicker and better developed in the centre of the basin, thinning and/or onlapping towards the edges of the basin. This stage continues until the basin welds; after welding the basin can sink no further, but while salt remains under the periphery of the basin, the basin flanks can continue to subside, resulting in the development of a new depocenter fringing the basin. Clastic sediments in this second phase tend to be thicker and better developed around the fringe of the basin, thinning and/or onlapping towards the centre of the basin (Jackson & Hudec, 2017).

The resulting simulation, shown in Figure 2.10, illustrates how the interplay of two different structural growth profiles can successfully recreate the overall form of a turtle anticline. Figure 2.10 shows that applying a simple, sinusoidal growth curve to the Clastic Limiting Surface can replicate the general pattern of clastic sedimentation distribution, thickness variation, an onlap within such a basin, matching the overall patterns seen in nature.

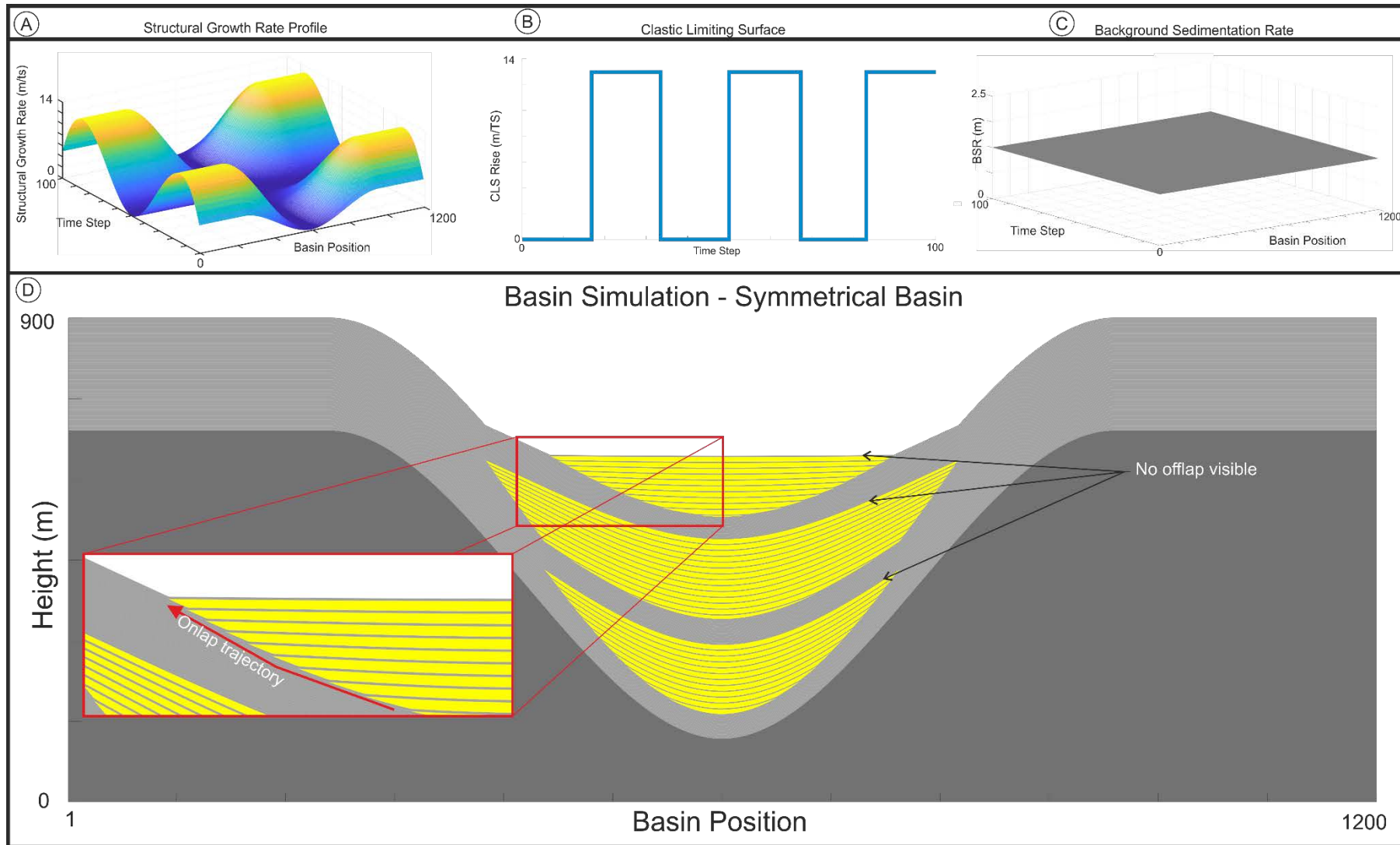


Figure 2.7 Inputs used to model the evolution of a simple symmetrical basin. A) 3D representation of the Structural Growth Profile; X axis represents position in space, Y axis represents the position in time, Z axis represents the growth that the structure grows in meters per time step. B) The rate of rise of the Clastic Limiting Surface shown is binary, either at a constant rate of rise of 13m or 0m per Time Step. C) Background Sedimentation Rate is kept temporally and spatially uniform. D) The red box highlights the trajectory of the overlapping surfaces and highlights a lack of offlapping surfaces.

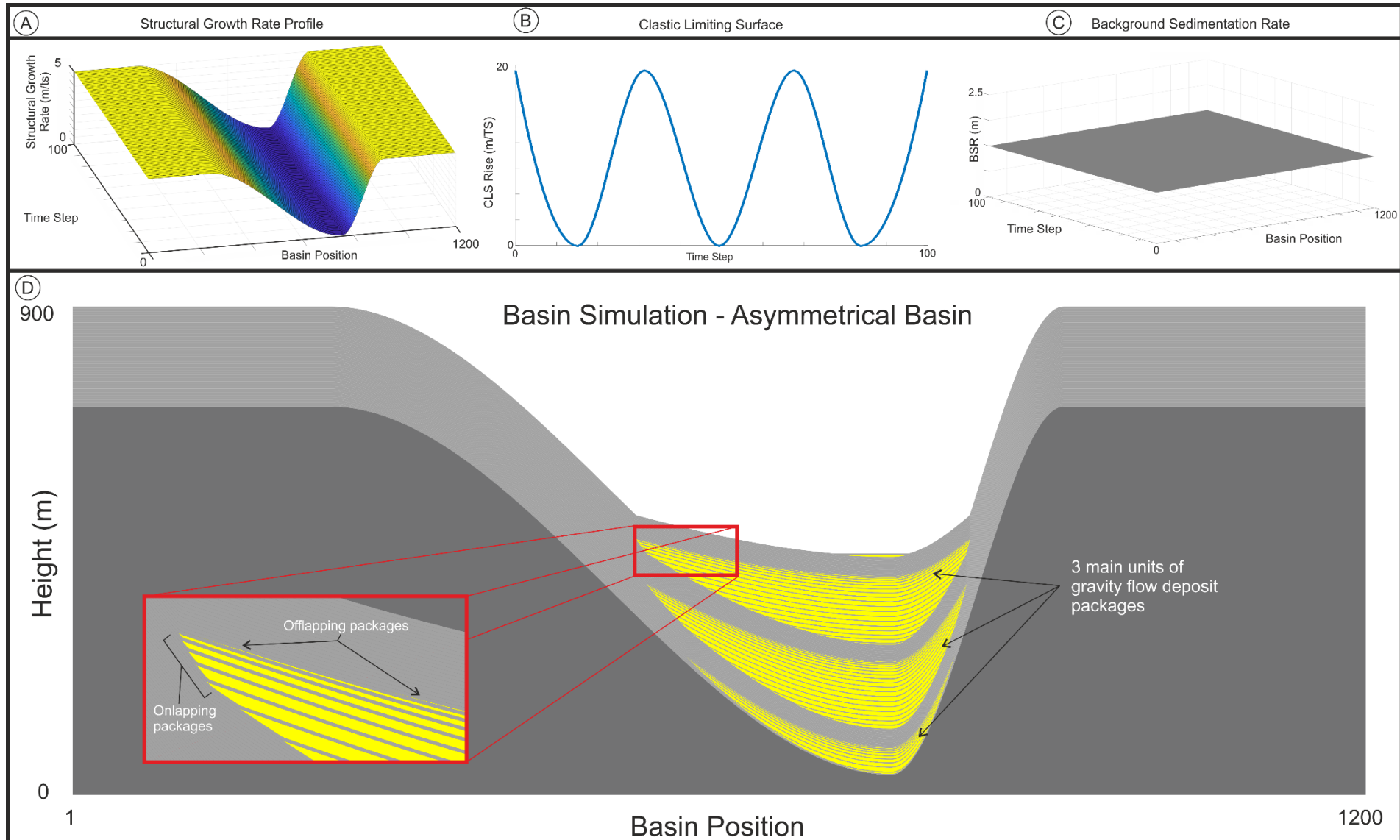


Figure 2.8 Basin simulation of an Asymmetrical Basin. A) A simple asymmetrical Structural Growth Profile is combined with a rate of rise of the Clastic Limiting Surface (B) that is sinusoidal, along with a temporally and spatially uniform Background Sedimentation Rate (C) these inputs combine to produce the basin simulation shown in D) Three main units of gravity flow deposit packages occur. Each contains onlapping and offlapping packages that are highlighted by the red box

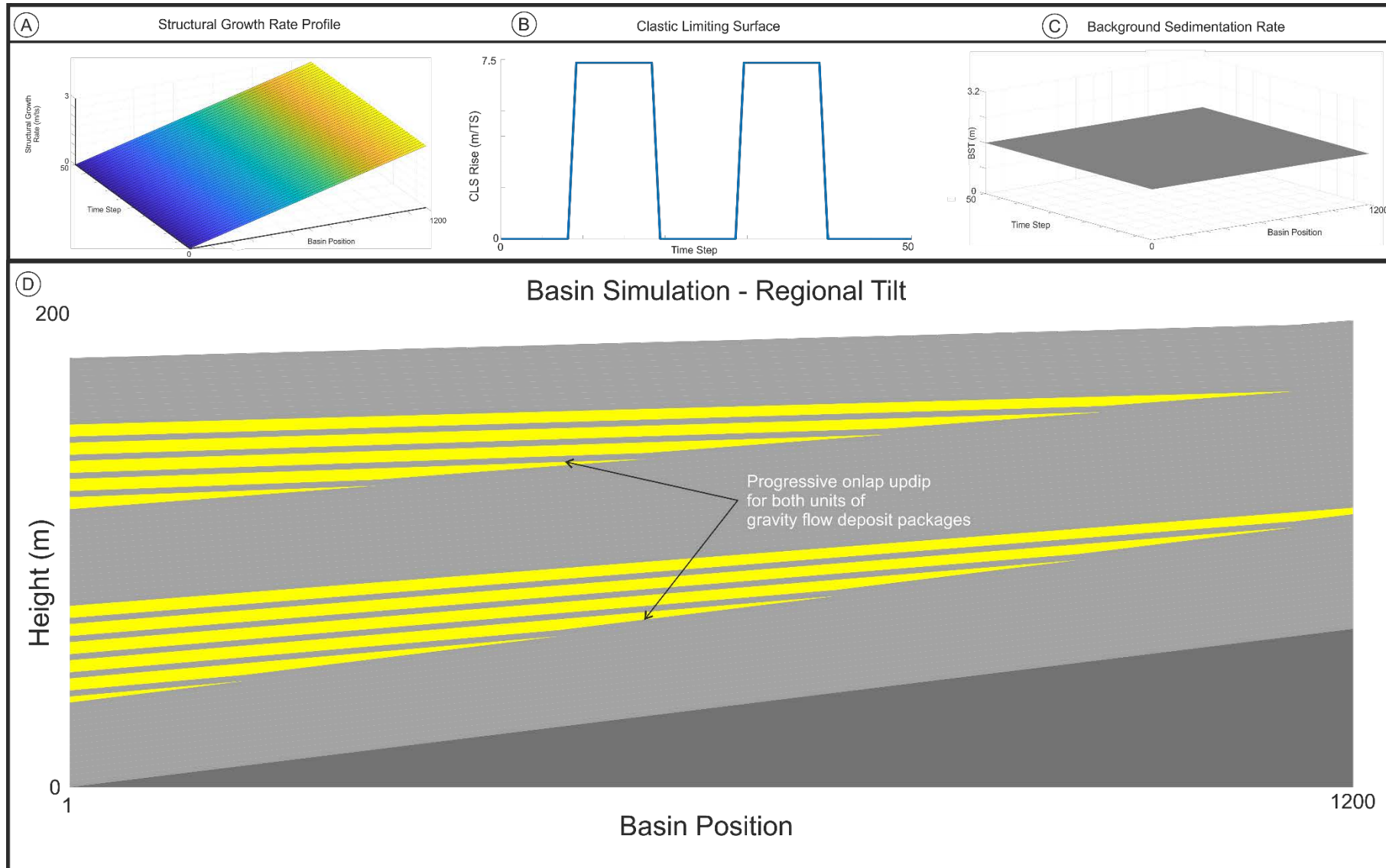


Figure 2.9 A) The Structural Growth Rate simulates tilting to the right-hand side of the cross section, B) along with a binary rate of rise of the Clastic Limiting Surface, and C) a Background Sedimentation Rate that is kept spatially and temporally uniform. These combine to produce D) two distinct units of progressively onlapping updip gravity flow deposit packages.

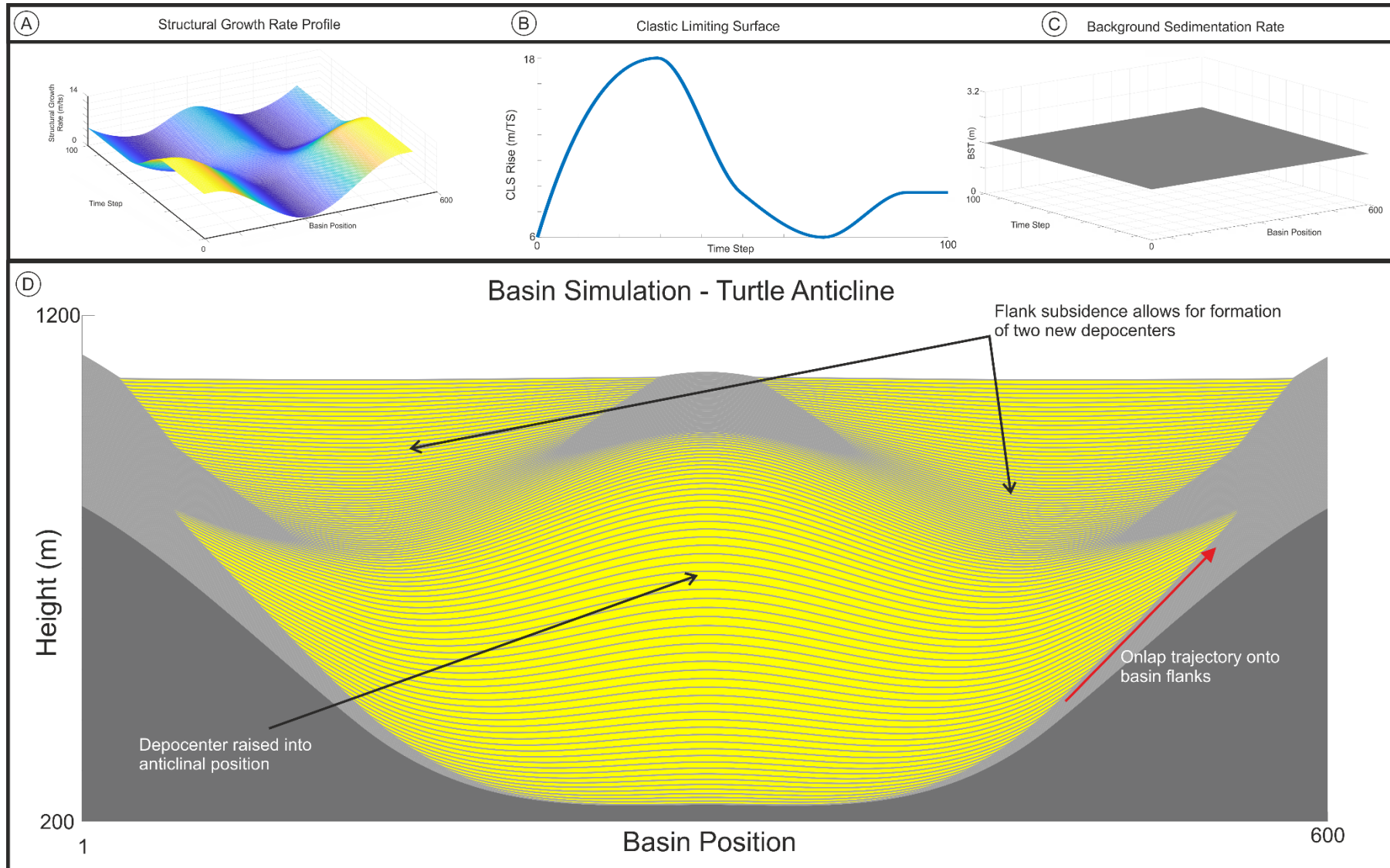


Figure 2.10 A) The Structural Growth Rate Profile is a combination of two distinct Structural Growth Profiles, which simulates the processes of salt withdrawal (a single depocenter), welding, and then flank subsidence (simulated by the development of two depocenters to the left and right of the original depocenter in the middle). B) The rate of rise of the Clastic Limiting Surface is variable through time but shows that sediment was continually deposited within the system. C) Background Sedimentation Rate is kept temporally and spatially uniform. D) The process of welding has raised the depocenter in the lower part of the interval into an anticlinal structure while the flank subsidence has allowed for the formation of two new depocenters

2.4.2 Case Study

2.4.2.1 SymB1 Basin – Central Gulf of Mexico (Figure 2.11)

Creating a simulation of a real mini-basin, in which we attempt to match the precise structure and stratal architecture seen on subsurface data, was a critical test of *Onlapse-2D*. Allowing us to demonstrate that *Onlapse-2D* can be applied to real basins not just conceptual mini-basins. We chose to model a near symmetrical mini-basin, from the central Gulf of Mexico with an apparently straightforward structural history we call this basin **SymB1** (Figure 2.11). Seven horizons up to the sea floor were mapped and the basin was split into six zones labelled from 1 to 6.

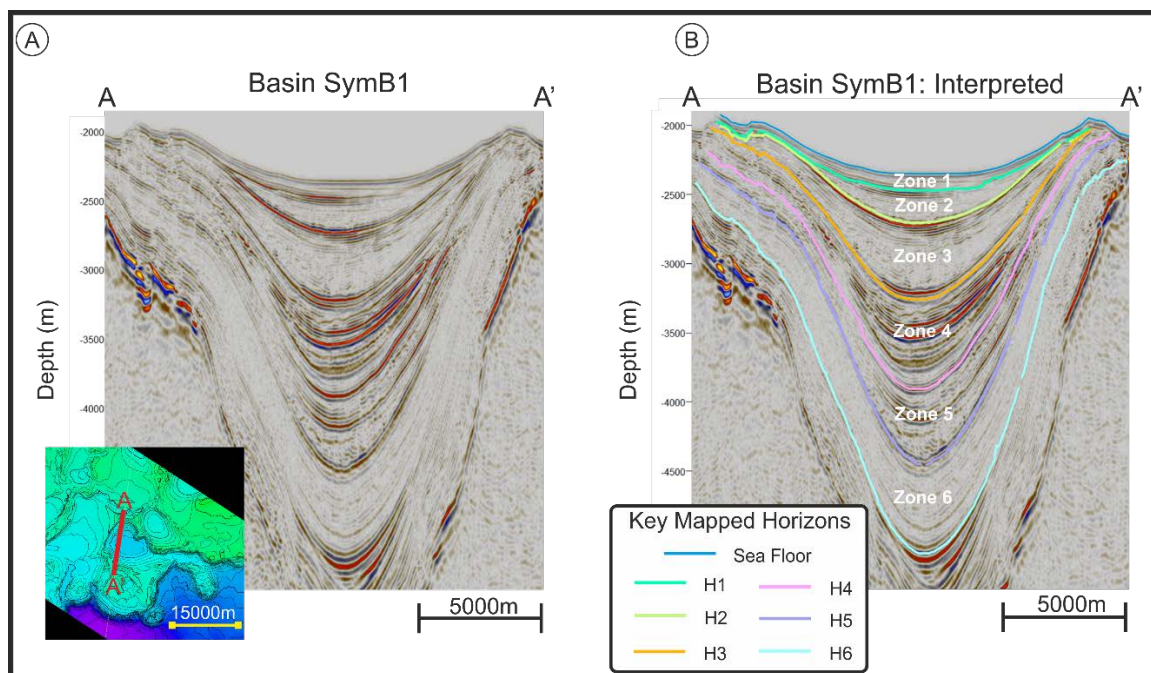


Figure 2.11 A) Near symmetrical apparently simple salt-withdrawal mini-basin from the Gulf of Mexico. B) Interpreted horizons on Seismic cross-section on the right hand side, along with the name of the zones that the mini-basin was split into.

For the first iteration of the model we applied a single simple structural growth profile, with temporally and spatially uniform background sedimentation, and applied a rate of rise to the Clastic Limiting Surface that varied in both the amount of rise per time step and the duration of that rise (Figure 2.12). When compared to the seismic dataset the *Onlapse-2D* model of **SymB1** matched the gross geometry of the basin overall (Figure 2.13). We consider there to be a discrepancy between the model and the real basin, when there is a difference in the thickness of modelled intervals or structural height greater than 25m. This was chosen because the typical resolution of good quality seismic is ~25m. We found that there was a discrepancy in the final structural height of the *Onlapse-2D* model in a small number of locations. There were discrepancies in all zones; for example, in zones 6 and 5 the centre of the basin was typically

under thickened while the basin flanks were over-thickened. There were several gravity flow deposit packages within zone 1 that were more laterally restricted in the modelled output, than in the seismic cross section (Figure 2.13).

Iteration is an important part of the process in simulating basin evolution with *Onlapse-2D*. The computational simplicity of *Onlapse-2D* allows us to make small changes to the input parameters and rapidly calculate their effect on the basin simulation. In order to improve upon the fit between our first iteration and the seismic cross-section we made a series of small changes to the Structural Growth Rate Profile and the Clastic Limiting Surface profile to create the final model simulation **SymB1** (Figure 2.14).

For the Clastic Limiting Surface profile, we increased the number of Time-Steps in which periods of hiatus occur, included short periods (one Time-Step) of rapid deposition (up to 350m/Time-Step) as well as periods of more moderate (35 – 45m/Time-Step) but prolonged (4 – 6 Time-Steps) rise in the Clastic Limiting Surface to best match the stratal geometries observed within the mini-basin. However, these improvements to the Clastic Limiting Surface profile were unable to account for a thickness miss-match in zone 6. The discrepancy within zone 6 occurs where a match in the model thickness is flanked by areas that are between 125-150m under thickened compared to the seismic data set. The first attempt to fix this discrepancy through altering the Initial Sea Floor Topography proved unsuccessful. A second, subtly different Structural Growth Rate Profile was added to the model which corrected the discrepancy. This second Structural Growth Rate Profile increased the structural accommodation available during the deposition of gravity flow deposit packages by lowering the growth rate where under-thickening occurred in Zone 6. As this type of under-thickening on the flanks was found only within Zone 6 and not in later zones the Structural Growth Rate Profile transitioned back to the first profile used after the end of Zone 6 (Figure 2.14).

We combined this new two-phase Structural Growth Rate profile with a Clastic Limiting Surface profile rise that provided a highly episodic sediment supply, along with brief periods of depositional hiatus, and brief periods of rapid Rise of the Clastic Limiting Surface. The geometries of several zones were simulated through moderate rates of rise over prolonged periods, which produced gravity flow deposit packages that progressively onlap updip onto the basin flanks. Very rapid rates of rise of the Clastic Limiting Surface correspond to laterally extensive and thick mass-transport complexes corresponding to zone 3 in the seismic which indeed has the chaotic seismic facies character that would be expected from a mass transport complex (Figure 2.11).

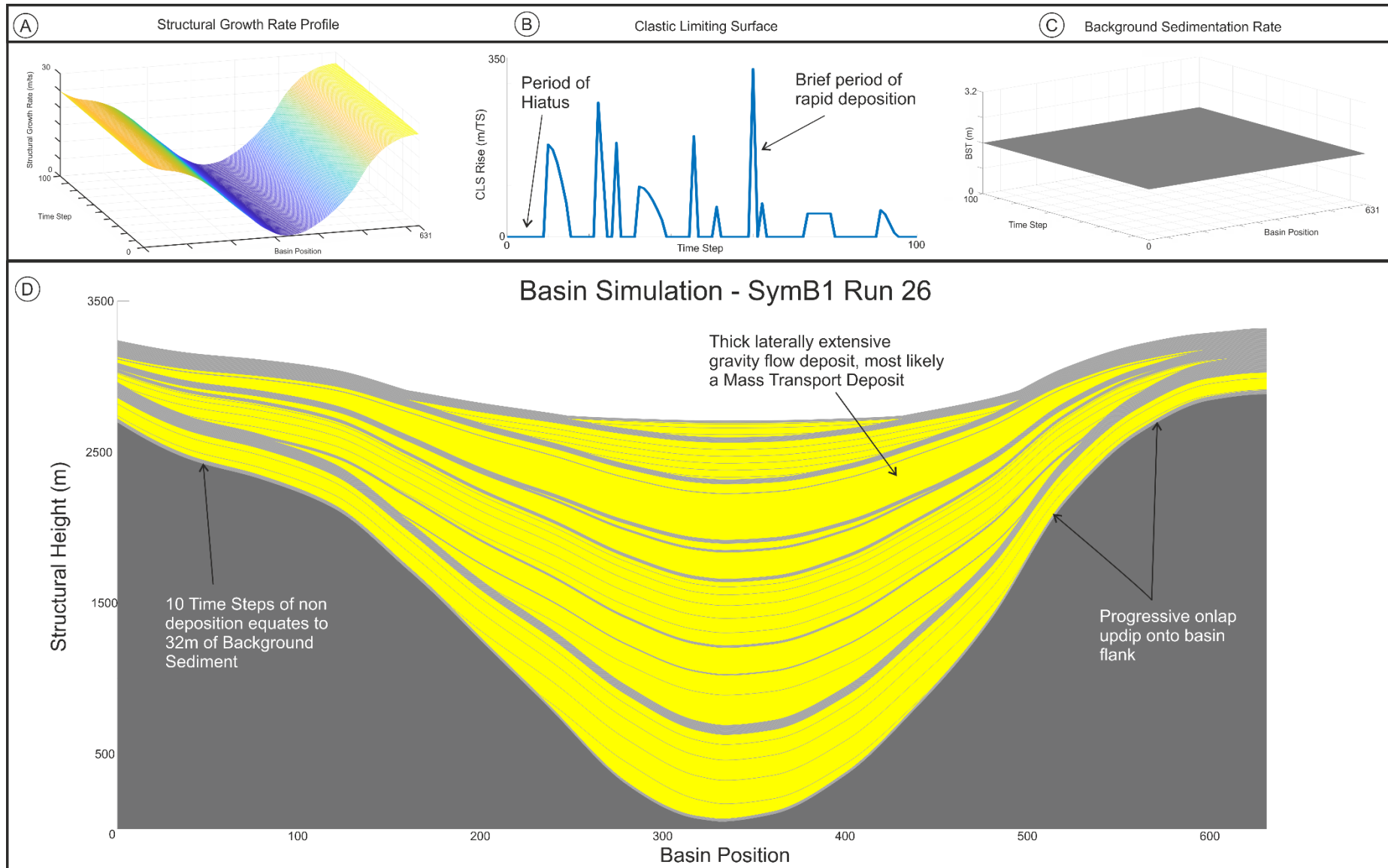


Figure 2.12 A) Simple, constant Structural Growth Rate Profile; B) the Clastic Limiting Surface that varies in the rate of rise and the length of the rise with periods of hiatus, and a Background Sedimentation Rate (C) that was spatially and temporally uniform combine to produce this Basin Simulation of SymB1 (D). The period of Hiatus at the start of the simulation produces ~32m of background sediment, while the brief period of rapid deposition that consists of a single Time Step produces a thick laterally extensive gravity flow deposit that is most likely a Mass Transport Complex.

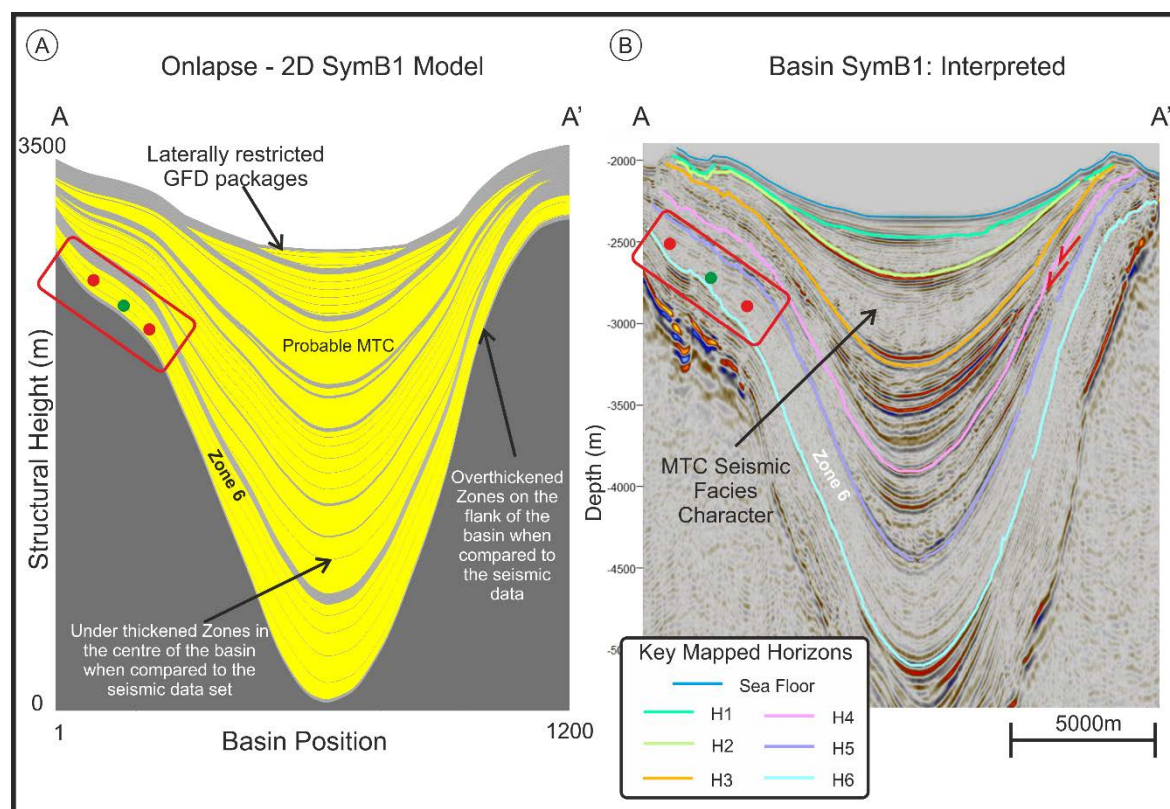
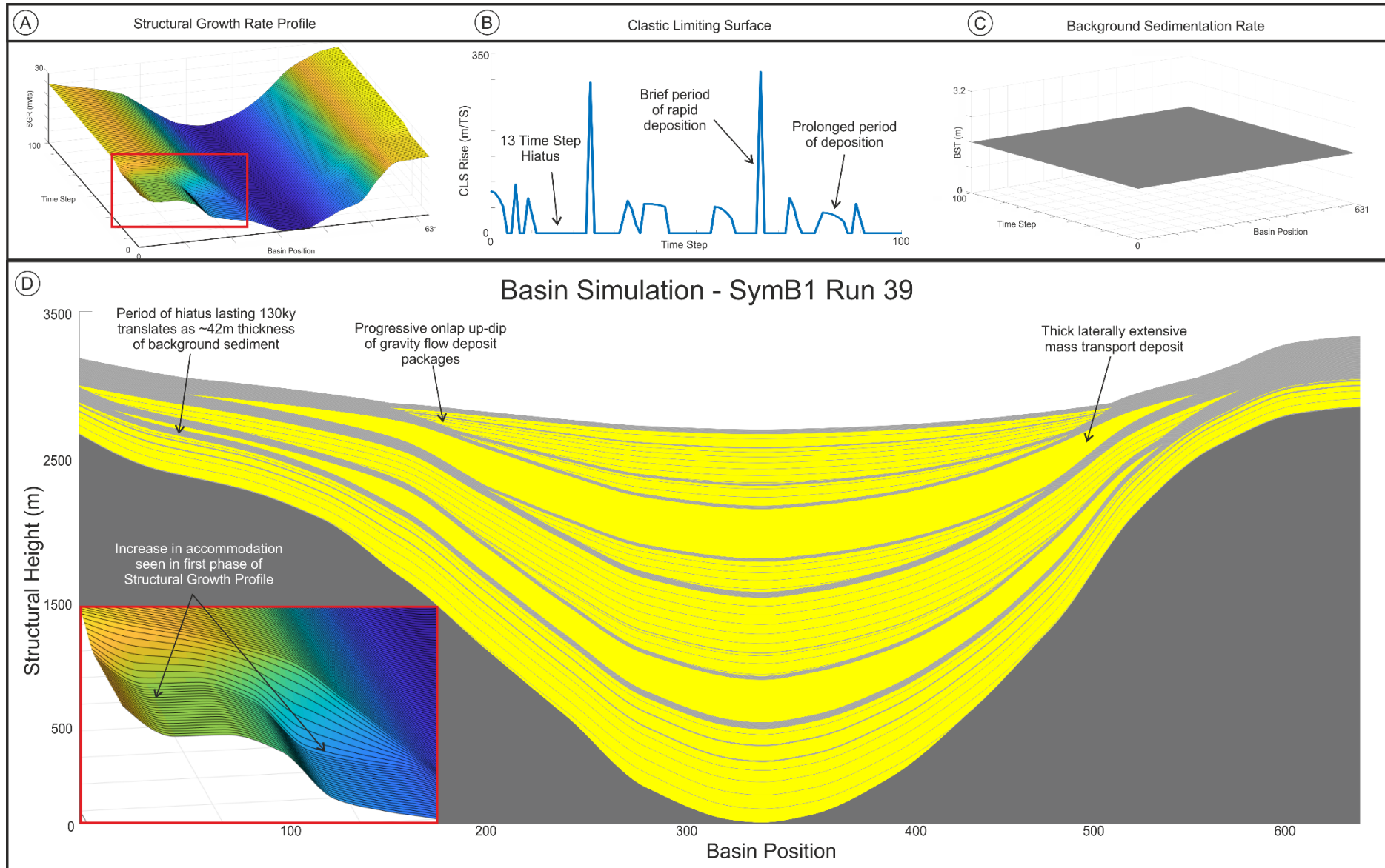


Figure 2.13 Comparison of the model produced by Onlapse-2D (A) and the seismic data set (B). Comparing the zones in the Onlapse-2D model with the seismic we found the depocenter was generally under-thickened in Zones 5 and 6 while the flanks were over thickened. Within Zone 1, the modelled output was predicting gravity flow deposit packages that were more laterally restricted than seen in the subsurface data. The red box in A) highlights an area where we were unable to use changes to the rate of rise of the Clastic Limiting Surface to correct the anomaly that had formed. Red circles indicate where Onlapse-2D models the thickness of the Gravity Flow Deposits 125 – 150m thinner than seismic data shows. The green circle represents a good match between the model and data. Seismic facies character of shows that “Probable” MTC is very likely an actual MTC



Chapter 2

Figure 2.14 Inputs used to simulate a more accurate basin evolution of SymB1 with a closer match to the seismic data. A) The addition of a second, subtly different structural profile that allowed for an increase in accommodation during the deposition of gravity flow deposits in Zone 6 (red box Insert). B) Changes in the rate of rise of the Clastic Limiting Surface allowed us to model the lateral extent and thicknesses seen in Zones 3 and 4 much more accurately as well as produce a closer match to the thickness and lateral extent of the MTC seen in the seismic data. Cf figures 2.9 & 2.10

2.5 Discussion

Our results show that *Onlapse-2D* is able to produce geologically realistic basin stratigraphy, including symmetrical basins, asymmetrical basins, tilted basins, and more tectonically complex turtle anticline basins. The **SymB1** case study in the central Gulf of Mexico shows that *Onlapse-2D* is able to recreate the structure, basin-fill stratigraphy and detailed stratal geometries of a real mini-basin. In the results section we discussed the iterative approach using multiple *Onlapse-2D* runs to get a good match between the modelled stratigraphy and the actual **SymB1** basin fill as measured in the seismic section. In this section we will provide a geological interpretation of our basin simulation, we will also evaluate how well the *Onlapse-2D* model performed in simulating both hypothetical basins and **SymB1** basin, and we will also discuss how *Onlapse-2D* can still provide valuable information through what we term informative discrepancies.

2.5.1 Discussion of SymB1 Results

In the **SymB1** case study we found that we were not able to match the seismic data using only a simple model, which used a single constant Structural Growth Profile growing at a constant rate. Discrepancies between the *Onlapse-2D* model and the seismic data could not be accounted for simply by modifying the Initial Bathymetry or the Clastic Limiting Surface Profile. As we could not correct the discrepancy by altering the rate of Clastic Limiting Surface or the Background Sedimentation Rate, we concluded that modifying the Structural Growth Profile for a limited period of time during the early stages of the simulation would be the most logical step. The addition of a second Structural Growth Profile (Figure 2.14) provided an increase in accommodation on the left flank by adding two depressions in the profile that grew at a lower rate. We believe that this second Structural Growth Profile relates to extrinsic events that caused a zone of contraction early in the life of the basin. Specifically, we infer that the **SymB1** basin was partially obstructed early in its formation, which caused deformation of the sea floor, which created more localised accommodation. Identifying the exact nature of the obstruction that the **SymB1** basin experienced is beyond the scope of the model. However, work by (Duffy, et al., 2019) on Gulf of Mexico supra-salt mini-basins shows that basins can be obstructed through a variety of processes including basal salt welding or basin collision). Such processes modify the local strain field, and cause a zone of contraction updip of the obstruction. We infer that the additional Structural Growth Profile, that was necessary in order to accurately model the basin stratigraphy of SymB1, represents the obstructional processes described by Duffy et al (2019).

To model the lateral extent and thicknesses of stratigraphic packages seen in zones 3 and 4 rapid increases in the Clastic Limiting Surface rate of rise were needed, which represent short periods of rapid deposition by sediment gravity flows. We infer that these geologically instantaneous periods of infill are probably mass transport complexes and this is supported by the chaotic facies character of zone 3 for example.

During the iterative process of improving the model for the **Symb1** basin we found that there are two ways to hone the simulation. Each method requires comparing the total thickness of the zones and measuring the lateral extent of the major gravity flow deposit packages found in the model with the subsurface data. The first method is to measure the thickness of each zone in the model separately and compare that to its subsurface equivalent in isolation (Figure 2.15a). This method does not take into account the accuracy of the zones modelled before or after, for example if Zone 2 are in comparison to the subsurface data. The second method is to fine tune each zone sequentially from the lowest to the uppermost zone in a cumulative manner taking into account the accuracy to which the preceding zone was modelled (Figure 2.15b). We found that the first method provides a better match for each zone however, it may create errors that while minor in each zone create cumulative errors that increase upwards through the model.

Having applied the above alterations to the Structural Growth Rate Profile and Clastic Limiting Surface Profile we reach a point of diminishing returns, i.e. where only small improvements in the thickness and lateral extent of the gravity flow deposit packages can be achieved. Any remaining inconsistencies are likely to be related to factors that *Onlapse-2D* is currently unable to model, such as erosion, depositional relief, and compaction.

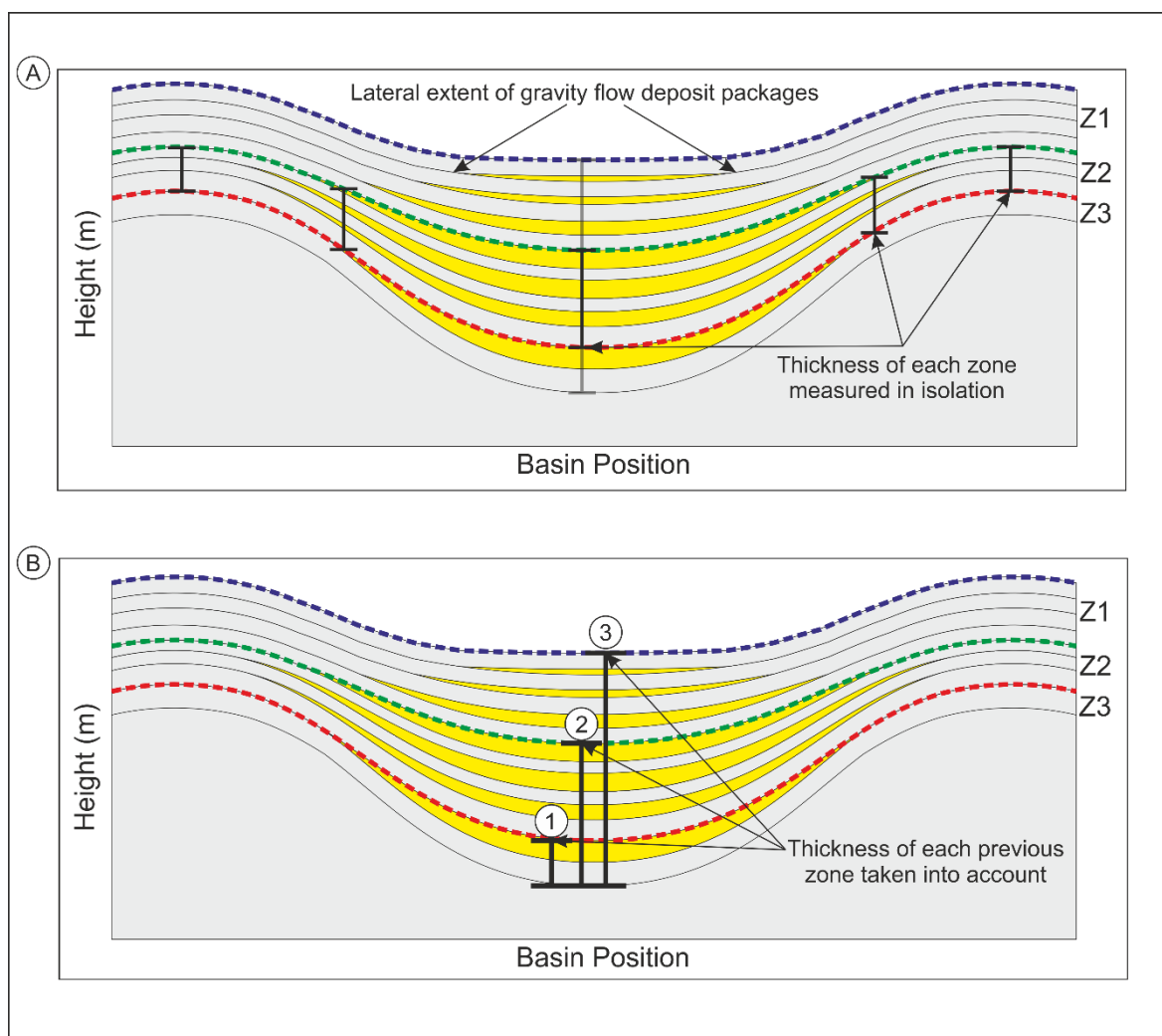


Figure 2.15 Two methods used to hone the final output in Onlapse-2D. A) Thickness of each zone is considered separately, e.g. Zone 1 within the seismic is compared to Zone 1 within the model. B) Second method that involves taking into account the total thickness of the sediment deposited in the model. The thickness of each zone contains the thickness of the zone(s) before it in a cumulative manner, e.g. Zone 2 has the thickness of Zone 1 added to it.

Having applied the above alterations to the Structural Growth Rate Profile and Clastic Limiting Surface Profile we reach a point of diminishing returns, i.e. where only small improvements in the thickness and lateral extent of the gravity flow deposit packages can be achieved. Any remaining inconsistencies are likely to be related to factors that *Onlapse-2D* is currently unable to model, such as erosion, depositional relief, and compaction.

2.5.2 Assumptions, Uncertainty, Useful anomalies, and Informative Discrepancies

2.5.2.1 Assumptions and Uncertainty

Several assumptions are made during the processes of producing simulations with *Onlapse-2D*. It is assumed that deposition only comes from sediment gravity flows and background sediment, there is no significant contributions from other processes (e.g. carbonate build-ups), all gravity flow deposit packages are horizontal at the time of deposition, there is no compaction, and no large scale erosion has taken place.

Erosion is not explicitly modelled in *Onlapse-2D*, and erosion is known to occur periodically throughout the evolution of deep-water mini-basins (e.g. scouring at the base of mass transport complexes (Moscardelli, et al., 2006), knick points (Heijnen, et al., 2020), channelization (Mayall, et al., 2006) etc. Because *Onlapse-2D* is unable to model erosion and assumes that all gravity flow deposit packages are horizontal at the time of deposition this means that *Onlapse-2D* is unable to directly model positive depositional topography (e.g. submarine lobes) or depositionally erosive features (e.g. mega scours).

Onlapse-2D assumes that all structural growth occurs through vertical shear, and that there are no major horizontal components to structural movement. *Onlapse-2D* also inherits all the assumptions that are made when matching subsurface data such as reflection seismic or well logs.

As structural growth occurs through vertical shear, faults with large horizontal displacements (e.g. normal faults) are unable to be modelled currently. Compaction is not currently included within the model; therefore, estimates on Background Sedimentation Rate and depositional rates of the Gravity Flow Deposit Packages are an underestimate. However, because we are able to obtain realistic simulations of real world examples (e.g. *SymB1*) of real world geometries we do not believe this is a significant factor. Compaction will be taken into account in later revisions of *Onlapse-2D*.

2.5.2.2 Useful anomalies and Informative Discrepancies

The decision to exclude erosion from *Onlapse-2D* does not invalidate the simulations produced by this software. Erosion is generally compensated for in the immediately overlying units therefore errors due to the lack of erosion in the model will tend to be localised (Figure 2.13). This is shown in Basin *SymB1*, where there is an erosional surface that has been compensated for in the overlying zone. Despite not modelling erosion, *Onlapse-2D* simulations provide understanding of the overall tectonostratigraphic evolution of basins and enables prediction of the temporal and

spatial distribution and thickness of sediment gravity flow packages (potential reservoirs) and background sediment packages (potential seals).

Whilst *Onlapse-2D* does not explicitly model erosion, or constructional topography, the simulation process does allow us to identify erosional or constructional anomalies, and to measure their magnitude as mismatches in zone thicknesses between the model, and the seismic data. These mismatches can be informative and interpreted within the geological context provided by the seismic data within the basin or regionally. We use the term *informative discrepancies* for the difference between the optimized solution and the geological control data. In some cases, the informative discrepancies correspond to surfaces or intervals that have clear evidence of seismic erosion (e.g. levees). However, on data with poorer imaging, such evidence may be less clear, and in these cases, the identification of informative discrepancies from an *Onlapse-2D* model may help to refine the seismic-stratigraphic interpretation.

The results of the modelling shown here illustrate that the inherent assumptions made when using *Onlapse-2D* to simulate the tectonostratigraphic evolution of structurally controlled deep-water mini-basins are reasonable and fit for purpose. The *Informative Discrepancies* described in **SymB1** provide evidence that even when *Onlapse-2D* is unable to provide a best-fit solution, important geological information can still be extracted. This learning may also be of use in other forms of forward modelling that attempt to replicate real world examples. Discovering where the simulation deviates from the subsurface data may illustrate a processes that is going on that is not taken into account during modelling.

However, the assumptions made within *Onlapse-2D* preclude it from being used in certain areas. For example, due to structural growth being modelled through vertical shear we would not recommend using *Onlapse-2D* in areas with strong components of horizontal displacement such as thrust ramp anticlines, complex incline anticlines in strike-slip regimes, or in salt-detached ramp syncline basins (Figure 2.16). As *Onlapse-2D* at present also is unable to model compaction or erosion, environments where these are common also present a challenge to model. For example, areas that experience significant erosion (Figure 2.16) or where differential compaction produces significant positive topography.

Salt-Detached Ramp Syncline Basin

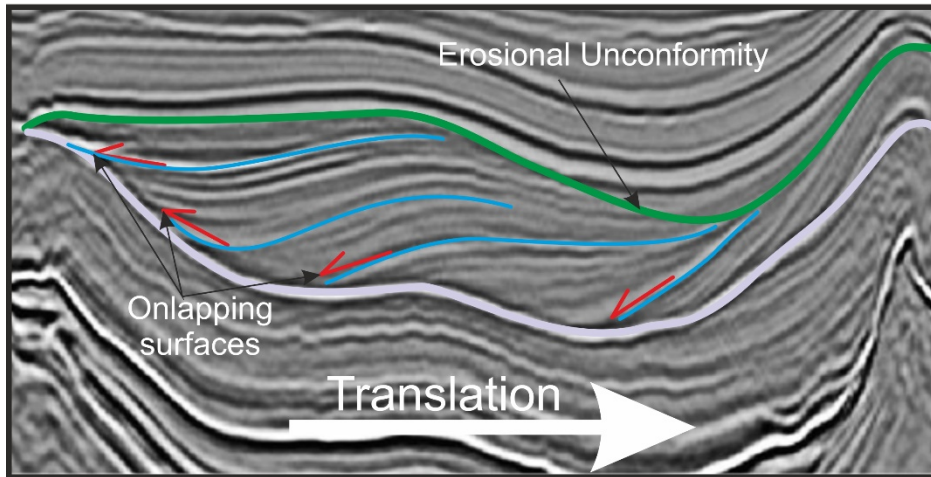


Figure 2.16 Interpreted seismic section of a Salt-Detached Ramp Syncline Basin, modified from (Pichel, et al., 2018) showing many features that Onlapse-2D would be unable to model. The large horizontal component of structural movement (white arrow) and major erosion unconformity would preclude this type of basin from being accurately modelled.

2.6 Conclusions

Onlapse-2D is a two-dimensional geometric based stratigraphic forward modelling program. It is designed as an analytical tool to aid in the exploration of hydrocarbons through the prediction of reservoir and seal distribution in deep-water sedimentary successions where data constraint and quality is poor.

Using only four input parameters, *Onlapse-2D* can successfully simulate the tectonostratigraphic evolution of idealized mini-basins and produce geologically realistic cross sections.

Onlapse-2D has successfully modelled the complex geometries of a real mini-basin in the Gulf of Mexico and it can be used to identify extrinsic autocyclic events that have a significant impact on the formation of basin stratigraphy through what we term, informative discrepancies.

Because each model is easy to set up and rapid to compute, it is possible to create a large number of simulations that can be used to explore the range of possible alternative geological scenarios for a single set of data, allowing the uncertainty of interpretation of a set of subsurface data to be visualized and quantified.

The software can also be used to create a suite of simulations of deep-water sediment architecture for different geological scenarios, .e.g. for research or testing purposes.

2.7 Appendix

Found in Appendix A is the inputs parameters for the Hypothetical Basins, as well as for Run 26 of Symb1 and Run 39 of Symb1. In supplementary material A is an excel spreadsheet that contains the input parameters for multiple iterations of Symb1.

Chapter 3 Conditions favouring Onlap and Offlap: Why are onlaps common, and offlaps rare?

Donald N Christie ¹, Frank J Peel ², Gillian M Apps ² and Esther J Sumner¹

¹ Ocean and Earth Science, University of Southampton, Southampton, United Kingdom

² Bureau of Economic Geology, Jackson School of Geosciences, The University of Texas at Austin, University Station, Austin, Texas, United States

Prepared for submission to GSA Bulletin

3.1 Abstract:

It is widely acknowledged that the sediment fill of deep-water mini-basins shows abundant onlapping units, while offlapping units are relatively uncommon; however, there has been no satisfactory explanation of this imbalance. We used simple forward modelling to create 180 simulations of the stratigraphy of structurally active mini-basins, each using different histories of structure growth and sediment supply. These models show an imbalance between offlap and onlap similar to that seen in nature. Our analysis suggests that development of an onlap-biased depositional stratigraphy may be the natural consequence of basin-fill processes in structurally active basins; the imbalance does not require any forcing asymmetry or imbalance in the controlling processes. In our models, inputs with a symmetrical pattern (e.g. sinusoidal variation of structure growth) create asymmetrical output (onlap-biased stratigraphy). In structurally active mini-basins, the development of onlap and offlap may be linked to local sediment supply in some cases, but in others such a link may be weak, out-of phase, or even non-existent. Thus there is no requirement for the patterns of onlap or offlap in deep-water mini-basins to have any link to extrinsic processes such as sea level change.

3.2 Introduction:

3.2.1 Why are Onlap and Offlap important in deep-water stratigraphy?

Bed terminations by onlap or offlap are important components of stratigraphic architecture. Such terminations may stack to create onlap and offlap surfaces, which are considered to be critical parts of sequence stratigraphy. However, the processes that generate these important surfaces in deep-water stratigraphy have received little attention, and fundamental questions remain: are deep-water onlap and offlap surfaces diagnostically related to sea level changes or can they be generated entirely by other, more local processes? Why is it that deep-water onlapping surfaces are a commonly observed feature but offlapping surfaces appear to be much less common? In this paper, we use a simple forward modelling technique to study the origins of onlap and offlap, and to address some of these outstanding questions.

Over recent years, stratigraphic traps in deep-water sedimentary successions have become an increasingly important focus for Hydrocarbon exploration. Stratigraphic trap components such as depositional onlap or offlap edges typically carry higher risk and uncertainty, and may be harder to define, than structural components (Allan, et al., 2006), so it is important to recognize the stratal geometries of onlap and offlap, and understand how they form. Better understanding of onlap and offlap edges can assist in identifying new stratigraphic trap prospects (Amy, 2019) and in risk estimation. This is because the principal risk factors are commonly the presence of a continuous trapping geometry and an effective seal along the length of the stratigraphic termination (Stirling, et al., 2018).

Sequestration of carbon dioxide in depleted oil and gas fields, or in previously uncharged structural and stratigraphic traps, is being explored as a means to mitigate anthropogenic CO₂ emissions. The previous containment of hydrocarbons within depleted fields demonstrates the integrity of the container, significantly reducing (while not eliminating) the risk of geological leakage of CO₂ (Szulczewski, et al., 2013). However, if previously uncharged structures without this evidence of prior container integrity are evaluated for CO₂ sequestration, it is vital to have a full understanding of all seal and trap components, especially of any stratigraphic trap components. Developing a better understanding of the origin of onlap and offlap may therefore be of value in our quest for CO₂ sequestration targets.

3.2.2 What are Onlap and Offlap?

The concepts of onlap and offlap were first introduced in the 1940s (Melton, 1947) (Lovely, 1948) (Swain, 1949) and further refinement occurring in the next several decades (Mitchum, 1977) (Mitchum, et al., 1977) (Christie-Blick, 1991) (Cartwright, et al., 1993).

We define onlap as the lateral termination of a bed against a surface of greater inclination. An onlapping interval is one in which the onlap point of each successive deposit progresses up-dip on the basin flank. An offlapping interval is one in which the onlap point of each successive deposit progresses down-dip towards the basin centre (Christie, et al., 2021) (Figure 3.1). The bounding surface that contains the individual bed terminations is an onlap surface (in an onlapping interval) or an offlap surface (in an offlapping interval). As demonstrated by Smith and Joseph (2004) and illustrated in Figure 3.1, these bounding surfaces may not correspond to classic unconformities, because each bed termination may be separated from the next by a layer of background sediment.

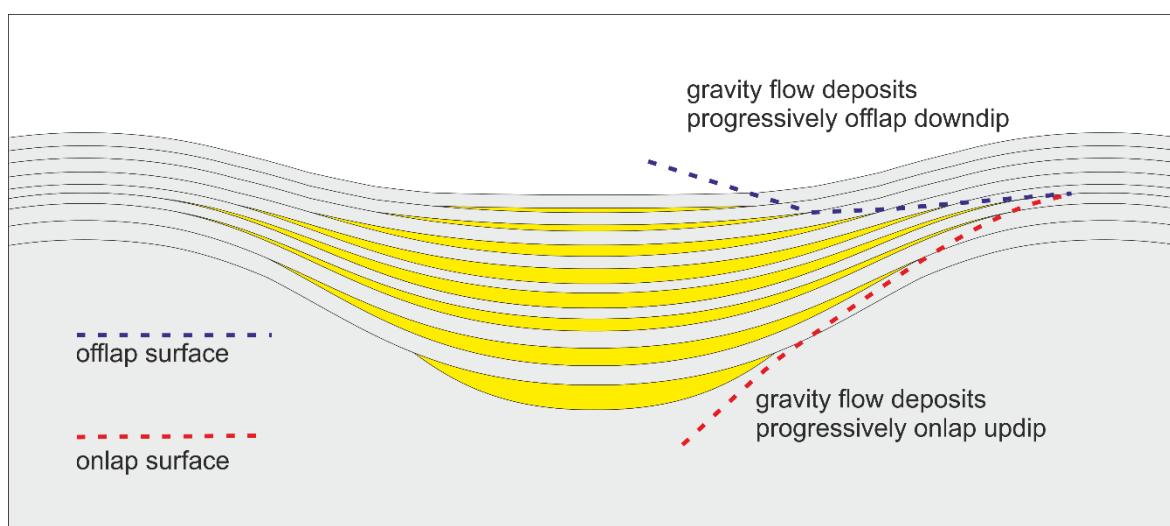


Figure 3.1 Onlapping interval where each successive stratal termination progresses up-dip towards the basin edge. The offlapping interval shows each progressive stratal termination progressing down-dip away from the basin edge.

If the bed terminations were to lie vertically above the terminations of these underlying beds, the interval would be neither onlapping nor offlapping, and we have termed this scenario as “static pinchout”. While we have never observed such a scenario in natural examples, apparent static pinchout is seen in some forward models due to limitations of spatial resolution (terminations fall within the same column of computational cells). The majority of existing publications relate the development of onlap and offlap to changes in relative sea-level (Christie-Blick, 1991), (Pomar & Ward, 1994), (Catuneanu, 2006) (Catuneanu, et al., 2009), (Catuneanu, et al., 2011) (Zhang, et al.,

2018). Catuneanu (2019) specifically related offlap to lowering of relative sea-level, and considers it diagnostic of forced regression. However, this relationship is based predominantly on the shallow parts of the sediment systems tract (shelf to upper slope and terrestrial) and we suggest that it may not apply the deeper part of the systems tract. Comparatively little work has been published investigating the development of offlap and onlap in deep-water sedimentary systems, with the noticeable exception of numerical forward modelling performed by Sylvester et al (2015).

In deep-water sedimentary systems there are multiple allogenic and autogenic factors that influence development of the sedimentary systems, including local & regional tectonics, sedimentary transport dynamics, shelf morphology, and climate. These factors can negate or overwhelm the effect of relative sea-level change on the rate of delivery of clastic sediments into the deep-water (Kneller, 2003) (Brunt, et al., 2004) (Carvajal, et al., 2009) (Dixon, et al., 2012) (Bourget, et al., 2014) (Liu, et al., 2016) (Harris, et al., 2018). This would suggest that the development of onlap and offlap geometries in deep-water systems may be controlled by other local factors, rather than relative sea-level changes.

3.2.3 Why does Onlap dominate over Offlap?

The statistical dominance of onlap over offlap in sedimentary successions is well-documented (Christie-Blick, 1991), (Sylvester, et al., 2015), (Catuneanu, 2019), (Yu, et al., 2021). Seismic data indicates that is a near-universal characteristic of deep-water sedimentation. Figure 3.2 shows a typical deep-water mini-basin, for which our interpretation (Figure 3.2a) shows multiple major onlap surfaces compared to one minor offlap surface. Inspection of all images of deep-water mini-basins from around the world in Jackson and Hudec (2017) reveals onlap surfaces in every section, while offlap surfaces are rare or absent.

Stratal architecture dominated by offlap is seen only in two specific deep-water settings, both involving high lateral displacements: i) the upper boundary of the growth package in salt-detached ramp syncline basins (Pichel, et al., 2018) and ii) above footwall ramps in trust-sheet-top basins (Corredor, et al., 2005).

The reason for the dominance of onlap is not intuitively obvious, as stratigraphic cycles which contain controlling processes that are both symmetrical and asymmetrical (Sharman, et al., 2019) (Catuneanu, 2019), one may expect to see as much a record of the waning phase as the waxing phase, but this is not the case. Numerical modelling that investigated the formation of stratigraphic sequences in intraslope deep-water mini-basins performed by Sylvester et al (2015) indicates that the development of offlap is tied to the rate of sediment input into the basin.

There, Sylvester et al (2015) showed even symmetrical cycles of increasing to decreasing sediment supply resulted in stratigraphic sequences with the familiar saw-tooth geometry of onlap dominated base and offlapping surfaces on the top, but this was not the case if sediment varied in an on-off pattern. This modelling showed that subsidence rates that vary through time coupled with constant sediment input can result in the development of both onlap and offlap. Our own observations also suggest that onlap tends to occur as the rate of growth of underlying structures decelerates, while offlap tends to form as structure growth accelerates. The statistical imbalance of onlap vs. offlap might therefore result from a global tendency for asymmetric structural history, with slow structural deceleration, coupled with rapid acceleration. However, we are unaware of any evidence for this temporal asymmetry.

An alternative possible hypothesis for the apparent dominance of onlap over offlap in natural examples might be that it might be an observational effect. If overlapping units tend to be thicker than offlapping units, is it possible that they exist in equal numbers, but we see fewer offlaps because the offlapping layers are thin and therefore not seismically resolved?

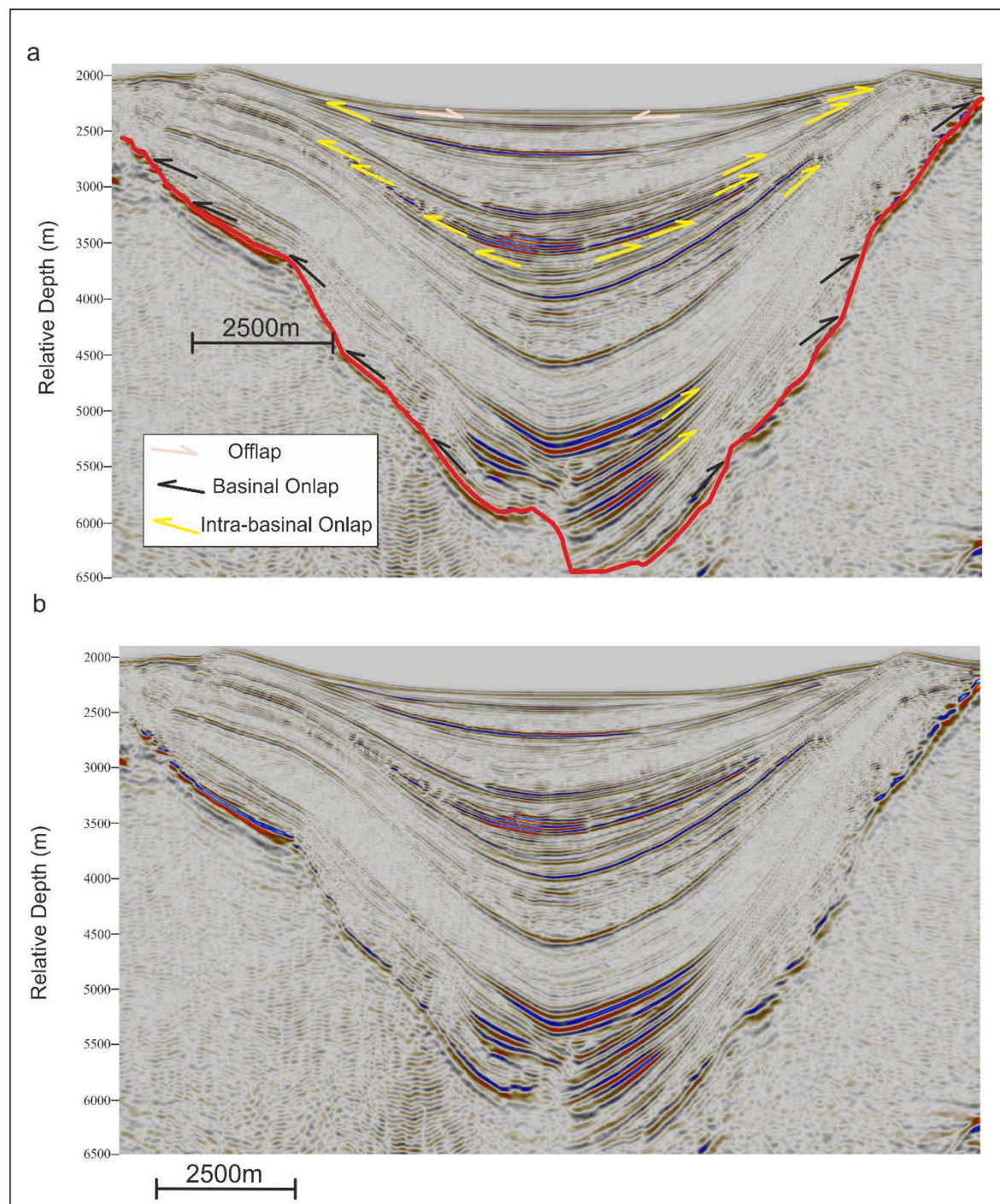


Figure 3.2 a) typical deep-water mini-basin demonstrating the apparent domination of onlap stratal terminations over offlap. b) uninterpreted seismic of Figure3.2a

3.2.4 Aims

The aim of this paper is to investigate how the interaction of sedimentation and accommodation control the development of onlap and offlap in deep-water sedimentary systems, and to explain the relative rarity of offlap surfaces in deep-water sediments.

To do this we used the *Onlapse-2D* forward modelling software, (Christie, et al., 2021), to generate a suite of 180 synthetic deep-water basin models, using a range of input parameters.

The simplicity of *Onlapse-2D* allows for a large number of simulations to be rapidly computed as a sensitivity study to investigate the development of onlap and offlap in deep-water sedimentary systems, and their dependence on the controlling factors.

As discussed above, one possible explanation of the observed dominance of onlap compared to offlap might require some global asymmetry in rates of sediment supply or structure growth rate (gradual waxing vs. rapid waning of sediment supply; slow deceleration vs. rapid acceleration of structure growth). In order to investigate whether this is a necessary condition for the imbalance, we created stratal simulations using inputs that have no such imposed asymmetry, for example as shown in Figure 3.3, with rates of structure growth and sediment supply represented by sinusoidal curves for which the duration of increase is equal to, and mirrored by, the duration of decrease. We sought to determine whether such perfectly symmetrical input curves could generate an asymmetrical output, with dominant onlap.

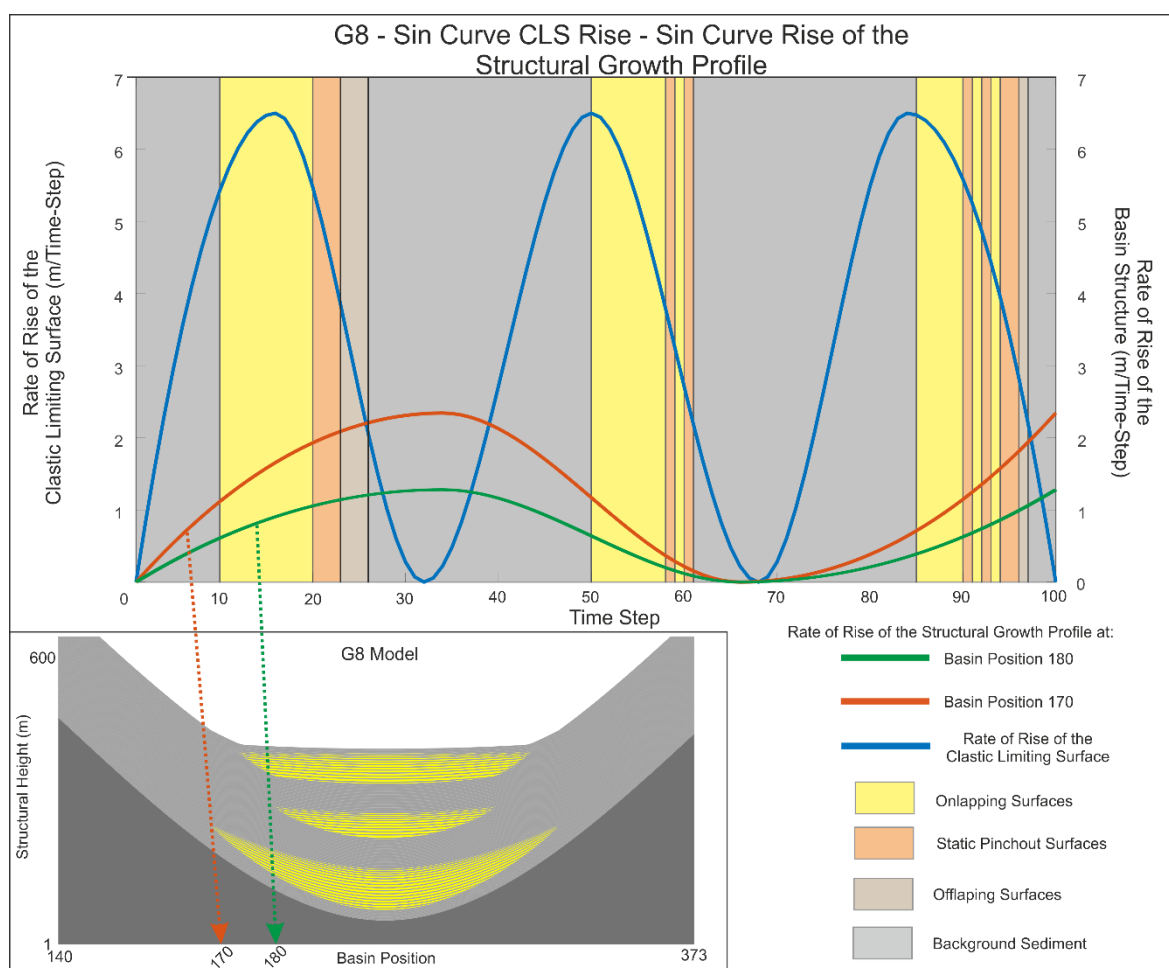


Figure 3.3 Example of basin simulation, corresponding to model G8. Fig. 3a, input parameters used for this model, 1 Time-Step equals 10ky; Fig 3b, output simulation. Onlap is able to form when both the rate of rise of

the Clastic Limiting Surface and the Structural Growth Profile are increasing and decreasing. Offlap forms only when the rate of rise of the Clastic Limiting Surface is decreasing.

3.3 Method

3.3.1 What is *Onlapse-2D*?

Onlapse-2D is a stratigraphic forward modelling program that simulates the structural and stratigraphic development of deep-water mini-basins (Christie, et al., 2021)(Chapter 2). It uses four inputs; Initial Basin Structure (the starting bathymetry), Structural Growth Profile and Rise (which control the structural development of the model), Background Sedimentation (both pelagic and hemi-pelagic), and a variable rate of rise of a Clastic Limiting Surface (which controls clastic sediment deposition within the mini-basin). *Onlapse-2D* combines these inputs using simple rules to generate realistic looking basin architectures. The software, input parameters, and computational logic are described in Christie et al. (2021). *Onlapse-2D* was principally developed as an aid to seismic interpretation and subsurface prediction in regions of limited data quality, using a process of iteration to create an output simulation model that is a detailed match to the equivalent real-world section. The final product of this process is a synthetic section that is geologically realistic, with fine-grain vertical variation in the thickness of stratigraphic units (Christie, et al., 2021), Thesis Chapters 2 and 4). This study uses a different approach, in which the software is used to generate synthetic sections that explore the stratigraphic effect of combining different types of input parameters, rather than to replicate natural examples or to produce geometries that are in every case realistic in appearance.

3.3.2 Initial Basin set up:

Each run of the sensitivity test begins with the same simple symmetrical shaped basin, and we applied a variety of different rates of rise to the structural growth profile (also a symmetrical bowl shaped profile). We applied a variety of different rates of rise to the clastic limiting surface. The geological explanation for these variations will be explained below. We applied these different growth rates to both the structural growth profile and the clastic limiting surface in order to explore:

- a) Whether the basic model could produce onlapping and offlapping geometries;
- b) What proportion of basic models contain any representation of offlap geometry;
- c) Does increasing or decreasing the structural growth profile rate and rate of rise of the clastic limiting surface effect the development of offlap;

- d) How volumetrically significant the offlap section is in the models that do produce some offlapping geometry;
- e) Whether any basic principles could be extracted from this to explain the apparent dominance of onlap and scarcity of offlap in real-world examples.

3.3.3 What we varied:

Observation of real-world examples shows that there is an imbalance between the prevalence of onlap and offlap in nature. This study explores possible reasons for this imbalance through forward modelling. We simulated the development and infill of a simple symmetrical mini-basin using *Onlapse-2D* in order to investigate possible controls on the frequency of different types of stratal termination (onlap, offlap, static pinchout).

To this aim, we created a suite of 180 different models of synkinematic sedimentation, in which synthetic basin-fill stratigraphy was generated by combining a range of independent variables (Table 2). The input factors were varied as follows:

Structural Growth Rate: Four simple patterns for the variation of structural activity through time were considered – constant rate through time; two variants of pulsed structure growth, represented by sinusoidal variation with time; the rate uniformly increasing with time. These four types were applied at three overall rates: Low/Slow (0.075 mm/yr), Medium (1.5 mm/yr), and High/Fast (2.25 mm/yr) to create 12 different Structural Growth Rate inputs.

Rate of Rise of the Clastic Limiting Surface: Five simple patterns of the Clastic Limiting Surface Rise through time were considered: Uniform rate of rise through time; four different types of pulsed growth, comprising two sinusoidal variants and two bimodal (square wave) variants. These five types were applied at three overall rates: Low/Slow (0.55 mm/yr), Medium (0.65 mm/yr), and High/Fast (0.8 mm/yr). This created 15 different Clastic Limiting Surface rise inputs.

The form of the Structural Growth Rate and Clastic Limiting Surface curves that were used are shown in Table 2. These were combined to create 180 different simulations, each with different stratal architecture, and each showing different patterns and amounts of onlap and offlap.

Input factors that were common to all 180 models were the Background Sedimentation Rate (uniform through time in all models), and the shape of the growing structure (a symmetrical mini-basin between two growing highs in all models). Our experience with *Onlapse-2D* simulations shows that while these factors may change the bed thickness or spatial location of onlaps and offlaps, they tend not to change the temporal distribution of onlaps and offlaps.

These combinations are intended to create a representative range of stratal patterns, rather than to create simulations that represent any particular natural example, so the input Clastic Limiting Surface and Structural Growth Rate variations are in the form of idealized curves and do not attempt to match any real-world location. The numbers shown here represent realistic orders of magnitudes for both growth of structure and sediment input rates in deep-water sedimentary systems. Jackson and Hudec (2017) show that the rate of rise of buried salt diapirs can range from 0.0008mm/yr – 4 mm/yr, and Suppe et al (1992) calculates that folding rates range from 1 – 2 mm/yr from examples including in the Gulf of Mexico, the Philippines, and Venezuela. Within the Sureste Basin of Mexico, sediment accumulation rates of Neogene sediments varies widely as well, with the mean accumulation rate between 0.16mm/yr – 4.5mm/yr (Gómez-Cabrera & Jackson, 2009).

However, each of these represents a geologically plausible scenario, for example pulsed structural growth is seen in some gravity-driven deep-water fold belts (e.g. (Corredor, et al., 2005)); and accelerating structural growth is seen in density-driven salt-withdrawal basins (e.g. (Jackson & Hudec, 2017)). For the Clastic Limiting Surface curves, a binary variation (square wave) might represent the effects of updip avulsion or lobe switching, and a sinusoidal variation might represent gradually changing processes such as climate. We appreciate that a multitude of real-world scenarios exist between these end-members.

3.4 Results:

3.4.1 Model Observations:

The initial campaign of forward modelling described above created a suite of 180 models of simulated basin-fill stratigraphy, each with a different geometry, different arrangement of gravity flow deposit packages, and displayed onlap and offlap onto the basin flanks. Examples of these simulations are shown in Figure 3.3, 3.4, & 3.5.

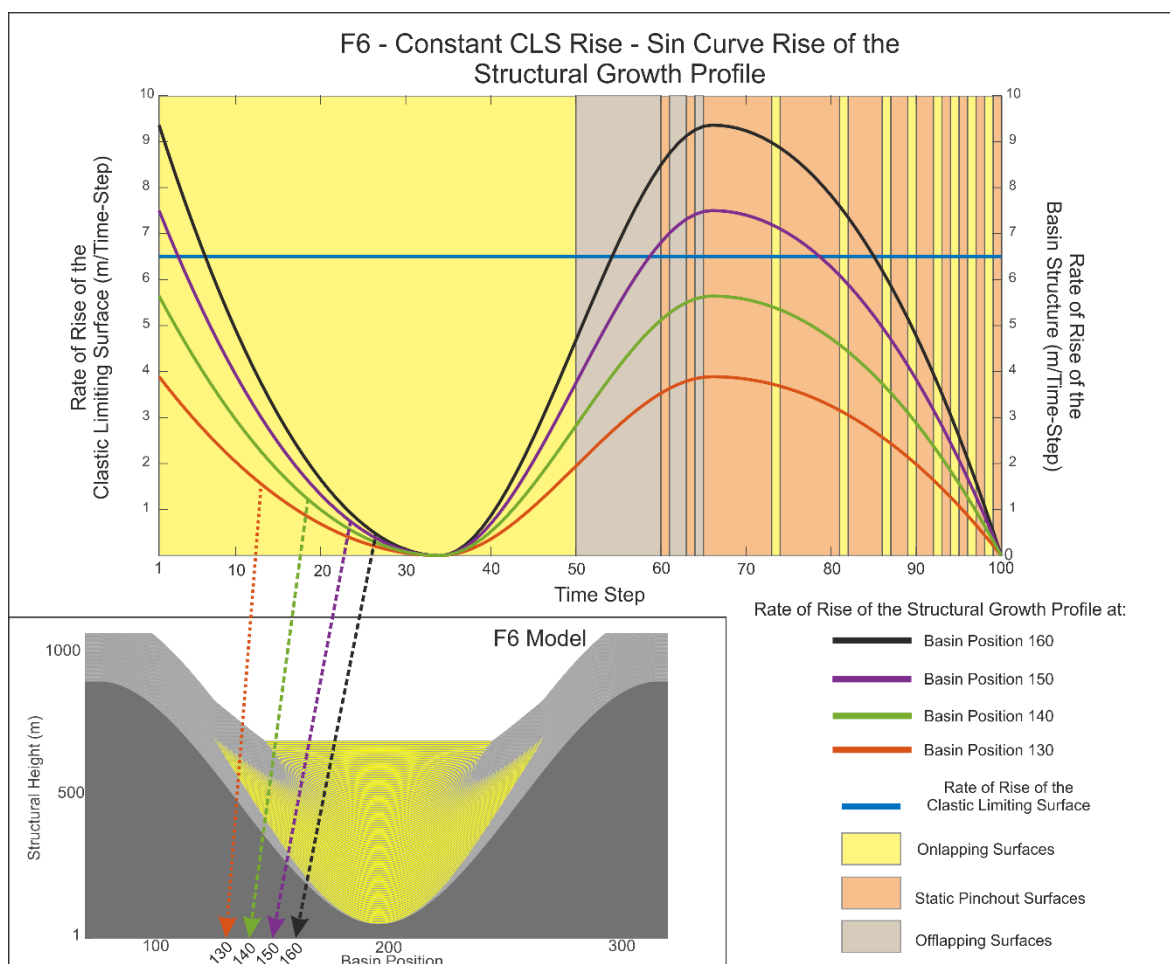


Figure 3.4 Example of basin simulation, corresponding to model F6. Fig 3.4a, input parameters used for this model; Fig 3.4b, output simulation. See text for discussion of highlighted points.

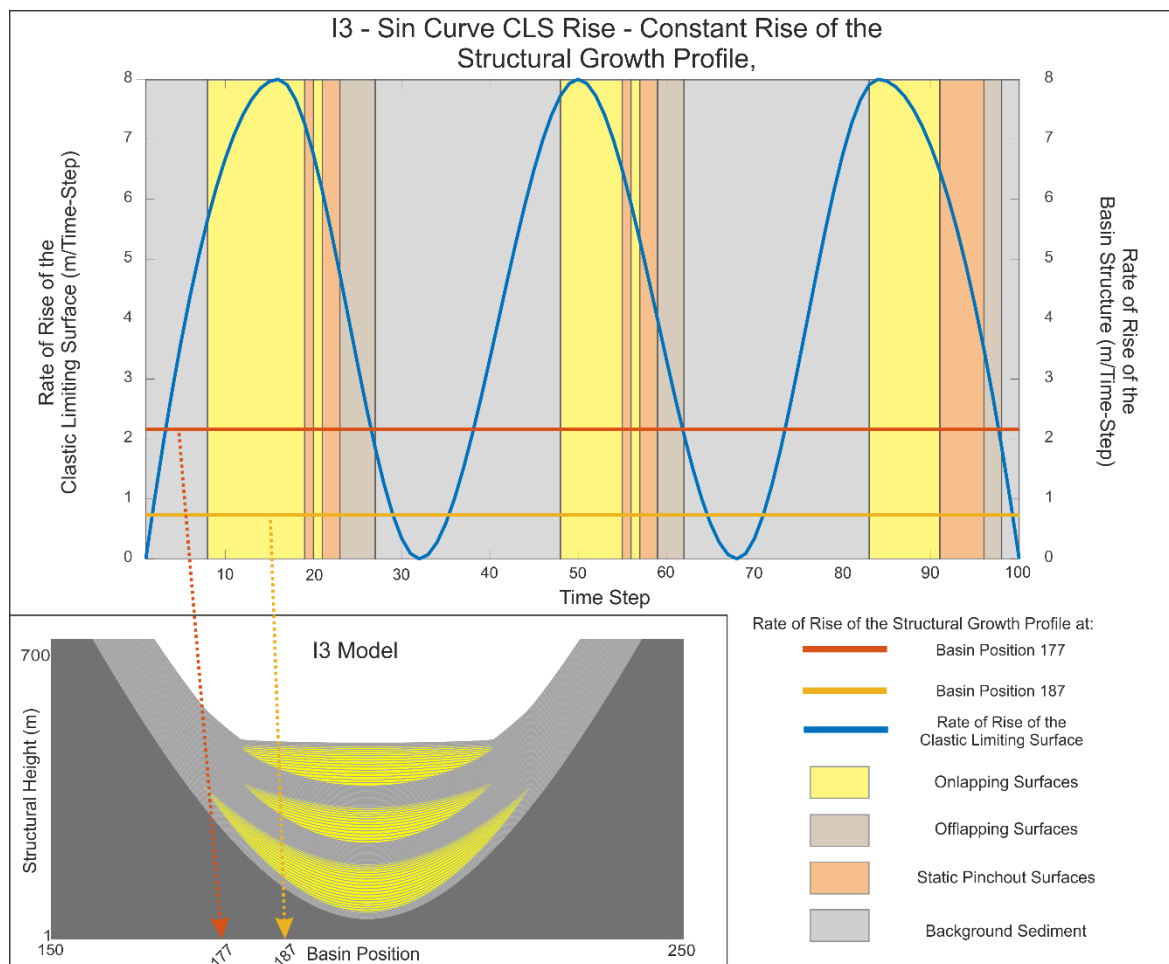


Figure 3.5 Example of basin simulation, corresponding to model I3. Fig 5.5a, input parameters used for this model; Fig 5.5b, output simulation. See text for discussion of highlighted points.

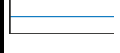
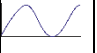


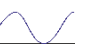
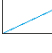

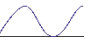








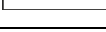

3.4.2 Prevalence of onlap, offlap, and static pinchout:

3.4.2.1 Analysis by population size:

For each of the 180 models, stratal geometries were analysed by counting the number of bed terminations of each type (onlap, offlap, and static pinchout), the results of this count are shown in three tables. Table 2 shows the proportion of gravity flow deposit packages which terminate in offlap for each simulation; Table 3 shows the proportion of gravity flow deposit packages which terminate in onlap for each simulation; Table 4 shows the ratio of offlap to onlap terminations, Figure 3.6 shows the histogram of this result.

Overall, onlap terminations were significantly more common than offlap (88% onlap, 7% offlap, 5% static pinchout). Onlaps were seen in every model output, only 54% of models contained offlap terminations. The dominance of onlap over offlap corresponds to observed natural examples.

Percentage of clastic intervals showing offlap

Percentage of clastic intervals showing offlap				Structural Growth Rate												
				Low				Medium				High				
				Constant	Sine D	Sine I	Inc	Constant	Sine D	Sine I	Inc	Constant	Sine D	Sine I	Inc	
																
				A	B	C	D	E	F	G	H	I	J	K	L	
Rate of Rise of the Clastic Limiting Surface	High	Constant		1	0%	10%	4%	11%	0%	15%	15%	9%	0%	15%	20%	9%
		Sine - D		2	14%	14%	9%	14%	17%	14%	11%	14%	17%	17%	11%	20%
		Sine - I		3	16%	14%	12%	18%	18%	16%	16%	18%	18%	16%	18%	20%
		Binary - On		4	0%	0%	0%	0%	0%	0%	12%	0%	0%	0%	18%	0%
		Binary - Off		5	0%	0%	0%	0%	0%	0%	0%	0%	0%	0%	0%	0%
	Medium	Constant		6	0%	13%	7%	7%	0%	13%	14%	8%	0%	15%	17%	7%
		Sine - D		7	12%	15%	4%	8%	12%	15%	8%	12%	15%	15%	8%	12%
		Sine - I		8	12%	7%	12%	14%	12%	12%	14%	17%	12%	14%	14%	17%
		Binary - On		9	0%	0%	0%	0%	0%	0%	11%	0%	0%	0%	14%	0%
		Binary - Off		10	0%	0%	0%	0%	0%	0%	0%	0%	0%	0%	0%	0%
	Low	Constant		11	0%	13%	7%	5%	0%	12%	13%	6%	0%	13%	15%	6%
		Sine - D		12	0%	0%	0%	0%	6%	6%	0%	0%	6%	13%	0%	6%
		Sine - I		13	10%	6%	10%	6%	10%	6%	13%	13%	10%	6%	13%	10%



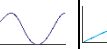

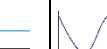
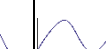
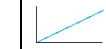


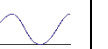
















Clastic Limiting Surface	LOW	Structural Growth Rate													
		Percentage of Clastic intervals showing offlap cont	Low				Medium				High				
			Constant	Sine D	Sine I	Inc	Constant	Sine D	Sine I	Inc	Constant	Sine D	Sine I	Inc	
															
			A	B	C	D	E	F	G	H	I	J	K	L	
		Binary – On 		14	0%	0%	0%	0%	0%	9%	0%	0%	0%	13%	0%
		Binary – Off 		15	0%	0%	0%	0%	0%	0%	0%	0%	0%	0%	0%

Table 2 Shows the results of modelling 180 different combinations of clastic limiting surface rise and structural growth profiles. The colour of the cells represent either the lack of (red) or relative amount of offlapping surfaces (orange – green) modelled to develop. Percentages in those cells represent the total percentage of clastic beds that terminate in an offlapping manner. While a red cell indicates that no offlap is found, it does not necessarily mean that only onlap stratal terminations are produced, as static pinchout terminations may also develop.

**Percentage of
clastic intervals
showing onlap**

Structural Growth Rate

Rate of Rise of the Clastic Limiting Surface	High	Constant		1	36%	55%	49%	43%	21%	57%	39%	24%	15%	52%	30%	18%
		Sine - D		2	63%	80%	71%	71%	63%	69%	69%	66%	60%	66%	66%	66%
		Sine - I		3	73%	76%	76%	75%	67%	69%	65%	69%	61%	67%	61%	67%
		Binary – On		4	85%	97%	85%	95%	63%	88%	65%	73%	50%	83%	57%	60%
		Binary – Off		5	85%	100%	89%	96%	72%	94%	65%	76%	65%	87%	56%	69%
	Medium	Constant		6	30%	64%	55%	35%	19%	54%	33%	22%	14%	43%	26%	17%
		Sine - D		7	69%	73%	77%	73%	62%	69%	69%	73%	58%	65%	62%	65%
		Sine - I		8	79%	74%	76%	76%	62%	69%	67%	69%	62%	67%	60%	67%
		Binary – On		9	77%	95%	77%	86%	58%	88%	63%	67%	49%	79%	56%	56%
		Binary – Off		10	83%	100%	77%	92%	69%	90%	56%	73%	60%	81%	50%	67%
	Low	Constant		11	27%	59%	42%	31%	17%	47%	28%	19%	12%	38%	22%	15%
		Sine - D		12	69%	69%	88%	81%	69%	69%	69%	75%	63%	44%	69%	75%
		Sine - I		13	71%	77%	77%	77%	65%	74%	68%	71%	65%	71%	65%	81%



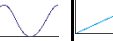

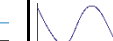

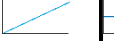


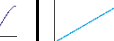














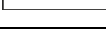

Clastic Limiting Surface	Low	Structural Growth Rate													
		Percentage of Clastic intervals showing onlap cont	Low				Medium				High				
			Constant	Sine D	Sine I	Inc	Constant	Sine D	Sine I	Inc	Constant	Sine D	Sine I	Inc	
															
			A	B	C	D	E	F	G	H	I	J	K	L	
		Binary – On 	14	72%	96%	72%	83%	55%	87%	60%	62%	43%	72%	53%	51%
		Binary – Off 	15	83%	100%	73%	78%	71%	93%	54%	73%	59%	80%	49%	66%

Table 3 Shows the results of modelling 180 different combinations of clastic limiting surface rise and structural growth profiles. The percentages in each cell represent the number of beds that terminate in an onlapping manner.

Offlap / Onlap

Ratio

Structural Growth Rate

Rate of Rise of the Clastic Limiting Surface																	
	High	Constant		1	0	0.18	0.08	0.26	0	0.26	0.38	0.38	0	0.29	0.67	0.5	
		Sine - D		2	0.22	0.18	0.13	0.2	0.27	0.2	0.16	0.21	0.28	0.26	0.17	0.3	
		Sine - I		3	0.22	0.18	0.16	0.24	0.27	0.23	0.25	0.26	0.3	0.24	0.3	0.3	
		Binary - On		4	0	0	0	0	0	0	0.18	0	0	0	0	0.32	0
		Binary - Off		5	0	0	0	0	0	0	0	0	0	0	0	0	0
	Medium	Constant		6	0	0.2	0.13	0.2	0	0.24	0.42	0.36	0	0.35	0.65	0.41	
		Sine - D		7	0.17	0.21	0.05	0.11	0.19	0.22	0.12	0.16	0.26	0.23	0.13	0.18	
		Sine - I		8	0.15	0.09	0.16	0.18	0.19	0.17	0.21	0.25	0.19	0.21	0.23	0.25	
		Binary - On		9	0	0	0	0	0	0	0.17	0	0	0	0	0.25	0
		Binary - Off		10	0	0	0	0	0	0	0	0	0	0	0	0	0
	Low	Constant		11	0	0.22	0.17	0.16	0	0.26	0.46	0.32	0	0.34	0.68	0.4	
		Sine - D		12	0	0	0	0	0.09	0.09	0	0	0.1	0.3	0	0.08	
		Sine - I		13	0.14	0.08	0.13	0.08	0.15	0.08	0.19	0.18	0.15	0.08	0.2	0.12	














Clastic Limiting Surface	Low	Structural Growth Rate												
		Offlap / Onlap Ratio cont.	Low				Medium				High			
			Constant	Sine D	Sine I	Inc	Constant	Sine D	Sine I	Inc	Constant	Sine D	Sine I	Inc
														
			A	B	C	D	E	F	G	H	I	J	K	L
			Binary – On 	14	0	0	0	0	0	0.15	0	0	0	0.25
		Binary – Off 	15	0	0	0	0	0	0	0	0	0	0	0

Table 4 Shows the ratio of Onlap:Offlap in terms of number of beds from 180 different combinations of clastic limiting surface rise and structural growth profiles.

3.4.2.2 Analysis by Area:

The apparent visual dominance of any stratigraphic component seen in a cross section depends not only on its frequency of occurrence, but also on the relative area of sediment within which that component is expressed. A property that is expressed in thick and/or aerially extensive beds may seem more significant than another property that is only expressed in thin and/or less extensive beds, even if the number of beds displaying each property is the same.

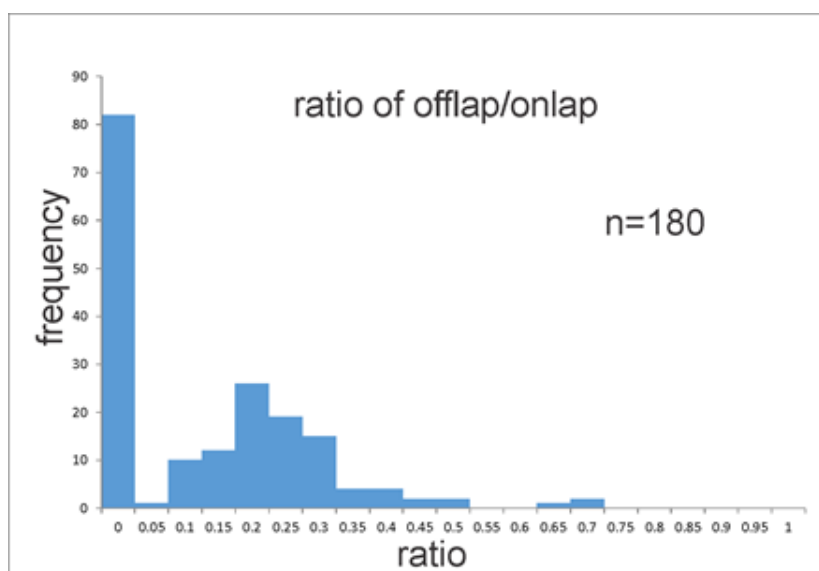


Figure 3.6 Histogram of the ratio of the number of intervals displaying offlap/onlap in the 180 base case simulation models

A key question in this study is the volumetric significance of offlapping units compared to onlapping units; if a greater proportion of offlapping units are too thin to be seismically resolved, this effect might contribute to the apparent dominance of onlap over offlap on seismic data.

To investigate this, we also examined the volumetric expression of beds with a particular pinchout type. The models produced here are two-dimensional, so we examined the area occupied by gravity flow deposit packages that terminate in onlap vs. offlap vs. static pinchout. We measured the cross-sectional area of the onlapping and offlapping units within a subset of 27 *Onlapse-2D* models. A cross-plot of the measured proportion of offlapping gravity flow deposit packages by number with the percentage by area demonstrates significant areal bias (Figure 3.7). In each model within the set the offlapping units have a lower proportion by area than by number. Simulations in which the rate of rise of the Clastic Limiting Surface was the sole controlling factor in the development of offlap represent 2% of the total area, with a range of 1% - 4%. Simulations in which both structural growth and sediment flux contribute to the formation of offlap show an average of 4% of the total area, with a range of 2% - 6%. Simulations in which the rate of rise of the Structural Growth Profile was the sole controlling factor in the development of offlap show a

marked increase in % area taken up by offlap, with an average of 11%, and a range of 7% - 13%. The mean proportion of offlapping units was 14% by population number compared to 6% by area.

Visual inspection of output models confirms that offlapping gravity flow deposit packages tend to be both thinner and less extensive than equivalent onlapping gravity flow deposit packages. This observation is consistent with real-world stratigraphy seen on seismic reflection data (Figure 3.2).

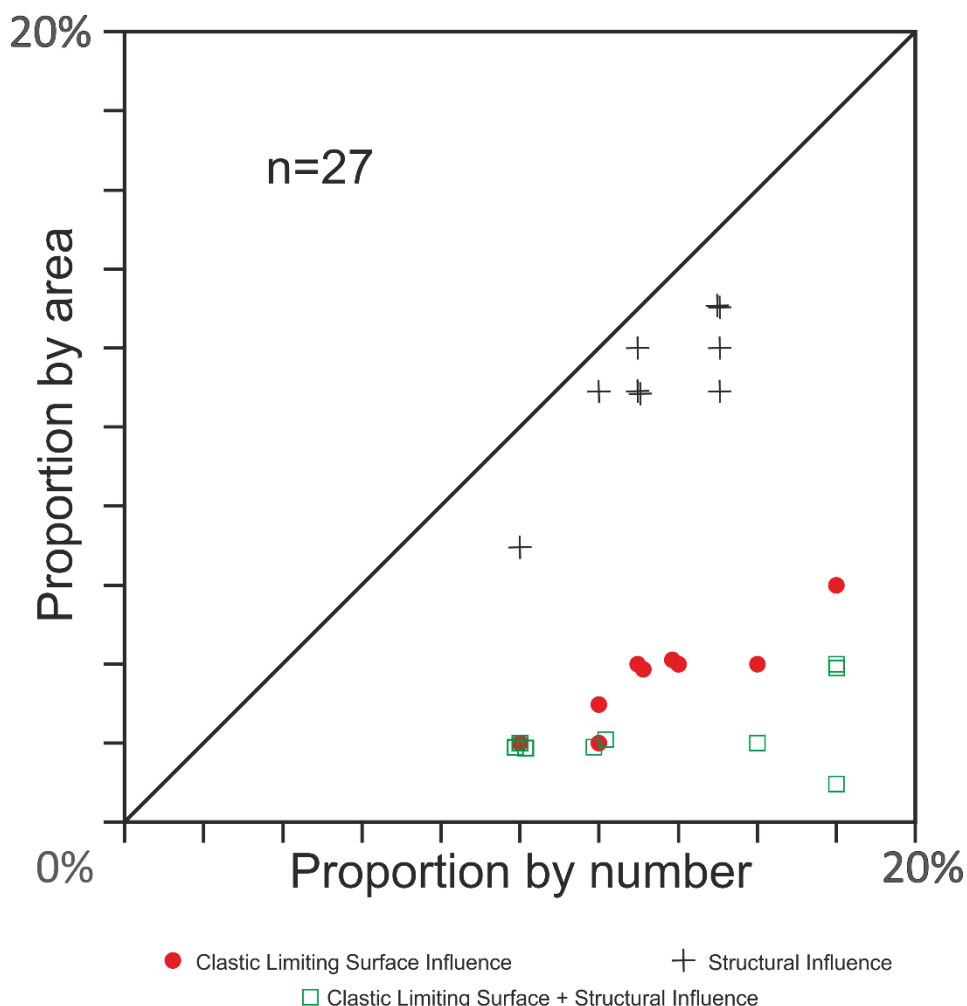


Figure 3.7 Comparison of the proportion of offlapping gravity flow deposit packages by number against the proportion by cross-sectional area.

3.4.2.3 Does changing the rate of rise of the Clastic Limiting Surface or Structural Growth Profile effect the development of offlap?

A key aim of this study is to investigate if the development of onlap or offlap corresponds to changes in rate of rise of the Structural Growth Profile or the Clastic Limiting Surface. For example, do times of onlap correspond to times of increasing rate of rise of the Clastic Limiting Surface (as a proxy for sediment supply), or times of decreasing rate of rise of the Structural Growth Profile. Figures 3.3, 3.4, and 3.5 illustrate how we investigate this, dividing the total time

duration of each output model into times of different stratal termination style; onlap, static pinchout, offlap, and non-deposition of gravity flow deposit packages.

The history of each model can also be divided into times when the rate of rise of the Structural Growth Profile or Clastic Limiting Surface was accelerating or decelerating. This was then compared with the style of stratal termination at each Time-Step. It is readily apparent that periods of onlap (yellow bands) occur in all phases; onlap may be developed as the rate of rise of the Clastic Limiting Surface is accelerating or decelerating. Onlap may also be developed as the rate of rise of the Structural Growth Profile is accelerating or decelerating. In contrast, offlap is only observed when the rate of rise of the Clastic Limiting Surface is decreasing or constant and/or the rate of rise of the Structural Growth Profile is increasing or constant.

3.4.2.4 Analysis by Numbers:

The magnitude (Low, Medium, or High) of the rate of rise of the Clastic Limiting Surface or Structural Growth Profile has an impact on the presence and prevalence of offlap. The most offlap is produced when both rates of rise of the Clastic Limiting Surface and Structural Growth Profile are “High”, and the least offlap is produced when both rates of rise are “Low”. Intermediate rates of rise produce intermediate amounts of offlap. See Appendix B for inputs used in models.

3.4.3 Sensitivity of model results to temporal and spatial resolutions:

The category of “static pinchout”, where a gravity flow deposit package termination lies precisely above the termination of the underlying package, is observed both in our forward models and by Sylvester et al (2015) who call term it “convergence”. This is an artefact of spatial resolution within the models; apparent static pinchout occurs when the stratal terminations fall within the same column of computational cells. Increasing the lateral resolution of a model enables the apparent static pinchouts to be identified as either onlap or offlap (Figure 3.8).

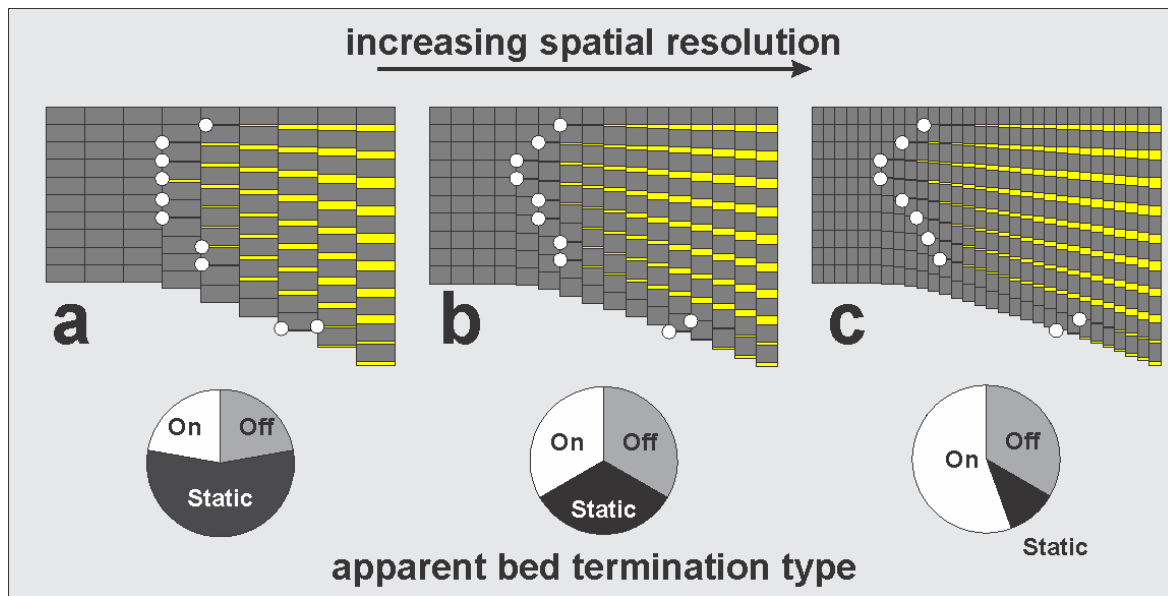


Figure 3.8 The effect of changing spatial resolution of the same 10-clastic-layer geometry by a factor of x2 (Figure 3.8b) and x4 (Figure 3.8c) on the proportion of apparent onlap, offlap and static pinchout. Figure 3.8a represents the base case. The pie-charts show the apparent proportions of layer terminations of different types; on = onlap, off = offlap, static = static pinchout

Increasing the temporal resolution of the simulation (by decreasing the duration of each Time-Step) increases the number of layers, and unless this is accompanied by a corresponding increase in spatial resolution, increasing the temporal resolution increase the number of static pinchouts.

To determine how dependent our model results are on the resolution of the model we conducted simulations of seven runs. The time per Time-Step decreased from 10ky to 5ky, while the horizontal resolution was increased from 25m to 10m. We measured the prevalence of offlapping, onlapping, and static pinchout terminations. The impact of changing the resolution was measured both by population size (Figure 3.9), and areally (Figure 3.10).

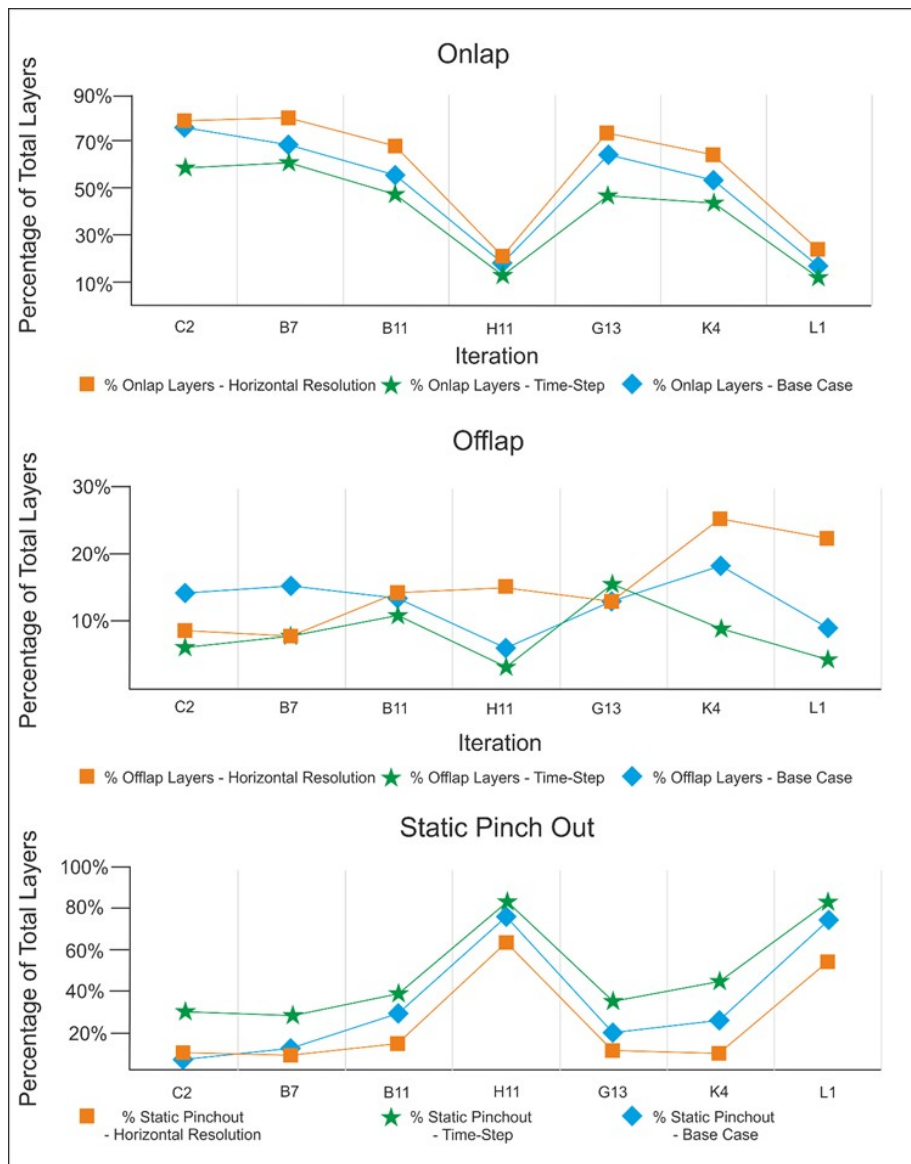


Figure 3.9 The effect of changing model resolution on the apparent proportion of onlap/offlap/static pinchout, determined by population size (number of layers). Blue diamond = base case; green stars = temporal resolution increase by factor of 2; orange squares = spatial resolution increased by a factor of 2.

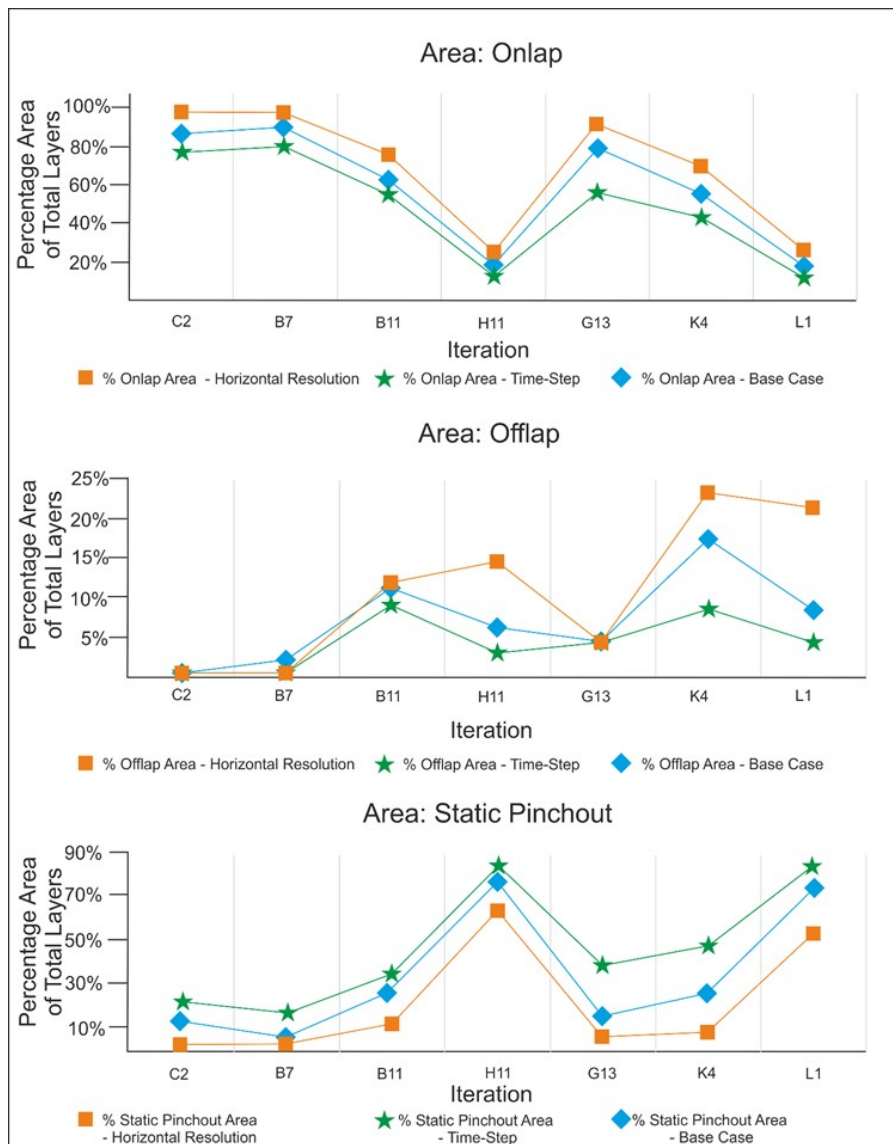


Figure 3.10 The effect of changing model resolution on the apparent volumetric proportion of layers showing onlap/offlap/static pinchout, (area of layers). Blue diamond = base case; green stars = temporal resolution increase by factor of 2; orange squares = spatial resolution increased by a factor of 2.

Increasing the horizontal resolution causes a decrease in the number of gravity flow deposit packages that terminate in static pinchout, resolving them as either onlap or offlap (Figure 3.9, 3.10). This redistribution results in a decrease in the proportion of static pinchouts and an increase in the proportion of onlap and (in most cases) offlap. The ratio of offlap to onlap is not significantly changed. These changes hold for both the number of gravity flow deposit packages and the area of gravity flow deposit packages.

Increasing the temporal resolution causes an increase in the number of gravity flow deposit packages that terminate in static pinchout, but it does not have a significant impact on the ratio of onlap to offlap.

This sensitivity study indicates that the dominance of onlap over offlap seen in our 180 base-case simulation models is not an artefact of modelling resolution. If all models had been run at higher spatial resolution, we would expect the proportion of static pinchouts to drop, but the ratio of offlap to onlap to not change significantly.

3.5 Discussion:

In the shallow marine setting, offlap is commonly interpreted in a sequence stratigraphic context, related to coastal offlap driven by relative sea-level fall e.g. (Catuneanu, 2019). In the deep-water environment, offlap is rarely interpreted this way. Sylvester et al (2015) postulates that offlap is more difficult to identify because of its limited thickness and the low angles between the stratigraphic surfaces compared to onlapping surfaces. Because there is little published study of the origin of offlap in deep-water with the exception of Sylvester et al (2015), we sought the opinions of a number of geoscientists from different companies that are active in deep-water exploration. We found that these interpreters consider that offlap may reflect retreat, or lateral avulsion of a depositional system away from the region of interest implicating sediment input controlled by autogenic factors. The modelling presented here demonstrates that offlap only occurs when a particular set of conditions are fulfilled. These conditions can be achieved by changing the rate of structural growth and/or changing the sediment supply. In our models, offlap is generated most commonly by a combination of the two factors, expressed by the rate of rise of the Structural Growth Profile and the Clastic Limiting Surface. Thus in some circumstances the development of offlap may be controlled changes in sediment supply, however, in other instances autogenic factors within the basin itself such as the influence of structural growth may be a dominant control. This suggests that in some cases onlap and offlap may develop in some circumstances entirely through allogenic factors independent of any changes in sediment supply, however distinguishing between the two would be difficult. Modelling performed by Burgess et al (2019) shows that allogenic factors can influence the development of stratal geometries in submarine fans, but that it is very hard to distinguish this from autogenic signals without prior knowledge of how the sediment input curve evolved.

While we are not concerned here with describing the multitude of processes that control sediment supply into a deep-water mini-basin, we note that classic sequence stratigraphy models such as that of Vail, Mitchum & Thompson (1977) & Catuneanu (2020) suggest that lowering of the relative sea level results in an increase of sediment flux to the deep-water part of the systems

tract. If there is any link at all between deep-water onlap or offlap and sea level changes, it may be out-of-phase with the link in shallower parts of the same system.

One hypothesis to explain the dominance of onlap over offlap could be that this is a product of temporally asymmetric control factors (Figure 3.11a), in which the duration of acceleration of the rate of rise of the Structural Growth Profile or Clastic Limiting Surface is different from the duration of deceleration. However, our modelling indicates that an imbalance between the occurrence of onlap and offlap can arise in models in which the temporal variation of the control factors is symmetrical (Figure 3.11b). Sylvester et al (2015) also shows that symmetrical cycles of increasing-to-decreasing sediment supply coupled with a constant rate of subsidence will result in the formation of an offlapping unit.

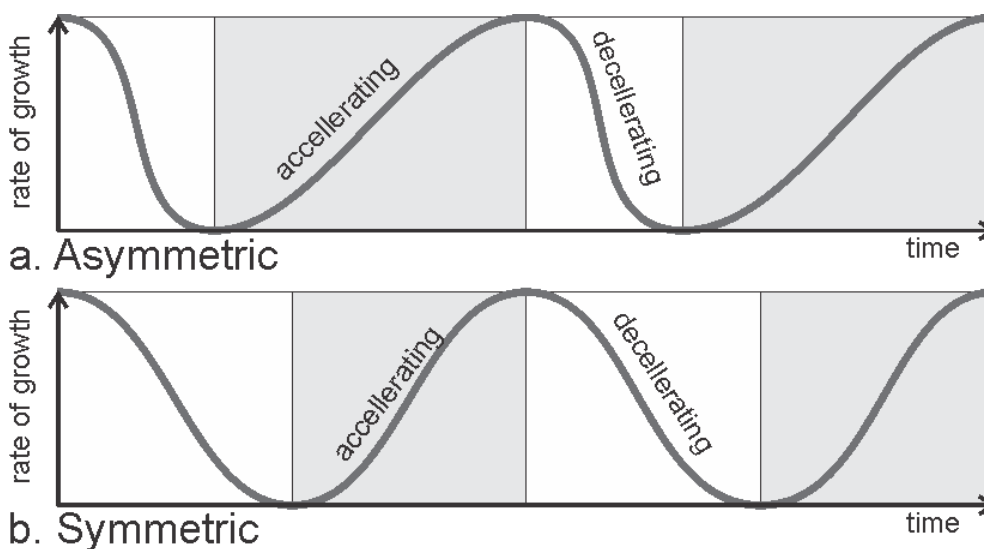


Figure 3.11 Schematic illustration of variation through time of a controlling factor (structural growth rate or CLS rise rate) that is asymmetric (3.11a) or symmetric (3.11b)

How then does the combination of temporally symmetrical factors give rise to an asymmetric population within the resulting stratigraphy? A simple graphical analysis (Figure 3.12) shows that although the variation of controlling factors such as the rate of rise of the Clastic Limiting Surface may be symmetric, the action of sediment accumulation imposes an asymmetric response. Offlap can only form during the short intervals of the time that the rate of rise of the Clastic Limiting Surface is decelerating, and also rising faster than the structural rise of the basin floor at the lowest point in the mini-basin, but it is slower than the structural rise of the basin floor at the depositional edge of the basin. This condition only applies for a minority of the time; this imbalance in time of offlap vs onlap is one reason for which there is a greater imbalance between the thickness of the gravity flow deposit packages that terminate in offlap and those that terminate in onlap. Similarly, this imbalance is noted by Sylvester et al (2015) who shows that

onlapping surfaces can continue to develop over a longer period of time, even when sedimentation rate in the basin is decreasing.

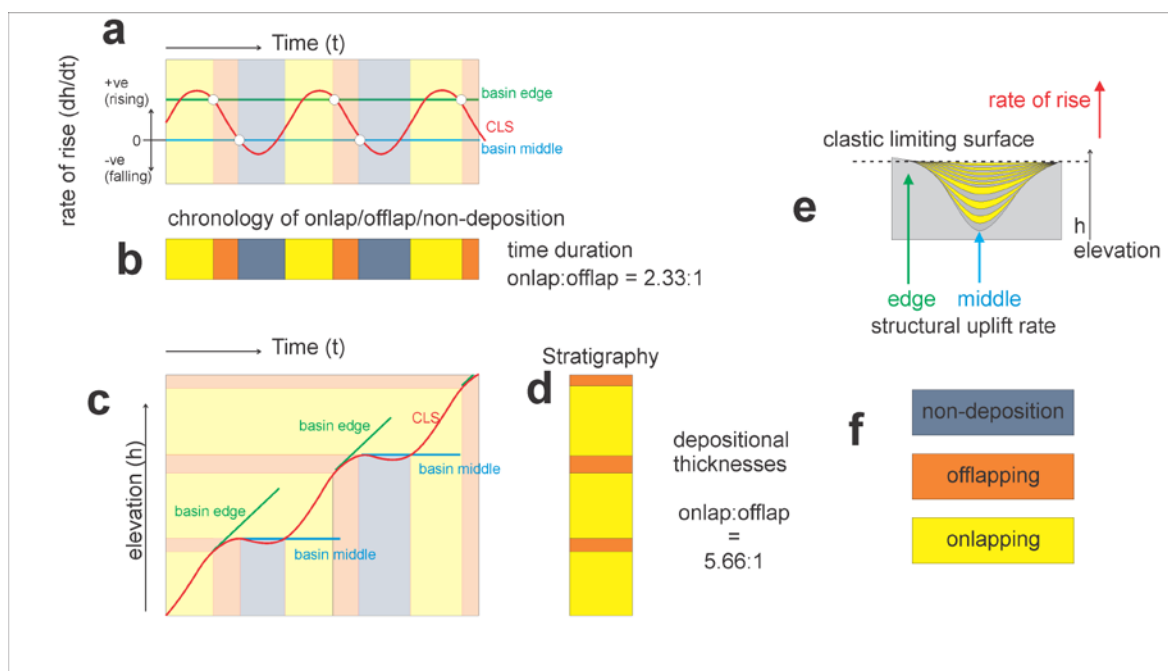


Figure 3.12 Construction used to illustrate the thicknesses of stratigraphy exhibiting onlap vs. offlap. Graphical analysis of a model similar to simulation run E2 (constant rate of structural growth, sinusoidal variation of rate of rise of CLS). For simplicity of construction, this analysis does not include any component of background sedimentation. a, rate of processes through time, red curve = CLS, green line = rate of structural uplift of edge of mini-basin, blue line = rate of uplift in the deepest part of the mini-basin; b, chronology of periods of onlap, offlap and non-deposition; c, graphical plot in elevation vs. time used to construct stratigraphic thicknesses. Colour key as in b; d, stratigraphic

The origin of this imbalance is expressed in Figure 3.13. For each Time-Step, the type of stratal termination is determined by whether the top of the gravity flow deposit package lies above or below the “Offlap Limit” surface shown here. The available space below this “Offlap Limit” surface is limited; this space is create by the increment of structural growth during the previous Time-Step. A gravity flow deposit package that produces an offlapping surface can only be deposited in this limited space. Because of this limitation, the thickness of that gravity flow deposit package is also limited. In contrast, the available space above the reference level, in which a gravity flow deposit package that terminates in onlap is not limited. Therefore, there is no limit imposed on the thickness of a package that terminates in onlap. Similarly, as shown by Figure 2 in Sylvester et al (2015) shows this as well, concluding that the development of offlap and onlap within a mini-

basin is determined by the balance between the volume needed to accommodate incoming sediment and the accommodation made through subsidence on top of the previous deposit.

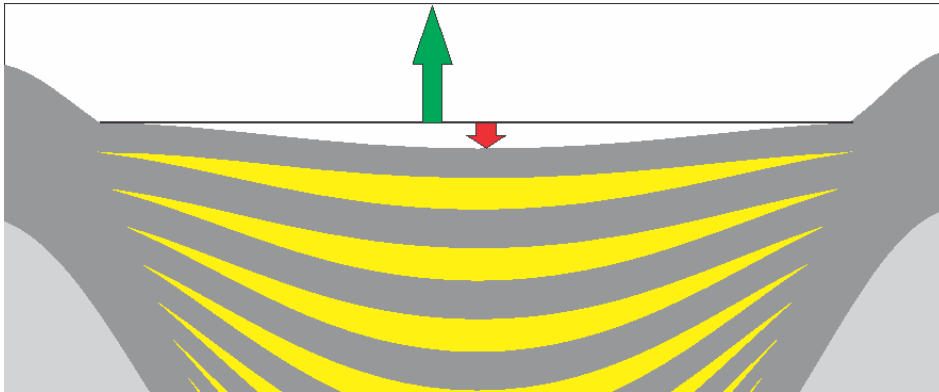


Figure 3.13 The orange line represents the Clastic Limiting Surface for the current Time-Step. The Offlap Limit line highlighting (black dotted line) highlights that the available accommodation for offlap is considerably lower than the available accommodation for Onlap.

3.6 Conclusions

Observations of deep-water clastic systems in nature show that onlapping geometries are relatively common, and offlapping geometries are relatively rare. This observed imbalance in deep-water systems has not hitherto been satisfactorily explained. However, published models for depositional systems in shallower parts of the systems tract suggest that offlap geometries result from falling relative sea-level.

Patterns of synthetic deep-water stratal architecture generated by simple forward modelling, presented here, also consistently show a similar imbalance with a strong prevalence of onlaps. The imbalance is seen both numerically (more onlap terminations than offlap terminations) and volumetrically (the amount of sediment within onlapping units is greater than the volume of sediment within offlapping units). The volumetric imbalance tends to be greater than the numerical imbalance, because offlapping units tend to be thinner than onlapping units.

In our models, the different patterns of simulated stratigraphy were generated by varying factors that describe the local rate of structure growth and the local clastic sediment supply. The imbalance of offlap to onlap is not the result of any imposed imbalance in the controlling variables; instead it is a necessary consequence of the way these combine to create stratigraphy in a structurally active mini-basin. Our models indicate that, while in some cases the temporal distribution of onlap vs. offlap may be related to changes in the regional sediment supply, in other cases it may be entirely controlled by changes in the rate of structural activity. Thus there is no

necessary hardwired link between the stratigraphic architecture seen in deep-water mini-basins and any extrinsic process such as sea level change.

3.7 Appendix Information

Found in Appendix B is the inputs parameters for the 180 simulations performed in the sensitivity study. Also included are the inputs that were changed for the increase in temporal and horizontal resolution, unless were show, the inputs remained the same as the base case. Tables for the number of gravity flow deposit packages are included, these were used to work out the data presented in Chapter 3. Within Supplementary Material B, is an excel spreadsheet that contains the data used to work out the percentages shown in Chapter 3. Within this spreadsheet is found an example of the raw numerical data generated by *Onlapse-2D*, including lateral extent of Gravity Flow Deposits, Background Sediment Thickness, and Height of Basin Structure.

Chapter 4 **Forward Stratigraphic Modelling with *Onlapse-2D* for Reservoir Prediction: Offshore Sureste Basin, Mexico**

***Donald N Christie*¹, *Frank J Peel*², *Gillian M Apps*² and *David “Stan” Stanbrook*³**

¹ Ocean and Earth Science, University of Southampton, Southampton, United Kingdom

² Bureau of Economic Geology, Jackson School of Geosciences, The University of Texas at Austin, University Station, Austin, Texas, United States

³ Murphy Exploration & Production Company, 9805 Katy Freeway Suite G-200, Houston, Texas, United States

Submitted and accepted for publication in *Frontiers in Earth Science*

4.1 Abstract:

A complex geological history and the fact that exploration has only recently begun to focus on deep-water makes the Sureste Basin in southern Mexico an ideal area to test the ability to *Onlapse-2D* to provide value to the exploration chain. The goal of this study was to help illuminate the tectonostratigraphic evolution of the study area and illustrate that *Onlapse-2D* can be used as an aid to exploration. Through integration of seismic reflection data, well data, and age dated horizon interpretations we were able to simulate the evolution of observed structural geometry and stratigraphic architecture of two cross-sections within the Late Miocene. From these simulations, we identified two distinct phases of compressional folding, defined the probable timing of salt withdrawal & diapirism, and recognise areas where there has been depositional topography created. We were also able to identify onlapping geometry of sediment gravity flows that represent a potential stratigraphic trap target for future consideration. These results show that *Onlapse-2D* is capable of illuminating the tectonostratigraphic evolution of complex deep-water mini-basins and add value to the exploration chain

4.2 Introduction:

The Sureste Basin, located in southern Mexico, is a world class basin for hydrocarbon exploration and production, with proven reserves of more than 50 Billion bbl of oil. Defined at its widest extent to cover both onshore and offshore areas (Shann, et al., 2020), it closely follows the outline of the Campeche salt basin (Figure 4.1) (Hudec & Norton, 2019). Most wildcat exploration wells until recent years were focused onshore and in shallow water. However, more than half of the basin is in the under-explored deep-water Campeche slope with less than 15 wildcat exploration wells in depths >500m. Large discoveries in recent years such as Zama-1 and Polok -1 have reinvigorated offshore exploration and highlighted the long term potential of the offshore Sureste Basin.

A complex geological history and the fact that exploration has only recently begun to focus on deep-water makes the Sureste Basin an ideal area to test the stratigraphic forward modelling program *Onlapse-2D*. Within the study area there is good quality seismic, however it lacks the vertical resolution to image detailed stratigraphic relationships. The overall tectonic history of the Sureste basin is well defined, but it is less so in the study area. Therefore, we believe that *Onlapse-2D* can be used to add value to the exploration chain.

4.2.1 Geological History of the Sureste Basin, Southern Mexico

4.2.1.1 Opening of the Gulf

The structural history of the Sureste Basin, and indeed the whole of the Gulf of Mexico is the manifestation of complex plate tectonics resulting from the breakup of Pangea around 250Ma – 170Ma. During the Middle Jurassic, counter-clockwise rotation of the Yucatan plate pulled the Sureste Basin away from the North American plate (Salvador, 1987), (Hudec & Norton, 2019), (Davison, et al., 2021).

4.2.1.2 Deposition of the Salt Basin and Oceanic Spreading

Deposition of the Louann Salt occurred in the Bajocian (Pindell, et al., 2019) across stretched continental crust of the Gulf of Mexico. Oceanic spreading is believed to have begun soon after deposition of the Salt and continued until the end of the Berriasian (Early Cretaceous) (Stern & Dickinson, 2010). This sea-floor spreading divided the Louann Salt into two segments with the salt provinces in the US Gulf of Mexico and Mexico's Sureste Basin (Figure 4.1) (Hudec & Norton, 2019).

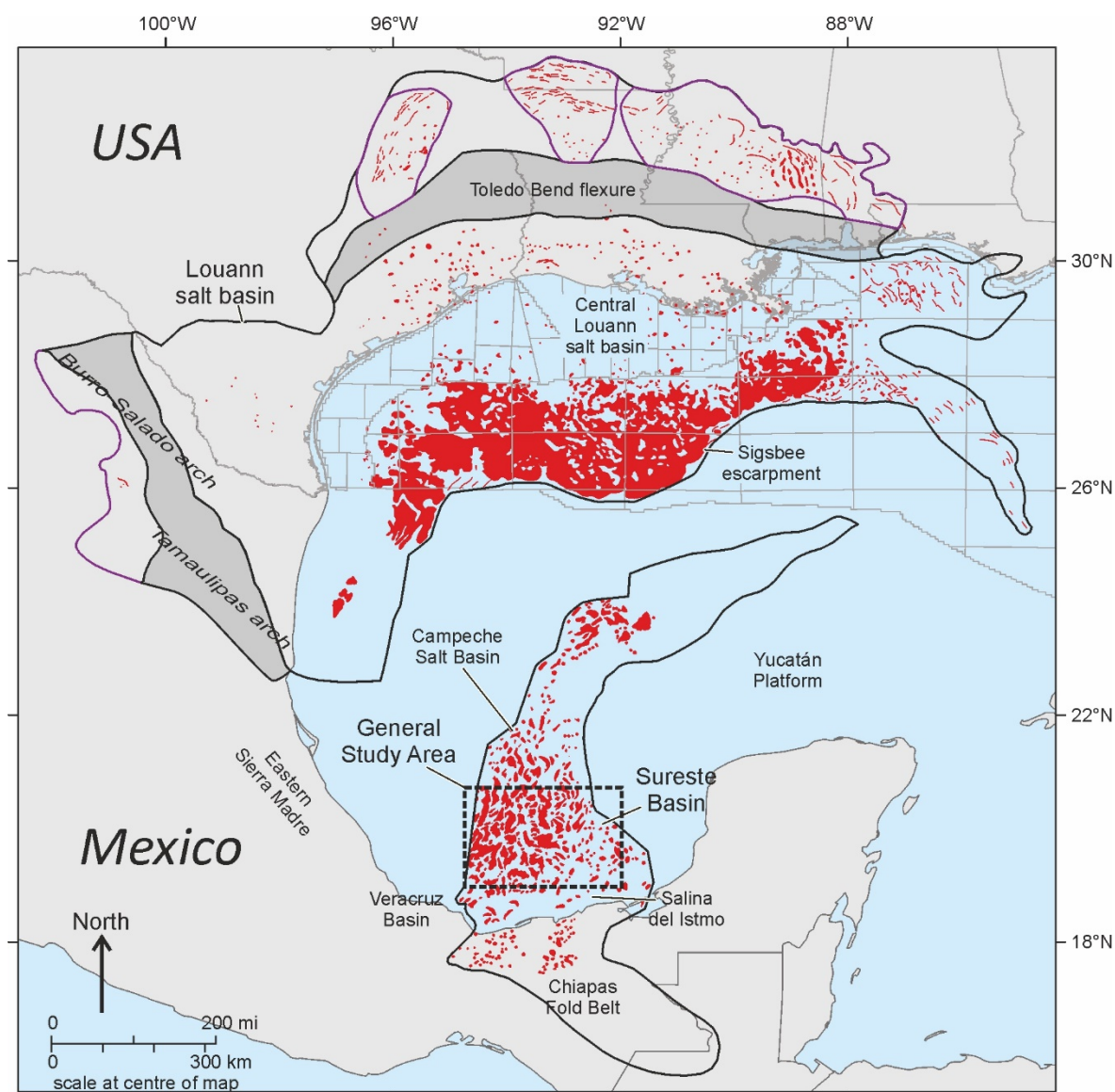


Figure 4.1 Outline of the Sureste Basin in Southern Mexico, the study area is located in the offshore section of the basin. Red shapes represent salt bodies.

4.2.1.3 Post-Rift Mesozoic

After cessation of rifting in the Early Cretaceous, the Gulf of Mexico began to slowly subside owing to thermal cooling and sediment loading, producing a northwest downward tilt to the Sureste Basin (Davison, 2020) (Davison, et al., 2021). For the remainder of the Cretaceous, carbonate deposition dominated the basin with shelfal systems found around the south and eastern rim of the Basin, and fine grained carbonate clastic sediments deposited in the deep-water areas of the Sureste Basin (Padilla y Sánchez, 2007) (Shann, et al., 2020).

4.2.1.4 Mexican Fold-and-Thrust Belt development

The passive margin phase of basin infill in the Sureste Basin came to an end at the start of the Late Cretaceous with the start of the Mexican Orogeny. Cover shortening, in the form of folding and

thrusting, propagated north-eastwards into the Sureste Basin (Shann, et al., 2020). Pre-orogenic salt diapirs were rejuvenated by squeezing, producing allochthonous salt sheets, which are most strongly developed in the onshore and shallow water zones (Davison, 2020).

The drowning of the carbonate reefs in the Lower Palaeocene marks the end of carbonate dominance in the Sureste Basin and from this point onwards deep-water clastic sedimentation dominated the basin, continuing until present day. However, carbonate sedimentation continued along the eastern rim of the basin along with isolated carbonate reef build ups (Davison, et al., 2021) (Shann, et al., 2020).

4.2.1.5 Miocene Tectonics and Stratigraphy

Thick Lower Miocene sands are evident across the offshore Sureste Basin and correspond to onshore formations (Shann, et al., 2020). The shelf margin in the Lower Miocene is located in the present day southern onshore region of the Sureste Basin. The shelf margin migrated northwards throughout the rest of the Miocene and until its present-day position in the offshore area of the Sureste basin (Gómez-Cabrera & Jackson, 2009). Throughout this time the main siliciclastic sediment input into the basin came from the southern part of the Eastern Siera Madre and Chiapas area.

The Chiapaneco Orogeny began during the Miocene (18.0Ma) (Davison, et al., 2021) and is responsible for a short lived but crucially important phase of compressional tectonics that affected the Sureste Basin. Between 13.8Ma – 11.6Ma, this phase triggered allochthonous salt sheet development across the basin. The tectonic event produced what is known as the Chiapas Fold-and-Thrust Belt (Mandujano-Velazquez & Keppie, 2009) and is associated with onshore volcanic activity (Stanbrook, et al., 2020). This event also produced intense deformation extending across a zone up to 600km North from the southern margin of the Sureste Basin (Davison, et al., 2021) (Shann, et al., 2020) (Davison, 2020). The culmination of this tectonic event is a regional strong erosional unconformity.

This Middle Miocene event effectively subdivides the stratigraphy into three units: (i) a pre-orogenic, Oligocene – Lower Miocene section, which was folded prior to emplacement of the extensive salt canopy; (ii) a syn-orogenic Middle Miocene deep-water turbidite system that is associated with the emplacement of an extensive salt canopy; (iii) a post-orogenic infill, of Late Miocene to Pliocene age, which is not affected by the Chiapaneco folding (Shann, et al., 2020).

Within the study area (Figure 4.2) sand injectites penetrate from Middle Miocene stratigraphy through the lower section of the Late Miocene, and are missing from the later stages of the Tortonian. In the later stages of the Tortonian pockmarks occur above the injectites (Figure 4.3).

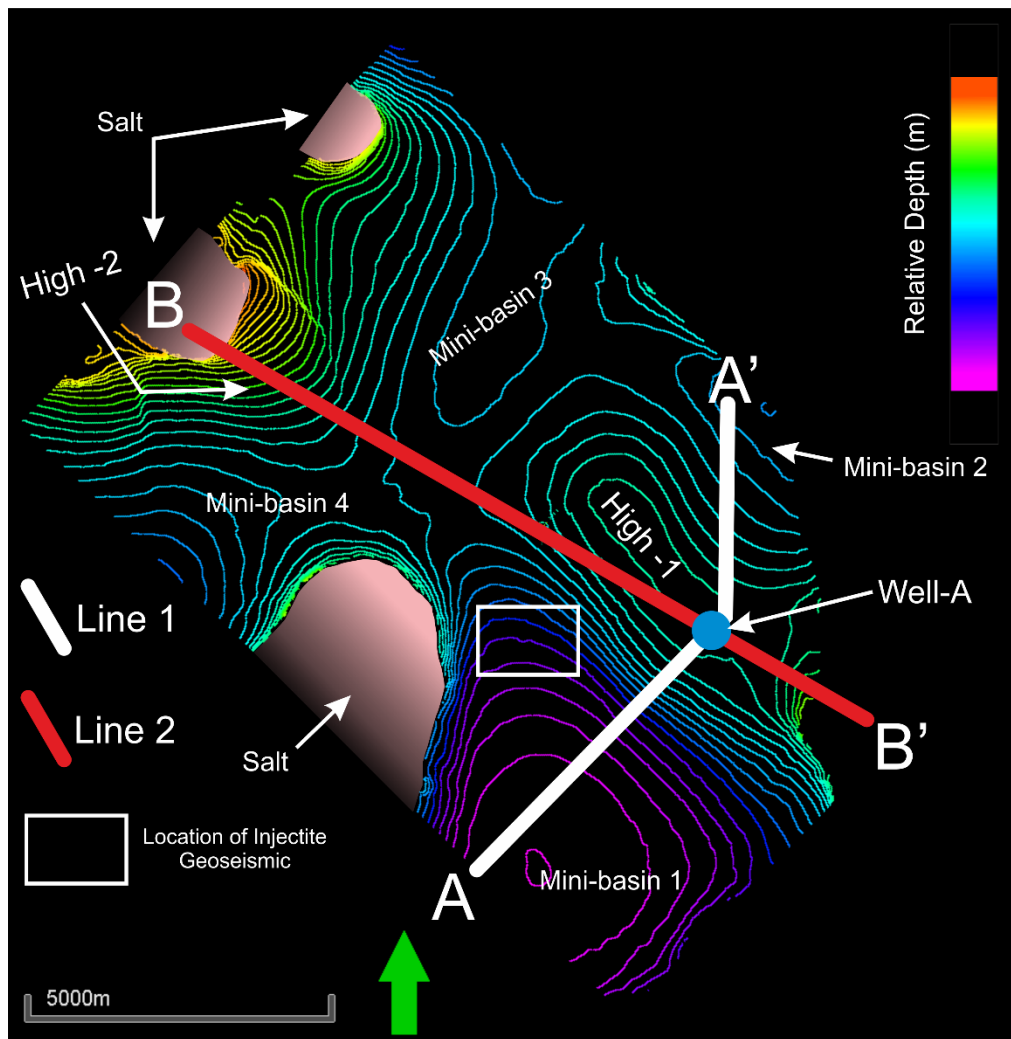


Figure 4.2 Location of Well A superimposed over a relative depth map of the 12.2Ma horizon interpretation, and the two modelled cross-sections Line 1 and Line 2. Colours represent relative depth, where Red contours are the highest, and purple contours represent the relatively deepest sections of the study area. Frame of reference has been rotated to preserve confidentiality.

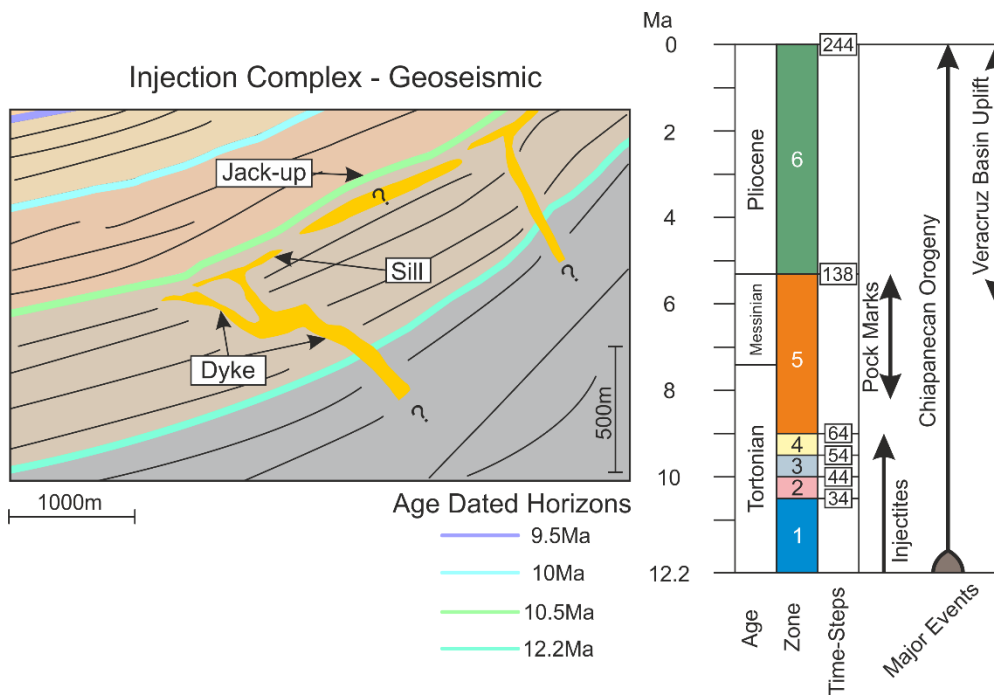


Figure 4.3 Geoseismic cross section of a Sand Injectite complex found to the south-west of High-1. Injectites observed to penetrate from Middle Miocene horizon (12.2Ma) into Upper Miocene stratigraphy, forming dyke and sill complex. Question marks show areas where presence of injectites is inferred, such as the 10.5Ma horizon jack-up structure. Chronostratigraphic chart show timing of injectites observed around High-1 from Middle Miocene before observations cease in the Upper Tortonian. After an absence of fluid flow structures, in the Upper Tortonian to Messinian pock marks are observed.

4.2.1.6 Post Miocene Tectonics to Present Day

After the Chiapaneco Orogeny the tectonic development of the Sureste Basin was dominated by two events. The first was a long lived gradual downslope gravity collapse over the shelf-slope sediments into the Gulf of Mexico. This divides offshore Sureste Basin into three regions; an updip set of extensional salt withdrawal mini-basins, a mid-slope translational area with widespread partly amalgamated salt canopy, and a lower-slope set of large compressional anticlinal folds (Shann, et al., 2020). The second late compressional event effects the south-eastern part of the Sureste basin, uplifting the entire Veracruz basin to the west of the Sureste Basin caused by Pliocene volcanic episodes (Padilla y Sánchez, 2007).

4.2.2 Aims of the Project

The overall aim of this study was to improve understanding of the tectonostratigraphic evolution of the Late Miocene section in three mini-basins in a geologically complex area located in the offshore Sureste Basin. The secondary objective was to validate and develop our stratigraphic forward modelling software *Onlapse-2D*. To do this we selected an area with good quality, high resolution seismic data and well control (good age dating) in a region with 3-dimensional

structural complexity. We constructed and modelled two cross sections. The first traverses Mini-basin-1 passing through Well-A and into adjacent Mini-basin-2. The second cross-section, Line 2 intersects Line 1 at Well-A, traversing Mini-basin-2 and Mini-basin-4.

4.2.3 Data Used

For this project, we utilized a subset of a 3D Kirchhoff Pre Stack Depth Migrated seismic with normal SEG polarity. The seismic data provided good image quality allowing for the mapping of structural and stratigraphic surfaces but lacked the vertical resolution to provide direct imaging of reservoir systems and stratal terminations. Structural and seismic surface interpretations were tied to and dated by biostratigraphic data in Well-A. We were provided access to full well log data that included, Gamma Ray, Resistivity, Neutron Porosity, Density, VShale and Image Logs interpretations.

4.3 Method:

4.3.1 What is *Onlapse-2D*?

Onlapse-2D is a stratigraphic forward modelling program that simulates the tectonostratigraphic evolution and development of deep-water mini-basins (Christie, et al., 2021). It uses four inputs; Initial Basin Structure, Background Sedimentation Rate, Structural Growth Profile and Rise, and a variable rate of rise of a Clastic Limiting Surface. *Onlapse-2D* combines these inputs using simple rules to generate realistic looking basin architectures. The software, input parameters, and computational logic are described in Christie et al (2021) (Chapter 2).

4.3.2 Study Area and Line Locations

This study was conducted in the offshore area of the southern Sureste Basin in Mexico. Cardinal points have been rotated to preserve confidentiality but we use a consistent reference direction as marked on Figure 4.2. Two 2D intersecting cross sections were modelled, with these locations chosen to investigate different phases and different styles of deformation in different orientations. The mini-basins within the study area contains a North-West to South-East trending long lived structural high that is flanked by four mini-basins. There are salt cored highs on the West and North-West flank of the study area (Figure 4.2). The main deep-water depositional systems entered at the south of the basin in Mini-basin-1 and 2, flowing axial to the long lived central High.

4.3.3 Boundary Conditions and Input Parameters

The boundary conditions for Lines 1 and 2 are as follows;

- Total Simulation Time: 12.2Mya (from Middle Miocene until present day)
- Time per Time-Step: 50ky
- Total number of Time-Steps: 244
- Basin Length:
 - o Line 1: 8550m
 - o Line 2: 10875m
- Horizontal Resolution: 25m.

Line 1 and 2 modelled a spanned time interval of 12.2Ma, but focused on modelling the period 12.2Ma to 5.3Ma (Mid-Miocene to Late Miocene). After 5.3Ma, the modelling is completed to a lower spatial resolution. The time interval of 12.2Ma is split into six zones that correspond to different Time-Steps.

- Zone 1: Time-Step 1 – 34 (12.2Ma – 10.5Ma)
- Zone 2: Time-Step 35 – 44 (10.45Ma – 10Ma)
- Zone 3: Time-Step 45 – 54 (9.95Ma – 9.5Ma)
- Zone 4: Time-Step 55 – 64 (9.45Ma – 9Ma)
- Zone 5: Time-Step 65 – 138 (8.95Ma – 5.3Ma)
- Zone 6: Time-Step 139 – 244 (5.15Ma – 0Ma)

4.3.3.1 Initial Basin Structure (Figure 4.4a)

The initial basin structure represents the basin floor bathymetry at the start of the model (Time-Step 0). The starting point for constructing this is to use the isopach of the interval beneath the deepest interpreted seismic horizon as a guide (Figure 4.5). Beyond the depositional edge of that deepest interpreted horizon, the isopach is not defined, and the Initial Basin Structure is derived by a process of iteration.

Inspection of the subsequent strata to identify the patterns of marginal onlap, internal onlap and wedging allow us to infer how much of the onlapped topography existed at the start of the model (at Time-Step 0) and how much of the topography was created by subsequent structural growth.

4.3.3.2 Rate of Rise of the Structural Growth Profile (Figure 4.4b)

This is the amount of rise in mm/yr converted to m/Time-Step that is applied to the basin structure through vertical shear. The first iteration is determined through taking the *Initial Basin Structure* and measuring its height from the lowest point in the basin. We then compare each

point along the cross-section to its height at the present day from the lowest point in the model, which gives us a simple way of calculating the average growth in mm/yr along the cross-section. This provides us a basic Structural Growth Profile, which is refined iteratively to match a predetermined set of criteria. For this study, two basic criteria were applied to the Structural Growth Profile. The first is that it must replicate the form of the final structure visually, and the second is that it must do so to a tolerance of $\pm 25\text{m}$. This can be done in a multitude of ways including, adding more Structural Growth Profiles to represent different components of the structural development (Salt Diapirism, Fold growth etc.), or adding more complexity to the rate of rise of the Structural Growth Profile.

4.3.3.3 Rate of Rise of the Clastic Limiting Surface (Figure 4.4c)

This is the amount of rise in mm/yr converted to m/Time-Step that is applied to the Clastic Limiting Surface. The Clastic Limiting Surface is used to determine whether new gravity flow sediment is deposited at a given position on the cross-section. The Clastic Limiting Surface is a line that delineates above which, no sediment gravity flow deposits are preserved, and below which if there is accommodation, they are preserved. This is a user defined horizontal level that can rise or fall with time.

The initial rate of rise applied to the Clastic Limiting Surface were based on the calculated average sedimentation rates from Gómez-Cabrera & Jackson (2009) which are not corrected for compaction so are likely to be an underestimate. Starting at the lowest zone, we work progressively up through the stratigraphy. Making adjustments to the Rate of Rise of the Clastic Limiting Surface so that the stratal patterns (onlap and offlap) and thickness within the zone match the subsurface data. The tolerance for thickness match is $\pm 25\text{m}$.

4.3.3.4 Background Sedimentation Rate (Figure 4.4d)

This is the amount of sediment deposited along the cross section through pelagic and hemipelagic settling. We calculated this from two interpreted condensed sections within the interval of study in Well-A that had good biostratigraphic age constraint. The deeper, oldest condensed section included an average background sedimentation rate of 0.022mm/yr , and the second condensed, younger section averaged 0.047mm/yr .

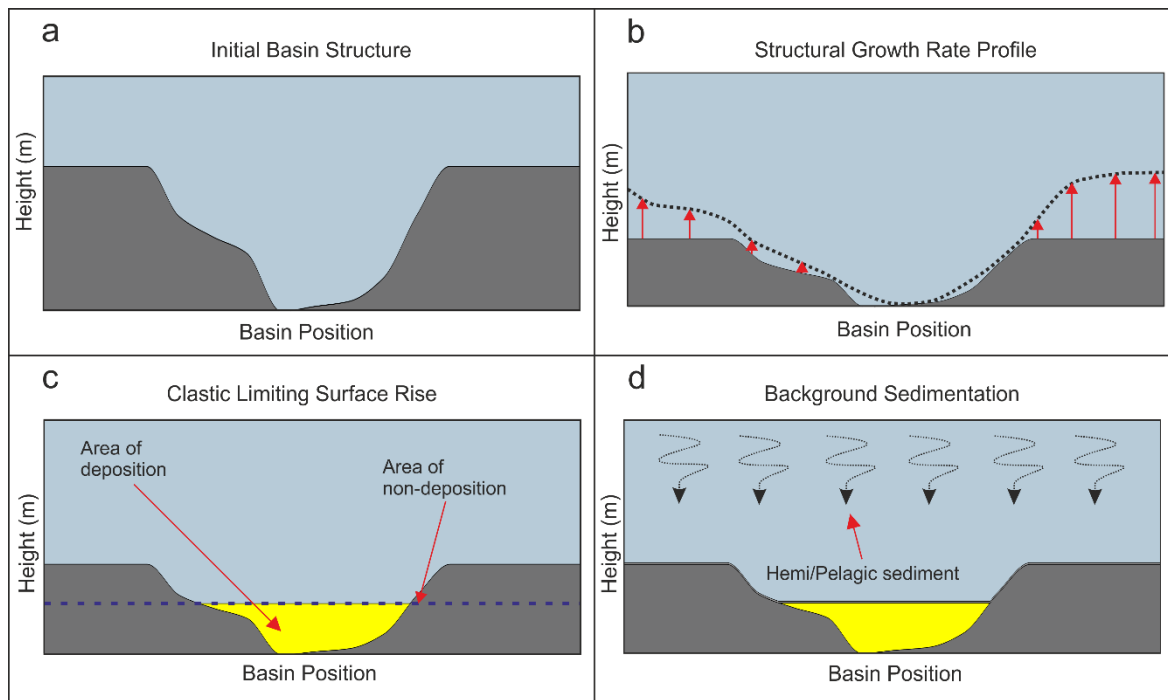


Figure 4.4 a) The Initial Basin Structure at Time-Step 0, Figure 4.5 illustrates how we derive this from seismic data. b) Dotted line represents the Structural Growth Profile, with red arrows indicating the rate of rise being applied to the Basin Structure (dark grey structure). The Structural Growth Rate Profile consist of multiple profiles, in this example it is a single profile. c) Blue dotted line is the Clastic Limiting Surface, if there is available accommodation space below then gravity flow deposit packages are deposited, if not then no deposition occurs. d) A uniform thickness of background sediment is deposited along the cross-section, through pelagic and hemi-pelagic settling.

4.3.3.5 A Note on Gravity Flow Deposit Packages

Geoscientists often associate yellow with sandy lithologies. *Onlapse-2D* does not assign a lithology to the modelled Gravity Flow Deposit Package, only stating that the rise of the Clastic Limiting Surface is generated by sediments deposited through gravity flow processes. The Gravity Flow Deposit Package represents any package of flow deposits, including low and high-density turbidites, calci-turbidites, and mass transport deposits. The interpreting geoscientist must, through their geological understanding (e.g. regional knowledge, seismic or well data, geological models) make an informed decision on what type of gravity flow deposit is represented in any given part of the active depositional package.

4.3.3.6 A Note on Compaction

Compaction is not currently included within the model, therefore estimates on the Background Sedimentation Rate and depositional rates of the Gravity Flow Deposit Packages are an underestimate. This does not invalidate the model because we are able to obtain realistic

simulations of the real world geometries. Further details on the software, input parameters, and computational logic are described in Christie et al (2021).

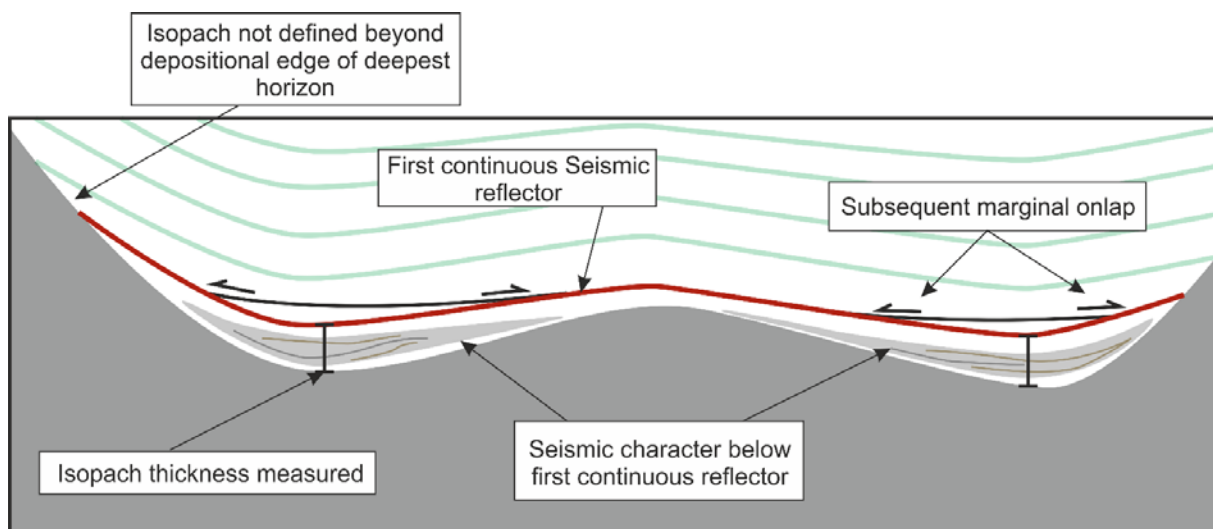


Figure 4.5 The Initial Basin Structure at Time-Step 0 is derived by mapping the first continuous seismic reflector (red) and measuring the thickness of the isopach below it. Inspection of the subsequent and underlying, strata to identify patterns of onlap and geometry allow us to infer how much topography existed at Time-Step 0 and how much topography may have been created by subsequent structure growth

4.3.4 Workflow

This study follows the same workflow as described within Chapter 2, Section 2.3.4 for both Line 1 and Line 2. After each iteration of the simulation, the generated stratigraphy was compared to the subsurface data to ascertain if the stratigraphy was consistent with the subsurface data, and what, if any differences can be found. First we measure the thicknesses of modelled intervals at key points along the cross-section. The key points are equally spaced along the cross-section at a distance of 1000m from each other, important features of interest such as the tops of anticlines or well positions are also included. This is compared to the same interval isopachs on the seismic section that is the basis for the modelled 2D profile. Second, we inspect the match between the stratal relationships generated in the model and those observed on the seismic line; for example, where there are onlaps on the seismic line, there should be onlaps on the model. Third, we consider the seismic facies of each zone, and the lithology. While *Onlapse-2D* does not explicitly define the lithology, the seismic facies, or mappable architectural elements within an interval, are good indicators of the type of gravity flow deposits and a proxy for the relatively speed at which the package was deposited. Intervals with active siliciclastic systems should match the zones in the *Onlapse-2D* model with high values for the Clastic Limiting Surface (more deposition per unit time). Spikes in the rate of Clastic Limiting Surface rise (i.e. zones deposited at the fastest rate) commonly correspond on seismic data to distinctive thick laterally extensive discontinuous,

chaotic seismic facies interpreted as probable mass transport complexes, however they could also represent anomalously high period of sediment input that gave rise to oversized turbidity current events such as megabeds.

If a good match is not achieved, in this case outside the tolerance of $\pm 25\text{m}$ for this study, then the input variables (e.g. Clastic Limiting Surface, Structural Growth Profile, and Initial Basin Structure) are altered until the modelled stratigraphy fits within an acceptable range. For example, alteration of the input variables can include increasing or decreasing the rates of rise of the Clastic Limiting Surface or the Structural Growth Profile, adding additional Structural Growth Profiles, changing the shape of the Initial Basin Structure. For this study the iteration process continued until the generated stratigraphy matches the subsurface data. If the changes do not iterate towards a good fit to the subsurface data, there are two principal reasons. The first is that the structural simulation may not include all the structural processes within the basin (e.g. salt withdrawal) in some cases the difference may be resolved by adding additional structural growth profiles that represent some of the missing processes. The second is that the discrepancy may be caused by a depositional process that cannot yet be modelled through the *Onlapse-2D* method (e.g. erosional or constructional depositional topography).

4.4 Results

4.4.1 Line 1

Generally we found that the modelled final basin structure, thicknesses of modelled zones, and lateral extent of Gravity Flow Deposit packages found within them was a good fit to seismic and well data (Figure 4.6). A single, simple Structural Growth Profile that grew at a constant rate at each Time-Step was used. The Background Sedimentation Rate, derived from well based condensed section information increased in increments through time. The rate of rise of the Clastic Limiting Surface was more varied in both magnitude of rise per Time-Step and the duration of each rise (Figure 4.7). The combination in Figure 4.7 is non-unique but provided us with the closest fit to the seismic and well data of multiple model runs.

Within Time-Step 45 – 54 (Zone 3) and Time-Step 55 – 64 (Zone 4) we found that on the northern flank of the High-1 there was a localized but significant mismatch between what the seismic data indicates, and what the *Onlapse-2D* model predicted to be deposited. We found there was an increasing amount of over thickening into the northern section of the basin. The implications of this discrepancy, and how we corrected for it will be discussed further in the discussion section.

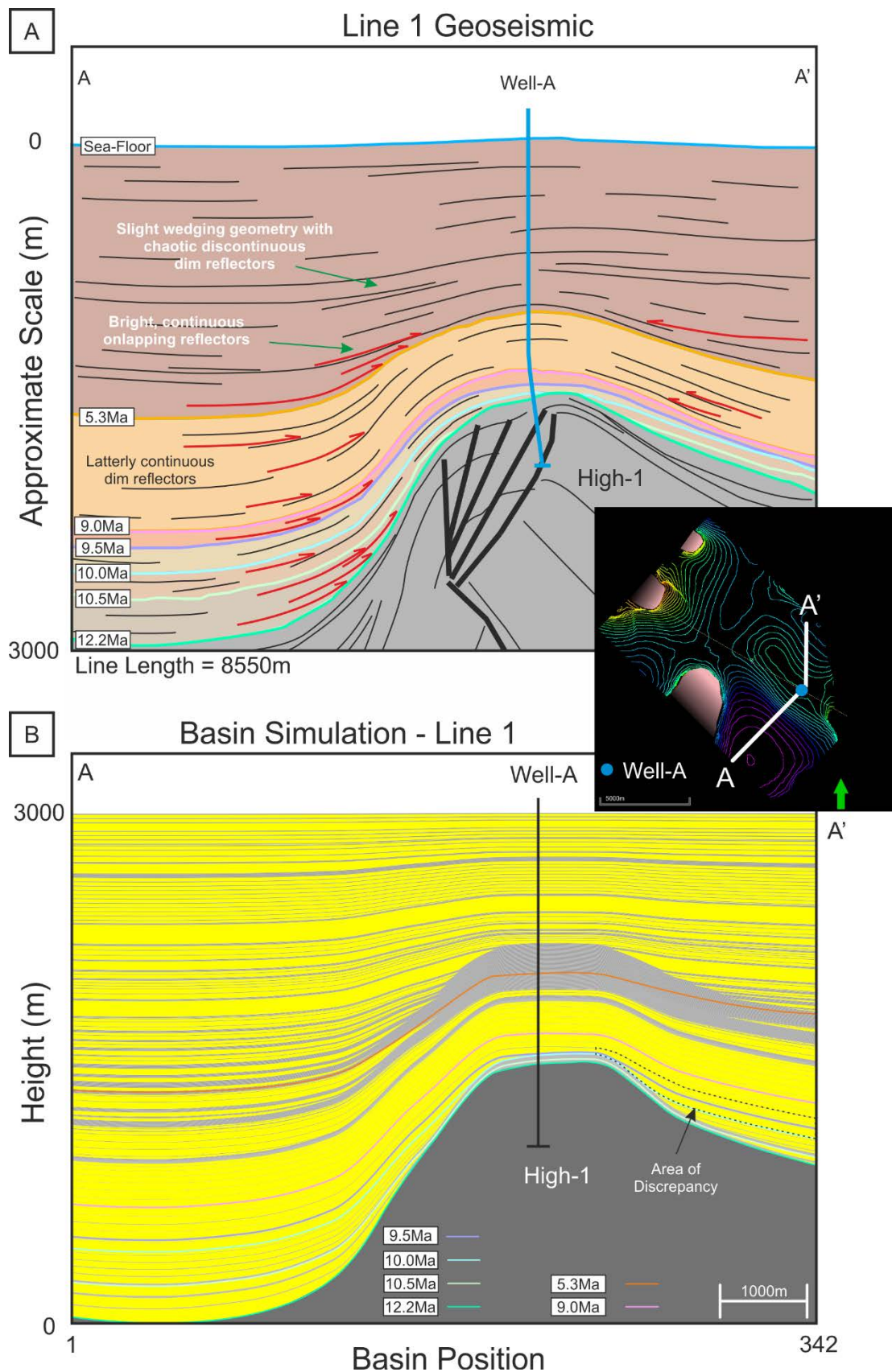


Figure 4.6 a) Line 1 geoseismic cross section, with major onlapping reflectors highlighted in red. Major horizons are age-dated with biostratigraphy from Well-A. Modelling was completed from 12.2Ma until present-day, with 12.2 Ma– 5.3 Ma being the focus, while 5.3Ma until Present day being modelled to a lower resolution. b) Onlapse-2D final simulation, overall there was a good match between the simulation and the geoseismic.

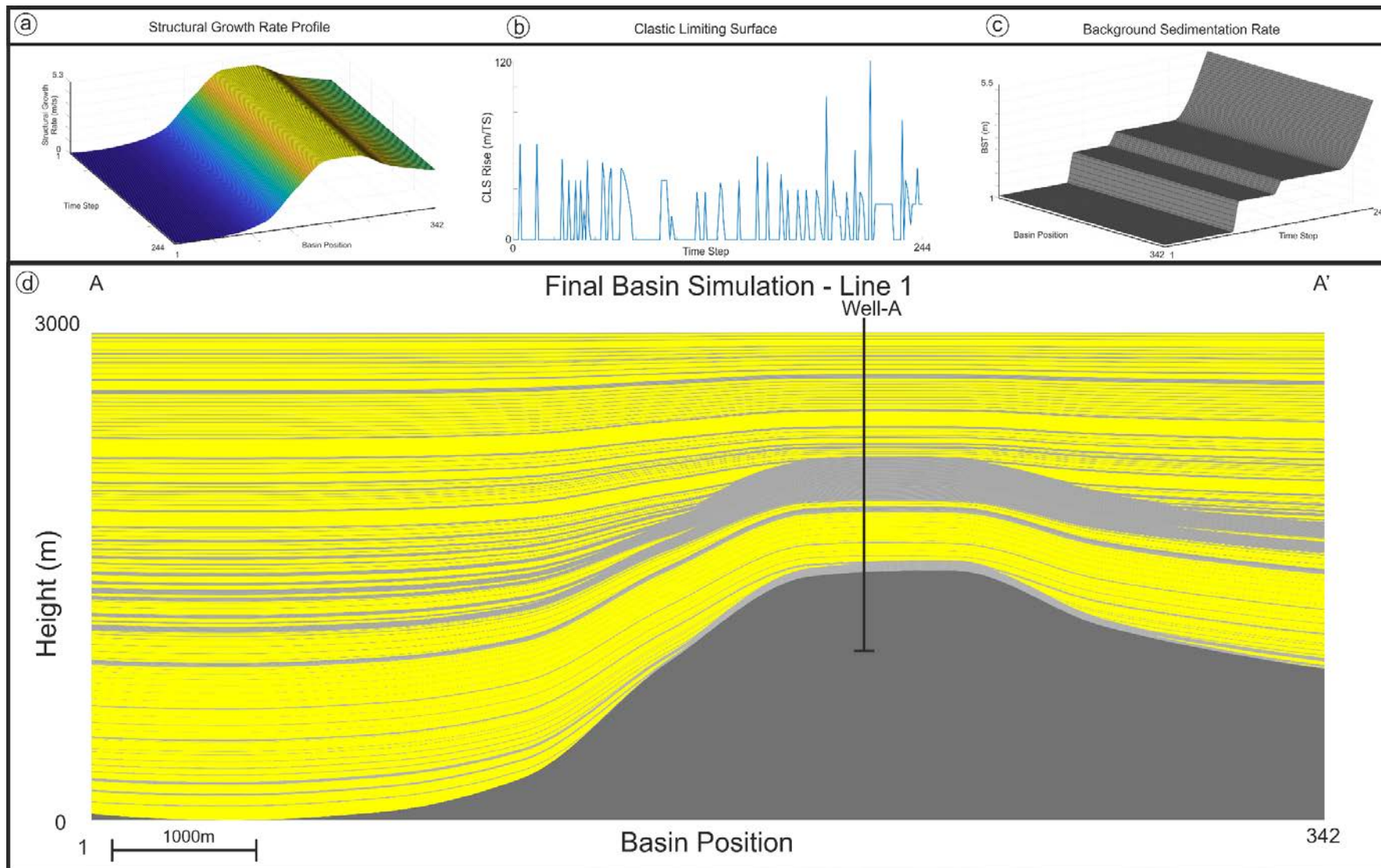


Figure 4.7 I Inputs used to model the evolution of Line 1. a) 3D Representation of the Structural Growth Profile, X axis represents position in space, Y Axis represents position in Time, Z axis represents the growth that the structure grows in meters per time step. b) The rate of rise of the clastic limiting surface; showing the sporadic nature and short lived time in which sediment gravity flows occur in the cross-section. c) Background Sedimentation Rate; derived from data from Well A. X Axis represents position in Space along the cross section, Y axis represents position in Time, and Z axis represents amount of background sediment deposited in meters. d) Final simulation for Line 1.

4.4.2 Line 2

As with Line 1, we found that overall the modelled basin structure, thickness of the zones within the interval of interest, as well as the lateral extent of the Gravity Flow Deposit Packages within those zones were a good fit to both the seismic and well data (Figure 4.8). All boundary conditions were consistent with Line 1, except the Basin Length which was 10875m. The area above the section of interest in Line 2 could not be modelled with a single, simple Structural Growth Profile. To fit the stratigraphy above the section interest, we required two different components of the Structural Growth Profile with different growth histories. The first component of the Structural Growth Profile was consistent with compressional folding, similar to Line 1, but with two discrete phases. The second component of the Structural Growth Profile was a longer time wavelength and was required to account for the significant structural high at the NW end of Mini-basin-4, and is consistent with salt withdrawal and diapirism. The timing of the interactions of the two Structural Growth Profiles is consistent with regional knowledge, and the spatial distribution is consistent with regional knowledge and structural geological principles. We will expand on this in the discussion. The changes to the Structural Growth Profile meant that we needed to create a new rate of rise of the Clastic Limiting Surface. However, the Background Sedimentation Rate remains the same (Figure 4.9).

Within Zone 4 (Time-Step 55 – 64) of Line 2 we found a localized but significant discrepancy between the final best fit simulation and the subsurface data. This mismatch could not be eliminated by simple adjustment of inputs. This discrepancy, which was focused around Well-A, was however informative. If the simulation matched the thicknesses found within Well-A, we found that there would be significant (up to 125m) of extra clastic sediment deposited within the mini-basin to the north-west. The implications of this informative discrepancy, as well as how we corrected the simulation are considered in the discussion.

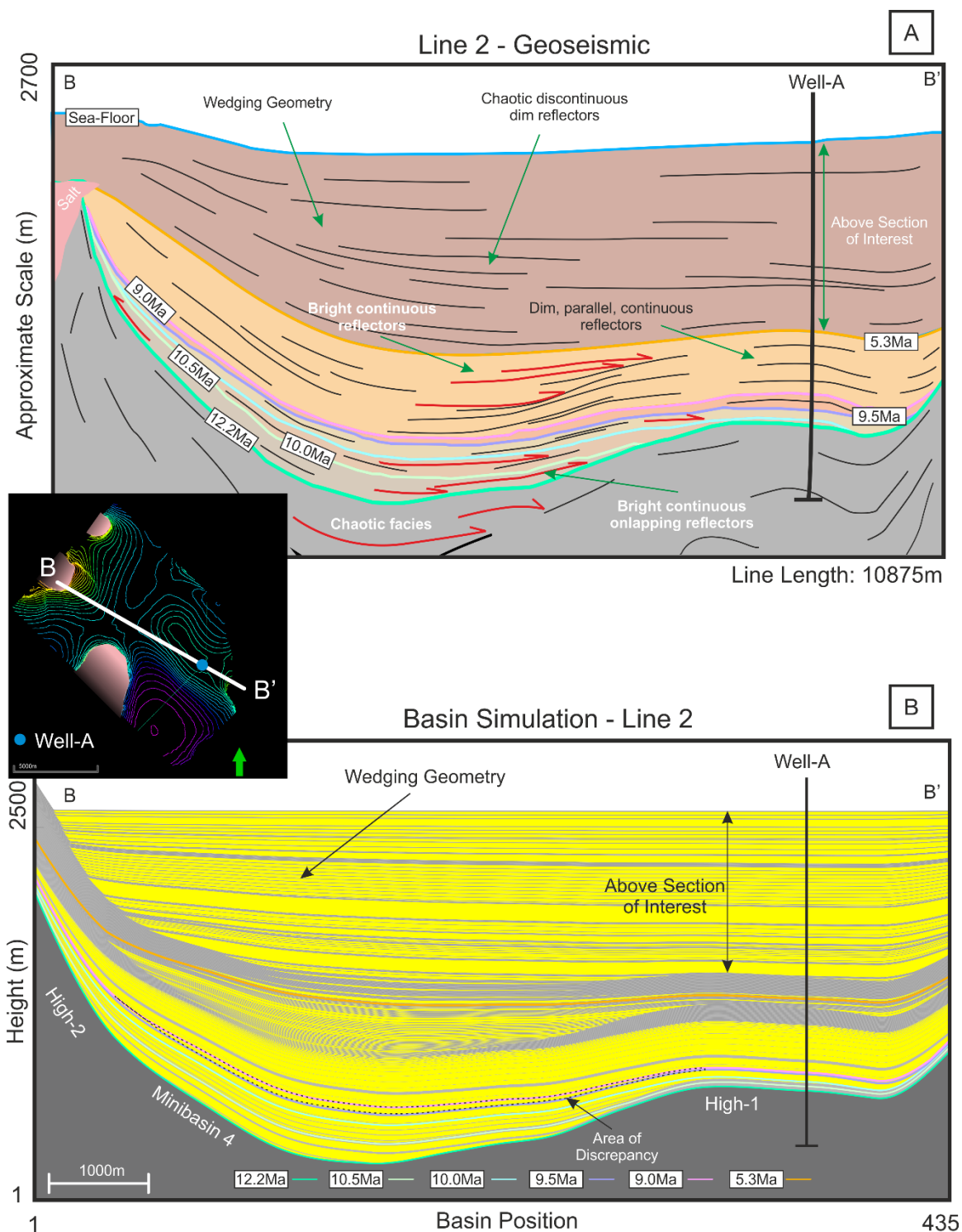


Figure 4.8 a) a) Geoseismic cross-section of Line 2. Line 2 crosses both High-1 and High-2, with High-2 containing salt. Wedging geometry seen in geoseismic cross-section is above our area of interest, but is still modelled at a lower resolution. b) Onlapse-2D final simulation, overall within the section of interest there is a good match between model and the geoseismic. The model is able to match the general form of the basin as well, and major onlapping reflectors seen in 8a, occur in the modelled simulation.

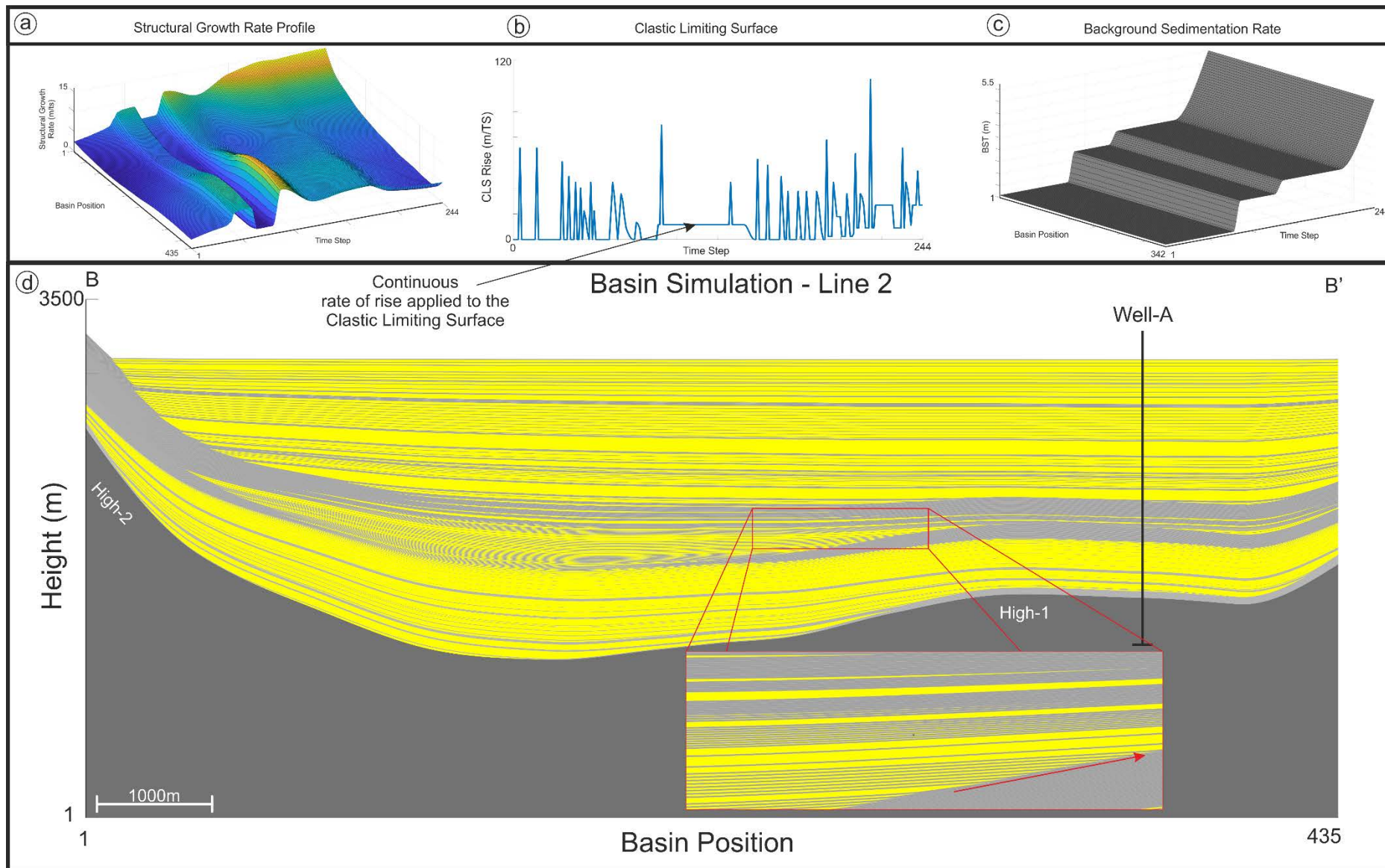


Figure 4.9 Inputs used to model the evolution of Line 2. a) 3D representation of the Structural Growth Profile, a much more complicated structural growth history is visible. A combination of 2 Structural Growth Profiles, one represent salt tectonics and the other focusing on growth of the Fold. b) The rate of rise of the Clastic Limiting Surface shows a more sustained input of gravity driven currents to achieve a good match compared to the more sporadic input in Line 1. c) Background Sedimentation Rate used in Line 1 is used in Line 2. d) Final simulation for Line 2. Insert section highlights thin gravity flow deposits, with red arrow showing the direction of onlap onto the basin flank

4.5 Discussion

4.5.1 Structural Evolution of Line 1 and Line 2

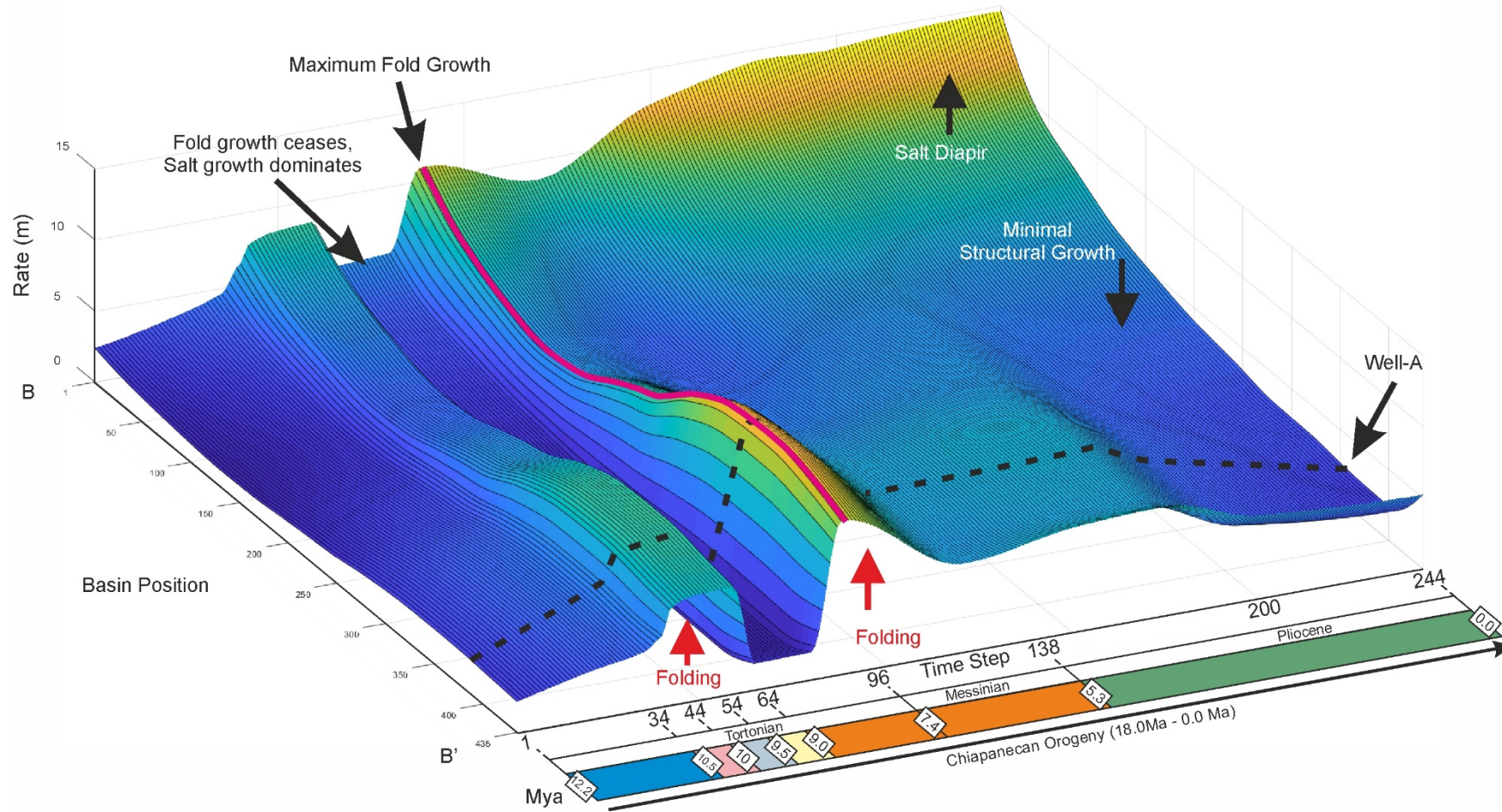
We deliberately kept the Structural Growth Profile and its rate of rise as simple, consistent, and geologically plausible as possible in order to make comparisons between iterations easier. In the model runs of Line 1, we found keeping a single, simple Structural Growth Profile that grew at a constant rate of rise per Time-Step produced the best fit model for our subsurface data.

For Line 2 we applied the same principle, starting with a single, simple Structural Growth Profile that grew at a constant rate of rise per time-step. The rate of rise of the Clastic Limiting Surface used for Line 1 was also used for Line 2. The rationale being that, if the modelling for Line 1 was the correct solution for Well-A, High-1 and surrounding mini-basins, we would be able to produce a close fit to the seismic and well data for Line 2. We would expect minor adjustments to either the rate of rise of the Clastic Limiting Surface or the Structural Growth Profile to occur simply because of the 3D nature basin evolution. However, using a simple, single Structural Growth Profile and the rate of rise of the Clastic Limiting Surface from Line 1 did not provide a good match in Line 2 for the seismic or well data. Minor iterative changes to the rate of rise of the Clastic Limiting Surface, the Structural Growth Profile, or the Initial Basin Structure could not overcome the differences in the model and the subsurface data.

Instead, major changes to the Structural Growth Profile were needed to get a close match to the subsurface data. The first major change was to significantly change the Structural Growth Profile (Figure 4.10), both temporally and spatially. The first profile was consistent two phases of folding, focused on the High-1 around Well-A that occur at different Time-Steps. The second profile included the growth of a salt diapir at the north western end of Line 2. Having three distinct phases of structural growth on Line 2 allowed us to have a much closer match to both the subsurface data. The last phase of structural growth had the greatest impact on the high at the northern end of Line 2, and that high is known to be a salt diapir.

So how can we have two lines that intersect that have apparently such different structural histories? We believe this is because both salt withdrawal and compressional folding are highly three dimensional in this basin. There are three distinct phases of structural activity represented on line 2, with two distinct structural processes active within the study area: salt diapirism and withdrawal, plus two distinct phases of folding.

Line 2 - 3D Structural Growth Profile Diagram



Chapter 4

Figure 4.10 3D representation of the rate of rise of the Structural Growth Profile through time. X –axis represents position in time, Y – axis represents basin position along Line 2, Z – axis showing the rate of rise in meters per Time-Step. Diagram shows the combination of two Structural Growth Profiles through time. Profile 1 was consistent with compressional folding over High-1, Profile 2 is focused on salt diapirism and withdrawal at High-2. Fold growth (Profile-1) dominates in two distinct phases, phase one occurs from 12.2Ma till ceasing at 9.0Ma, at this point Profile 2 (salt growth) dominates until 7.8Ma, at which point compressional folding begins again. Profile 1 continues to dominate until the middle Pliocene when fold growth tapers off. At this point, salt tectonics dominates, represented by Profile 2.

Why did we not see the two phases of folding in the model for Line 1? A line of section that is parallel to the fold axis of an episode of folding (i.e. strike to the shortening direction) may not show any sign of the existence of that fold episode. That folding episode may uniformly raise or lower the line across its whole length but we may not see differential uplift/subsidence in that direction. Conversely, a line that is at an oblique angle to a fold axis should show obvious evidence of that episode of folding.

In the study area we have 2 phases of folding whose orientations are nearly orthogonal (Figure 4.11). In the frame of reference used in this paper Phase 1 produces dominantly north-south fold axes, Phase 2 creates southwest-northeast fold axes. Line 1 is at a high angle to phase 1 and therefore shows phase 1 folding, but it does not cross any phase 2 structures. Conversely, line 2 intersects both structures of phase 1 and 2. For this reason line 1 can be modelled without requirement for phase 2 structuring as part of the model. Line 2, however, requires incorporation of both phase 1 and 2 of folding.

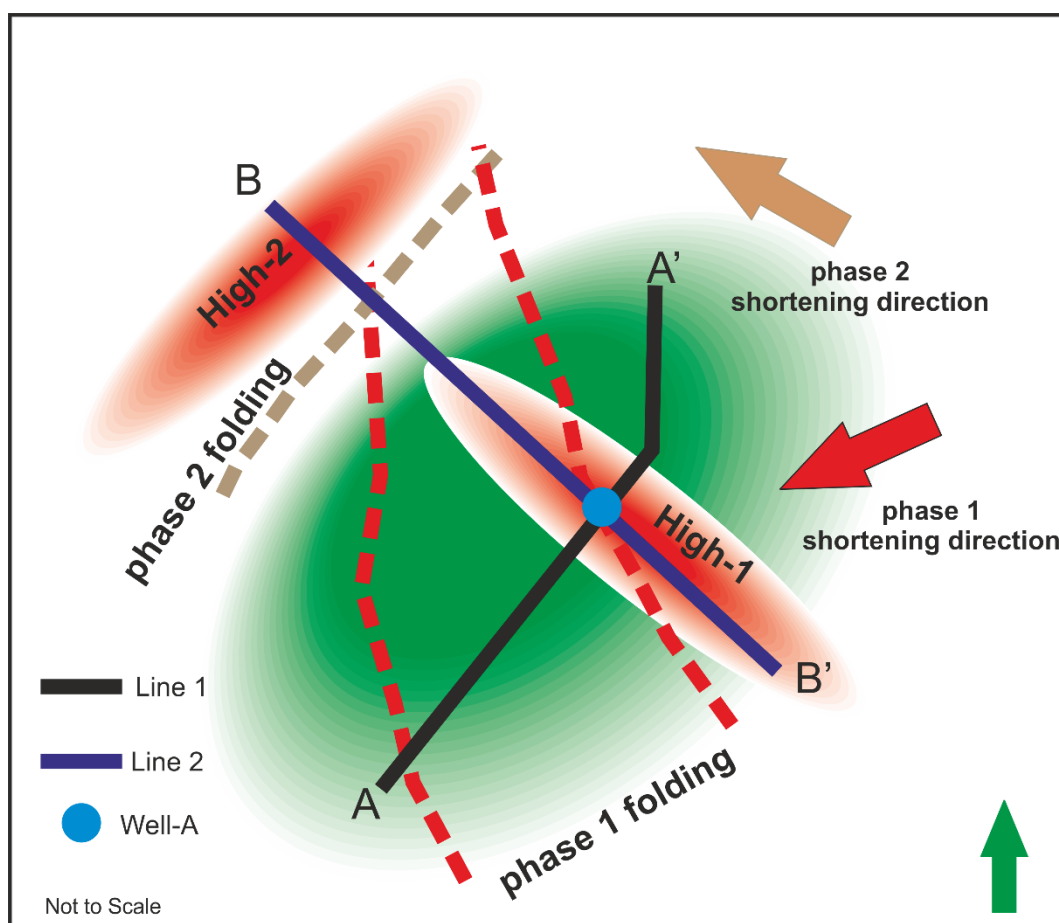


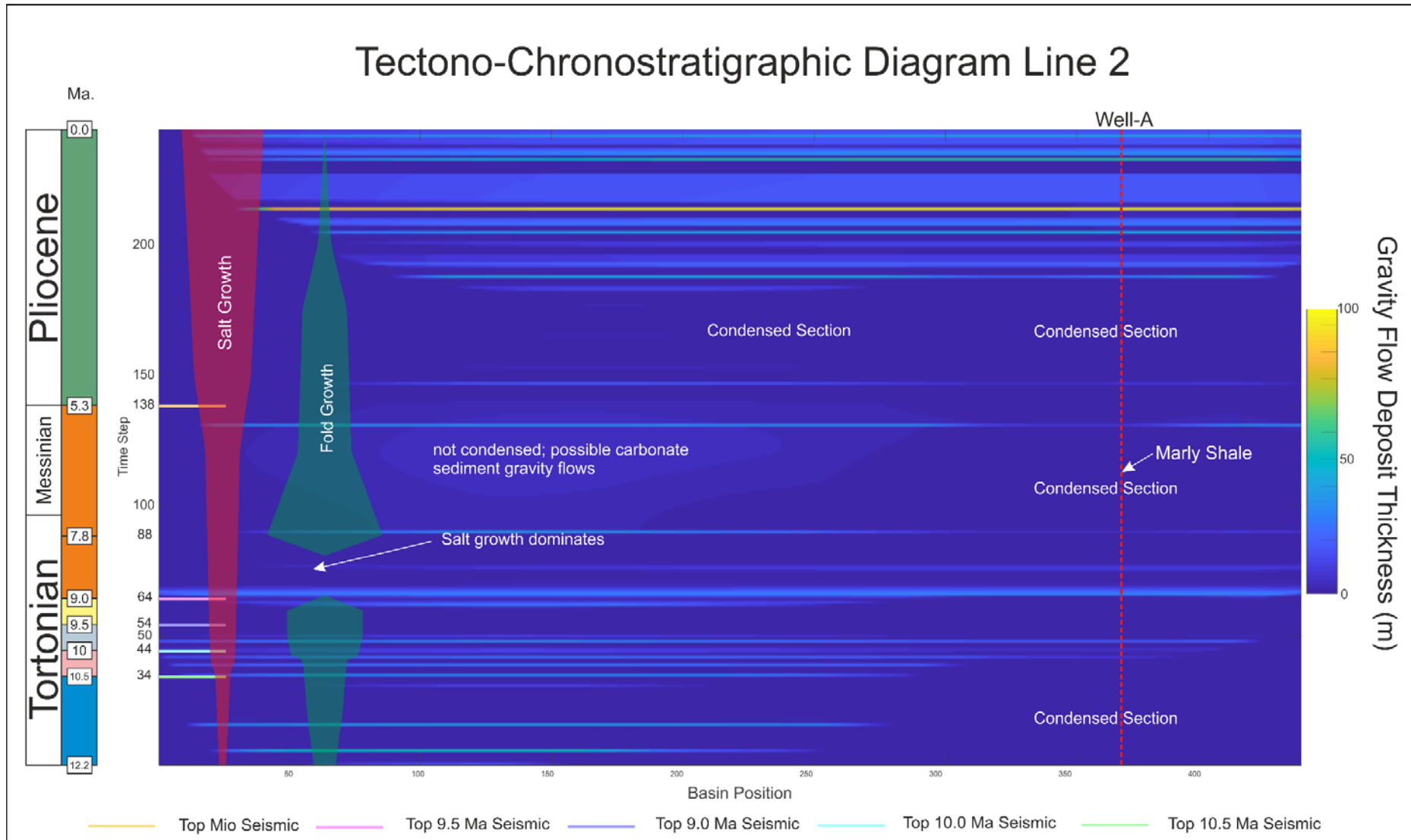
Figure 4.11 Schematic drawing of the structural components of study area. Red dotted line represents phase 1 fold axes that trend roughly east-west. Brown dotted line represents the phase-2 folding axes which trends southwest-northeast. Phase 1 shortening direction is towards the southwest, phase 2 shortening direction is northwest. Line 1 does not intersect the fold axis of phase 2 folding, while Line 2 intersects both phase 1 and 2.

Likewise, we did not identify a separate signature for salt withdrawal in Line 1 because the salt is withdrawing predominantly in a north-south direction to produce the High-2 diapir at the north end of line 2. For this reason, line 2 needed to incorporate salt withdrawal and diapirism.

Each component of the Structural Growth Profile reflects different structural controls on the basin, and show the amount of control that is exerted on the growth of structural accommodation through time (Figure 4.10). There are two distinct phases in the structural evolution of the cross-section where fold growth is dominant. Between these two phases, fold growth dramatically reduces from around 9.0Ma to 8.2Ma, before increasing rapidly, peaking at around 7.8Ma then decreasing over the course of the Pliocene (Figure 4.10). Salt tectonics dominates in the Pliocene, and this is what forms the wedge-shaped stratal geometry seen in the area above the Miocene section of interest in Zone 6.

Figure 4.12 is a tectono-chronostratigraphic chart we extracted from the *Onlapse-2D* model of Line 2, with the timing and relative importance of the two structural processes shown in red and green: salt tectonics exerts influence on the structural evolution of the cross-section throughout time, with increasing influence into the Pliocene; while the growth of High-1 through fold growth is a more variable event through time.

The observation of sand injectites around the High-1 in the study area provides important independent evidence of two discrete phases of folding in the *Onlapse-2D* model output (Figure 4.3). Sand injectites are observed to penetrate from the Middle Miocene through the lower section of the Late Miocene, and are not active in the Late Tortonian. The remobilization of sands occurs throughout the first phase of compression that is modelled in *Onlapse-2D* and, crucially, injectites are observed to terminate close to the time when the first phase of compression ceased in the model. No injectites are observed in the later stages of the Tortonian. Pockmarks are observed to occur around the time that the second phase of contraction occurs; vertical migration of fluids has continued, but the remobilization of sand had ceased.



Chapter 4

Figure 4.12 Tectono-Chronostratigraphic chart of Line 2. Representations of the two structural growth profiles superimposed upon a chronostratigraphic chart of Line 2. Chronostratigraphic chart shows the distribution and thickness of gravity flow deposits. Width of profiles represent relative strength, Salt Growth (Profile 2) continues throughout time while the Fold Growth (Profile 1) has two distinct phases, and can be seen to decrease rapidly in the Pliocene. Well-A shows multiple condensed sections in which no gravity flow deposits are intercepted. Section labelled not condensed is where Onlapse-2D had to introduce a small but continuous rise to the Clastic Limiting Surface, this deposited thin gravity flow deposits that onlap onto flanks of High-1.

4.5.2 Predicting Reservoir Properties with *Onlapse-2D*

To date *Onlapse-2D* has been used to match models with existing geometries within deep-water basins. However, one of the purposes of this study is to aid in the prediction of the stratigraphy prior to well placement. To this purpose we have used the interpretations of well data from Well-A, and combined this with the final simulation for Line 2 to make predictions about the stratigraphy in the Mini-basin-4 (Figure 4.13).

How would the stratigraphy change in Mini-basin-4 based on the modelling and what the well data shows us? Data from Zone 2 in Well-A is interpreted to be the distal lobe fringe of a deep-water turbidite system. The *Onlapse-2D* model shows sediment gravity flows that thicken into Mini-basin-4 from Well-A in Zone 2. These thicker sediment gravity flows could represent the sand-rich lobe axis of a lobe complex, which has progressively become unconfined through time with the lower section of Zone 2 having thick deposits that onlap onto the flanks of the high (Figure 4.13).

Within Zone 1 we see thick sediment gravity flow deposits confined within mini-basin-4 that onlap onto the flank of High-1. As these sediment gravity flow packages are not penetrated by Well-A, we cannot definitively state what the lithology of these are, but our interpretation is that they represent a confined submarine lobe-complex (*sensu* (Prélat, et al., 2009), (Groenenberg, et al., 2010)). The onlapping geometry of these sediment gravity flows represent a potential stratigraphic trap target for future consideration. Crucially, the modelling by *Onlapse-2D* predicts not only the positions of stratal terminations, which could not be imaged on seismic, but also a thick draping of background sediment above and below. Image Log analysis and well data shows that the background sediment here is made of exclusively of massive to stratified shales, which could provide a thick laterally continuous seal for the potential stratigraphic trap target (Figure 4.13).

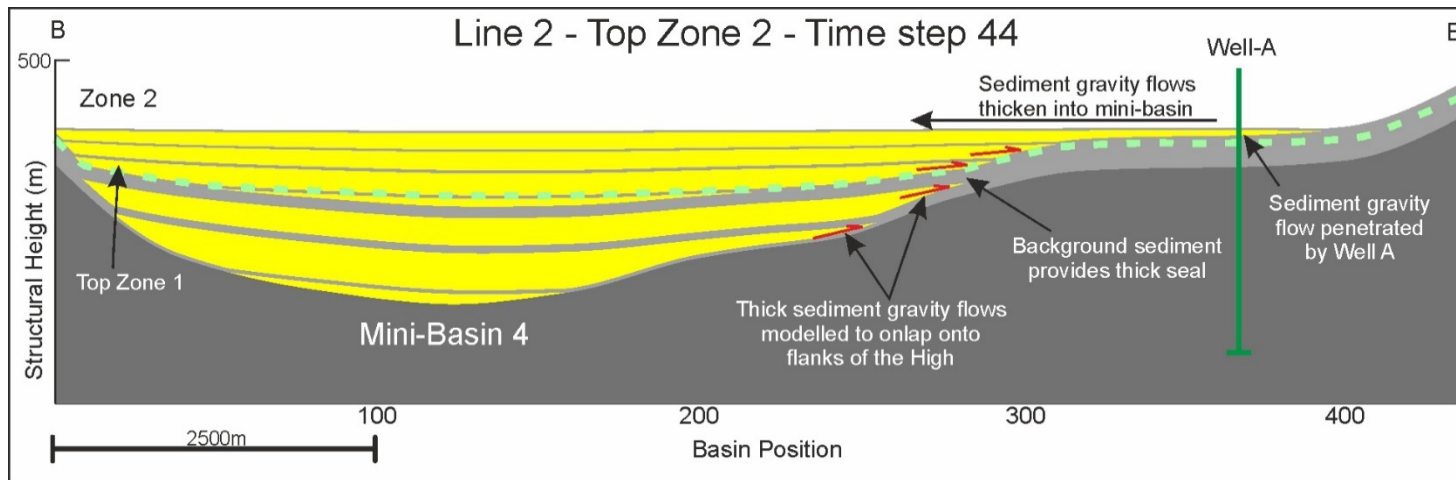


Figure 4.13 Time-Step 44 (10.0Ma) of Line 2, showing the predicted presence of sediment gravity flows in the Mini-basin-1. Thick sediment gravity flows modelled in Zone 1 onlap onto the high flanks, topped by a thick laterally extensive seal of draping mudstone. Thin unit penetrated by Well-A in Zone 2 would likely have a thicker, lateral equivalent found within the basin which is what the Onlapse-2D model has simulated to develop.

4.5.3 What is the significance of the different background sedimentation rates?

Data from Well-A indicates the presence of two condensed zones for which we have biostratigraphic age constraints. We used these to estimate the Background Sedimentation Rate, because these are regionally interpreted as condensed zones. The oldest condensed section occurred within the Middle Miocene, and gave us a rate of 0.022mm/yr, while the youngest condensed section occurred within the Late Miocene and gave us a rate of 0.044mm/yr, indicating a doubling of the Background Sedimentation Rate.

Lithology data from Well-A also shows that in the Late Miocene just before this doubling occurs in the background mudstone becomes considerably more carbonate-rich compared to the section below (Figure 4.14). We used this first appearance of a more marl-rich lithology to give us a reasonable estimate of which Time-Step the Background Sedimentation Rate should increase. Our interpretation of this increase in Background Sedimentation Rate is because of an increase in carbonate productivity within the region, consistent with the regional time-equivalent shelf carbonate stratigraphy. Sedimentation rates derived by Gómez-Cabrera & Jackson (2009) show a marked increase in the Pliocene, which we incorporated into our Background Sedimentation Rate curve.

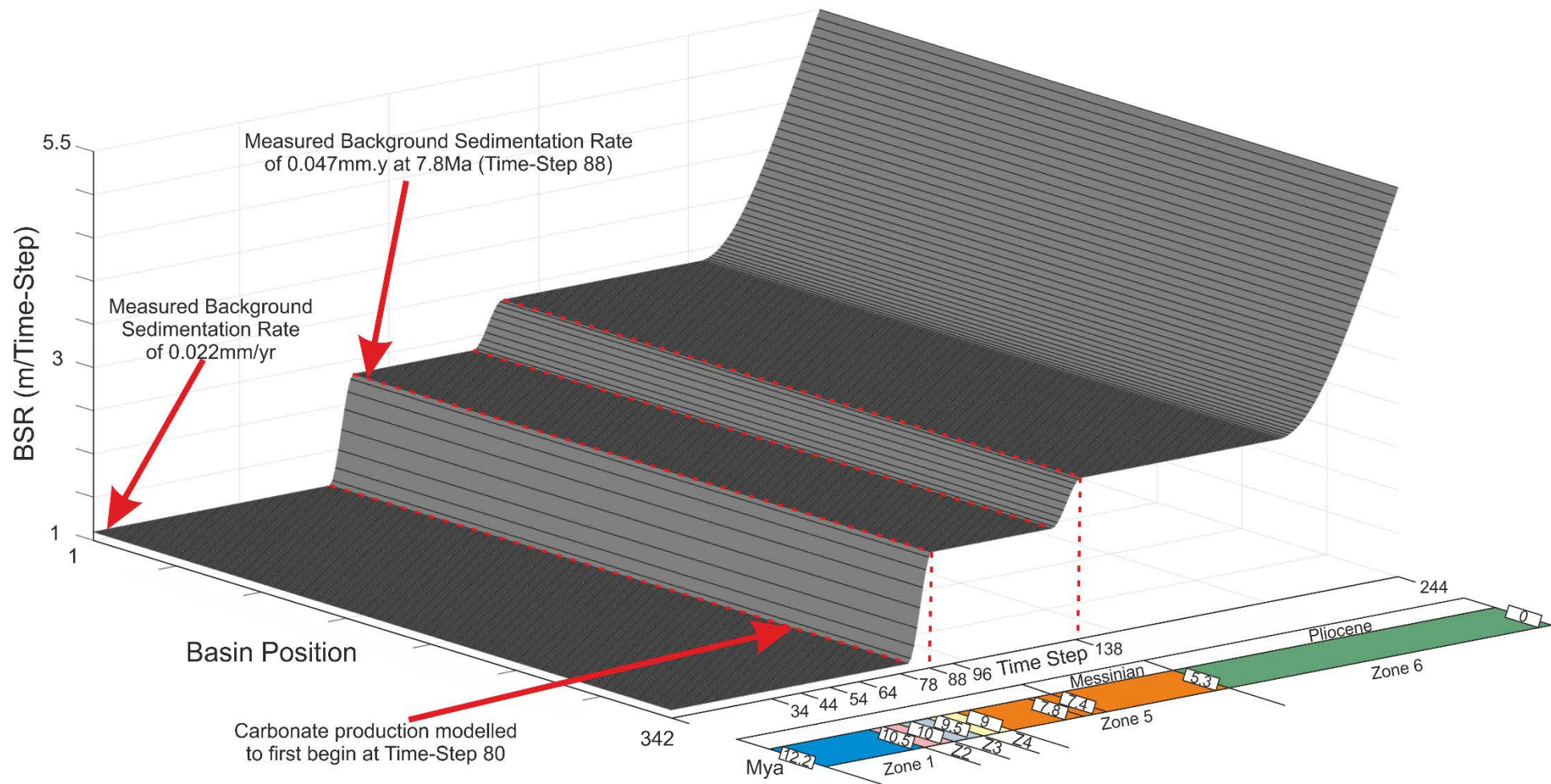


Figure 4.14 3D representation of Background Sedimentation Rate as it evolves through time. Derived from well data from Well A. X axis represents position in Time, showing both Time-Step and where in the chronostratigraphic column each event is. Y axis represents position along the cross-section. Z axis represents the rate of Background Sedimentation in meters.

4.5.4 Possible Carbonate Sediment Gravity Flows

There are marl-rich mudrocks penetrated in Zone 5 in Well-A. When we modelled these marls as background sediment, there was a significant mismatch between the seismic and the model as the Zone 5 interval extends northwards into Mini-basin-4; the model predicts a thin section, whereas the Zone 5 seismic interval thickens into the mini-basin.

Very thin sediment gravity flow deposits were observed in Zone 5 in Well-A, in a package that onlapped onto High-1 (Figure 4.9). Modelling active sedimentation of gravity flow packages that were restricted to Mini-basin-4 meant adding a small continuous rate of rise to the Clastic Limiting Surface. Doing so allowed us to account for differences in thicknesses observed between Well-A, and provide a better match to the subsurface data (Figure 4.9).

The presence of marl-rich shales in this interval at Well-A, and the fact there are known isolated carbonate build ups in the region at this time (Shann, et al., 2020), leads us to the interpretation that the modelled Gravity Flow Deposit packages which thicken northwards into mini-basin 3 in Zone 5 are likely to be calciturbidites.

4.5.5 Informative Discrepancies

What do we mean by an *Informative Discrepancy*? We are able to iterate towards a good solution where the model output provides a close match to the subsurface data. However, there are localized anomalies where it is not possible to iterate towards such a match using *Onlapse-2D*. We call these *Informative Discrepancies* because they point to valuable insights. *Informative Discrepancies* identify places in the model where the basic assumptions of the *Onlapse-2D* method, such as no erosion or positive topography do not apply.

Our purpose with *Onlapse-2D* is to attain a close as match as possible between the model output and observed subsurface data. However, in this study we demonstrate there is significant information and geological insight that can be obtained by quantifying the mismatch between the best fit model and the available data. Once we have identified an informative discrepancy, our objective shifts from attempting to make a perfect fit to making a best fit. Once this has been achieved, we can highlight the differences, quantify them, and then make a geological interpretation out of them. Thereby enabling us to potentially quantify the processes that lie outside the scope of the model. For example, estimate how much sediment at key points along the cross-section has been eroded or the height of positive depositional topography.

4.5.5.1 Informative Discrepancy in Line 1

Overall we found the simulation produced by *Onlapse-2D* provided a good match to the seismic and well data. However, we found a significant mismatch on the northern flank of the High-1 in Line 1 for both Zone 3 and Zone 4 (Figure 4.15). The model was simulating a significant thickness of gravity flow deposit packages when seismic data was showing us this was not the case. There was an increasing amount of over-thickening within Zone 3 and 4 extending into Mini-Basin-2 off of High-1, with up to 95m of extra sediment simulated as deposited.

To correct for this, we began by making iterative changes to the rate of rise of the Clastic Limiting Surface and the Structural Growth Profile, and we lowered the Initial Basin Structure for Time-Step 0. We were unable to lower the amount of over thickening in Zone 3 or 4 through these iterative changes, without substantially under-thickening the model in Well-A and in Mini-basin-1 (Figure 4.15). Therefore, the discrepancy is caused by a process that we do not model in the simulation (e.g. erosion or positive depositional topography).

As there is no evidence of this over thickening within our seismic, our interpretation is that there has been substantial erosion on the northern section of the High. Close inspection of the seismic data on the northern flank shows evidence of erosive features between the mapped horizons which agrees with our assessment (Figure 4.16). Taking into account the $\pm 25\text{m}$ tolerance of thickness within each modelled zone, we estimate that the amount of erosion at key points in the cross-section is from 0-25m on High-1, up to 70-95m in the deepest section of Mini-Basin-2 (Figure 4.15). We believe that this erosion is caused by the major sediment fairway that in the study area, where sediment enters Mini-Basin-2 from the south, flows northward running axially along High-1 into Mini-Basin-3. Quantifying the amount of eroded section could have implications for sediment delivery to successive mini-basins downslope, and possible reservoir intervals in those mini-basins.

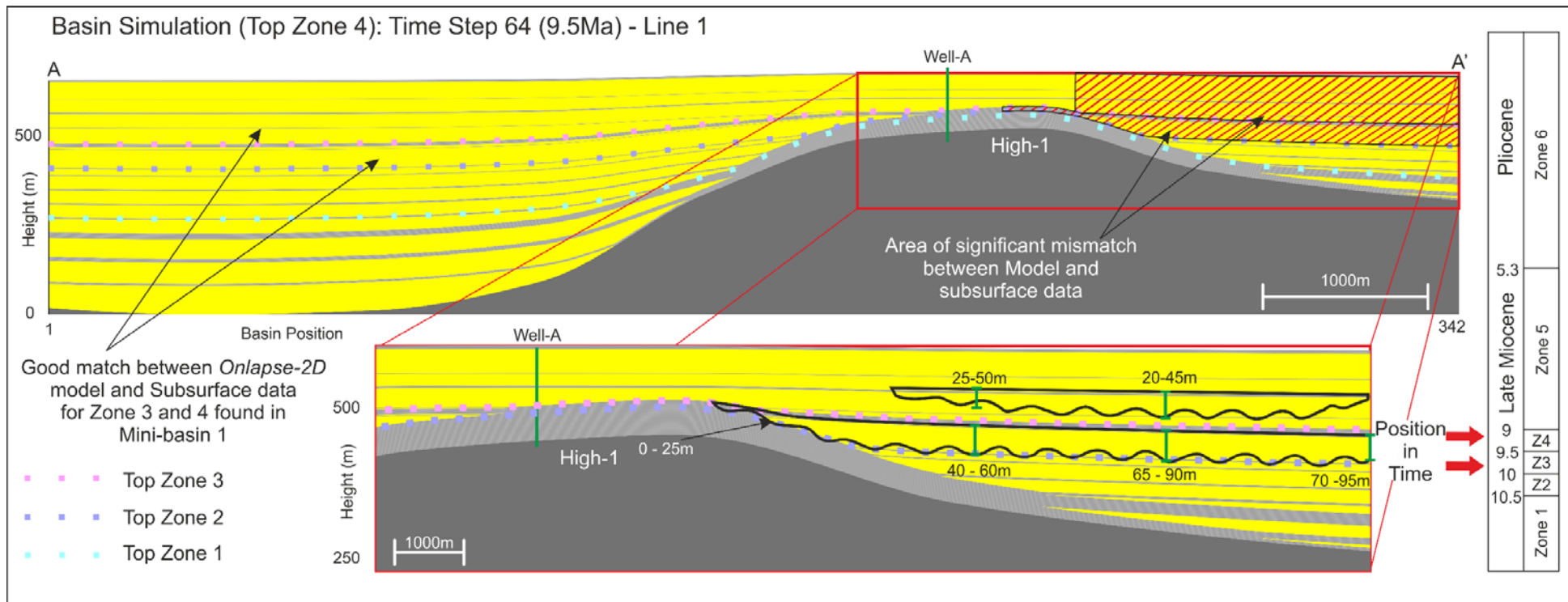


Figure 4.15 Basin simulation of Top Zone 4 of Line 1. A good match was achieved between the Onlapse-2D model and subsurface data in Zone – 3 & 4 in Mini-basin-1 and High-1. Red hashes show in Mini-basin 2 where for Zone 3 & 4 a significant mismatch occurred. Insert shows what Onlapse-2D simulated to develop, within Zone 3, an increasing amount of over-thickening is shown, and while for Zone 4 the over-thickening is more constrained to the centre of Mini-basin 2.

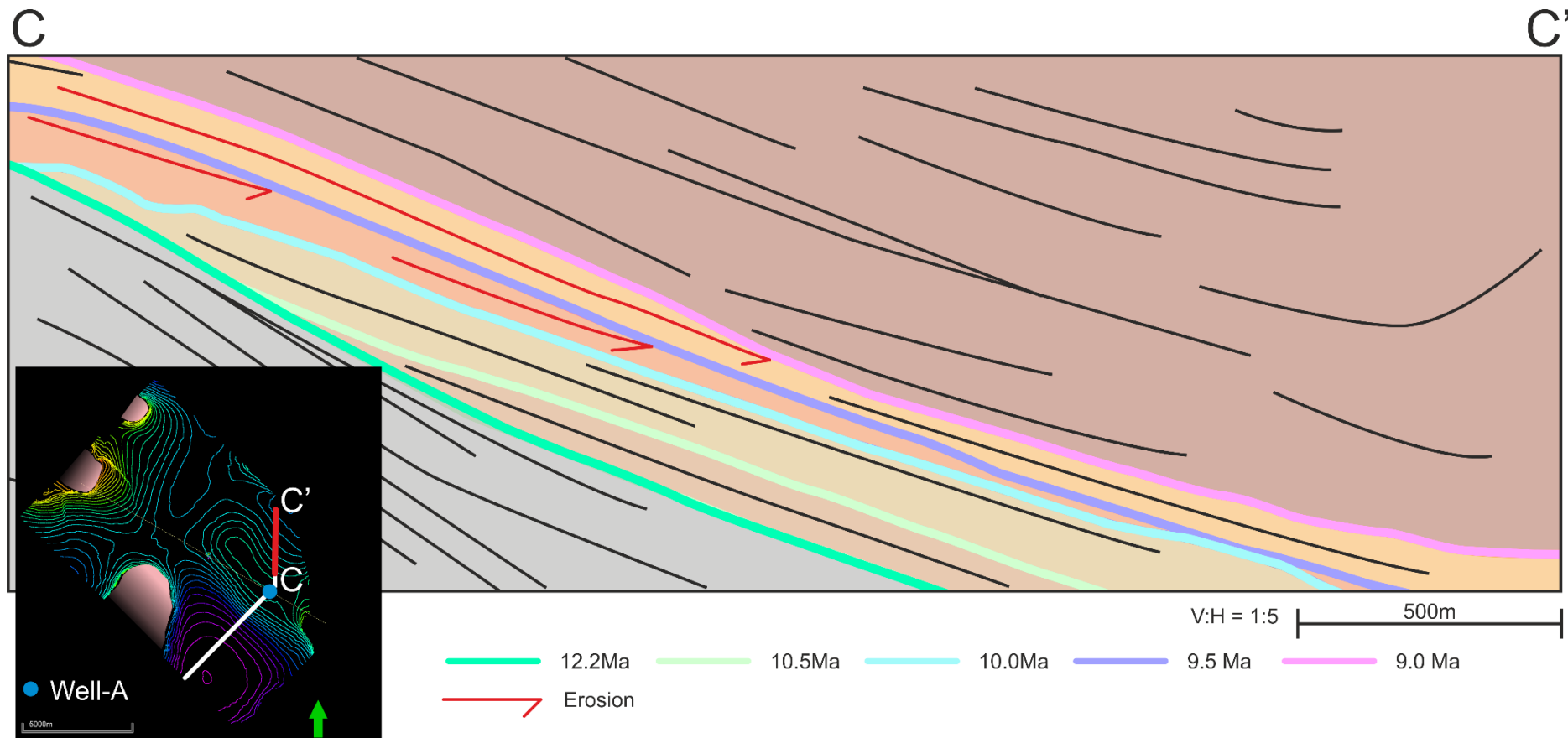


Figure 4.16 Geoseismic cross section focused on Mini-basin-2. Map insert shows location where geoseismic is taken from. Red arrows highlight that between 10.0Ma – 9.5Ma & 9.5Ma – 9.0Ma, seismic reflectors are eroded into by major horizons. This provides evidence that the mismatch between simulation and subsurface data occurs because there has been erosion within Mini-basin 2.

4.5.5.2 Informative Discrepancy in Line 2

Zone 4 of Line 2 contains another major discrepancy between the modelled *Onlapse-2D* simulation and the subsurface data. As shown in Table 5 matching the model to seismic data and Well-A, produced over-thickening of the clastic sediment deposited within the mini-basin to the north-west, ranging from 60m to 102m (Figure 4.17a).

Significant changes to the Structural Growth Profile, namely ceasing Fold Growth on High-1 (Figure 4.10) allowed us to lower this discrepancy between the model and the subsurface data. However, a discrepancy remained between the modelled simulation and the well and seismic data which we were unable to eliminate by means of further iterative changes in the inputs.

While there is evidence of erosion in Zone 3 and Zone 4 in the Line 1 seismic, close inspection of the seismic and well data provides no such evidence of erosion for either Zone in Line 2. This led us to the conclusion that positive topography found on High-1 was the cause of the significant mismatch between *Onlapse-2D* and the subsurface data. We attempted to match the thicknesses seen in Mini-basin-4 instead of attempting to match the thicknesses on High-1. This provided us with a much closer fit to the subsurface data, however we still found a mismatch in Well-A. This, however allowed us to estimate how much stratigraphy was missing within the model. From this we infer that the flanks of Mini-basin-4 there was around 5 – 30m of positive topography, and at Well-A there was between 45 – 70m (Figure 4.17b). Data from Well-A for Zone 4 supports this interpretation with the sands encountered in the well representing sedimentation in a proximal to marginal lobes position with thick intervals of stacked amalgamated sands.

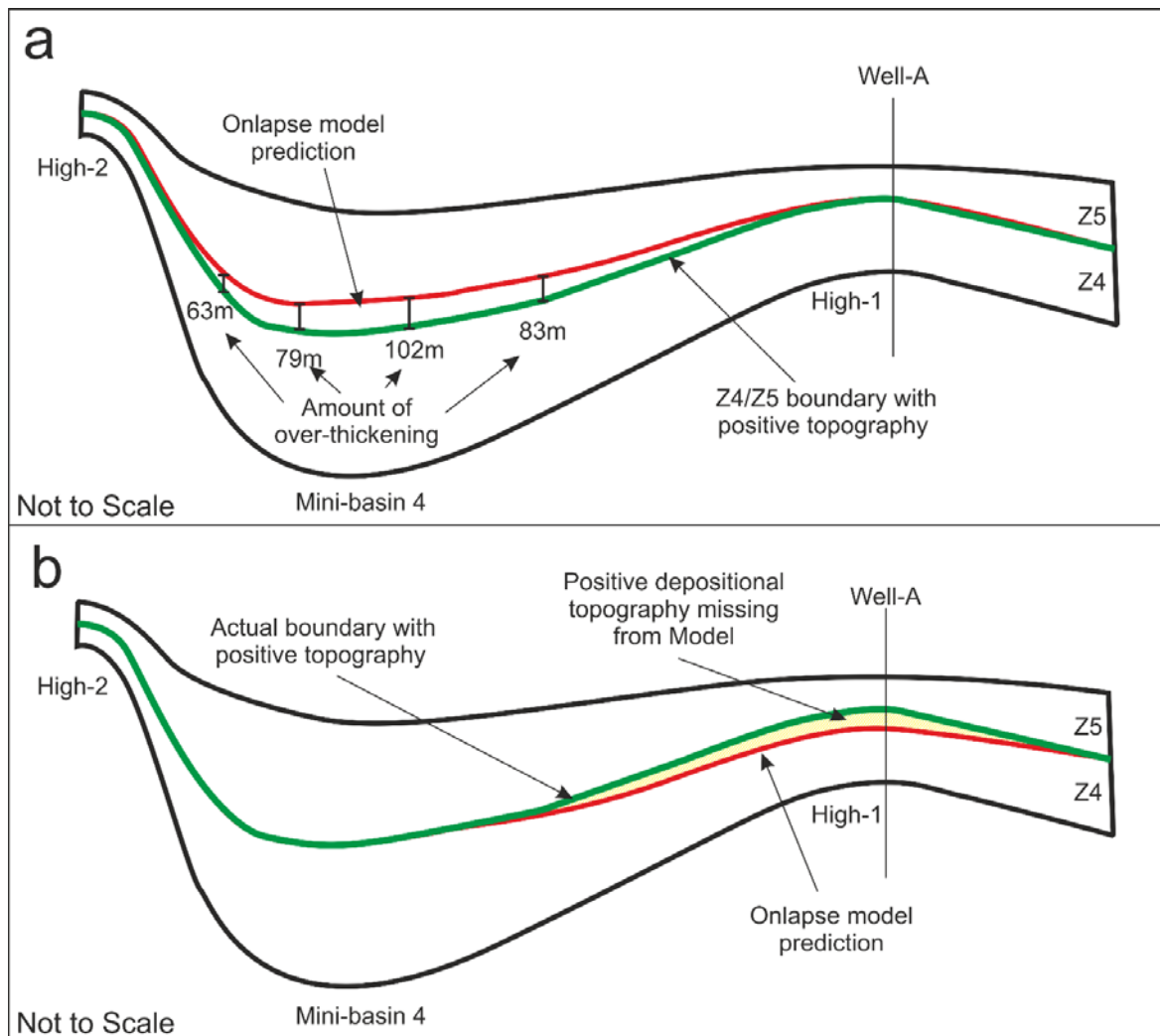


Figure 4.17 a) Schematic diagram of mismatch between the Onlapse-2D simulation and seismic data, with significant over-thickness within Mini-basin 4. Red horizon represents the original simulated boundary between Zone 4 & 5. Green horizon represents boundary between Zone 4 & 5 with positive depositional topography taken from seismic data. b) Schematic diagram of Onlapse-2D in final simulation, red horizon represents Onlapse-2D simulated horizon, which now matches the boundary seen in seismic in Mini-basin. From the difference between red and green horizon on High-1 we can infer the amount of positive depositional topography that is present

4.6 Conclusion

This case study has demonstrated the value of a modelling software that integrates dynamic topographic development of real structures with active deposition in the evolving palaeotopography. Specifically by seeking to precisely replicate the observed structural geometry and stratigraphic architecture provides powerful and unexpected insights into the processes of structural and stratigraphic evolution of the study area.

Through the integration of both seismic and well data into the *Onlapse*-2D model we have been able to successfully simulate the tectonostratigraphic evolution of two cross sections across the

study area in the Sureste Basin. We identified two distinct phases of compressional folding that were not parallel to each other and the long term effects of salt withdrawal and diapirism. We were able to integrate well data, age dated horizon interpretations, and seismic data to constrain and improve the modelled simulations produced by *Onlapse-2D* through a processes of iteration.

The best fit model for Line 2 illustrates that folding alone could not account for the stratal patterns observed in the seismic and well data and shows that structural movement resulting from salt tectonic patterns is required throughout the evolution of the cross-section. We are able to define the probable timing and rate of uplift during two phases of fold growth in the Late Miocene, and we were able to define the probable timing of salt withdrawal and diapirism which dominates the tectonics in the Late Pliocene. This is supported by independent evidence of timing of sand injectites.

While we achieve a good match between the final simulation and the subsurface data for much of the sections, there are minor but significant intervals in which the model is unable to produce a simulation that matches the data. These discrepancies prove to be valuable and correspond to intervals where there has been depositional topography created via erosion of previous deposits and constructional depositional topography. We term these *Informative Discrepancies*, and we are able to use their magnitude to estimate the amount of erosion or positive depositional topography that we could not model.

We have also demonstrated that the *Onlapse-2D* model outputs predict the distribution of potential reservoir and seal lithologies in parts of the basin away from direct well control.

4.7 Appendix Information

Found in Appendix C are the input parameters for Line 1, and Line 2.

Chapter 5 Conclusions

5.1 Main Findings

The main aim of this PhD was to develop a stratigraphic forward modelling program to aid in the exploration of hydrocarbons in deep-water sedimentary systems that occur in areas of poor data quality and coverage. To achieve this, the forward modelling program must be able to simulate the evolution of dynamic structural topography and sediment input in deep-water basins from real, readily available subsurface information. It must also be able to create geologically realistic simulations using only a small number of inputs so that the computational time and power needed is kept to a minimum. The forward modelling program must also establish its effectiveness in not only aiding in the exploration of hydrocarbons, but demonstrating its capability to better understand fundamental concepts.

Throughout this thesis I have demonstrated that the primary goals set out have been achieved. *Onlapse-2D* is a reduced complexity geometric based stratigraphic forward modelling program, it uses four physical inputs that can be derived from real subsurface data, to simulate the tectonostratigraphic evolution of deep-water mini-basins. It does this by a processes of iteration towards a best fit solution through hundreds of simulations. *Onlapse-2D* was also utilized to explore the domination of onlap over offlap in deep-water sedimentary systems. It illustrated that while offlap may in some circumstances be linked to changes in sediment supply there are instances in which the development of offlap is controlled primarily by local structural growth. Finally, I demonstrated that *Onlapse-2D* can be used as an aid in hydrocarbon exploration. It does this by simulating the tectonostratigraphic evolution of real basins and makes predictions on the distribution, thickness, and lateral extent of potential reservoir and sealing lithologies away from direct well control.

5.2 Chapter 2

The main findings of Chapter 2 are that I have successfully developed a 2D geometric stratigraphic forward modelling program, *Onlapse-2D* using a small number of inputs. The four inputs used are; Initial Basin Structure, rate of rise of a Structural Growth Profile, rate of rise of a Clastic Limiting Surface, and Background Sedimentation Rate. I have shown that *Onlapse-2D* is able to successfully simulate geologically realistic models of the tectonostratigraphic evolution of a range of idealized mini-basins. Using data from reflection seismic only, I was able to illustrate *Onlapse-2D*'s ability to accurately simulate the development of a real mini-basin from the Gulf of Mexico. Through this

modelling I was able to identify extrinsic autocyclic events that had a significant impact on the formation of basin stratigraphy.

5.3 Chapter 3

Chapter 3 shows how *Onlapse-2D* can be used to explore the fundamental concepts that govern deposition in deep-water sedimentary systems. This chapter highlights that the simulations produced by *Onlapse-2D* show a consistently similar imbalance where onlap dominates over offlap, both numerically and volumetrically to real world examples. This volumetric imbalance tends to be greater than the numerical imbalance due to the fact that offlapping units tend to be thinner than those that terminate in onlap.

Different patterns of simulated stratigraphy are generated by varying factors that describe the local rate of structural growth and sediment supply. The modelling suggests that the imbalance of offlap to onlap is not the result of an imbalance in the controlling factors, but a consequence of the way they combine to create stratigraphy in a structurally active basin. The modelling also indicates that in some cases, the temporal distribution of onlap and offlap can be entirely controlled by changes in the rate of structural activity. Therefore there is no necessary hardwired link between stratigraphic architecture in deep-water mini-basins and extrinsic processes such as changes in the relative sea-level.

5.4 Chapter 4

This chapter demonstrates the value of integrating dynamic topographic development of real structures with active deposition in an evolving palaeotopography using *Onlapse-2D*. Through this I was able to successfully simulate the tectonostratigraphic evolution of two cross-sections of Upper Miocene stratigraphy in age through the study area in the Sureste Basin matching seismic and well data. Using *Onlapse-2D* I was able to identify three phases of structural activity within the Upper Miocene, this included; two distinct phases of compressional folding that were not parallel to each other and a structural phase dominated by salt withdrawal and diapirism. I demonstrated that where the model could not be iterated towards a consensus with the subsurface data, it can be used to identify important geological factors through *Informative Discrepancies*. This included highlighting areas of depositional topography created through processes such as erosion or constructional deposition.

This chapter shows that *Onlapse-2D* is able to provide valuable information that can be used to predict the distribution of potential reservoir and seal rocks in areas away from direct well

control. Highlighting its potential to be used as an aid to exploration of hydrocarbons in deep-water sedimentary systems.

5.5 Future Work

While this thesis was ultimately successful in achieving the main aim, the development, testing and optimization process conducted throughout highlights where limitations remain. These limitations however, also provide a starting point when discussing the future direction of the research.

Several assumptions and uncertainties are made during the process of simulating models with *Onlapse-2D*. For example, the assumption is made that deposition comes from exclusively sediment gravity flows, there is no significant contribution from other processes such as carbonate build ups, and that all gravity flow deposit packages are horizontal at time of deposition. While these are good approximations for many simulations, this is not always the case. For example, mass-transport complexes do not always have a planar top or have to be laterally extensive. Investigating how to replicate this with the Clastic Limiting Surface could be useful in broadening the areas where *Onlapse-2D* can be utilized.

So far, *Onlapse-2D* has been used in continental margins affected by salt tectonics and thin-skinned fold and thrust belts. Exploring the use of *Onlapse-2D* in a diverse array of tectonic environments is an area which needs further research. Future testing should examine *Onlapse-2D*'s applicability to other basin types such as foreland basins, rift basins, and other tectonic settings such as extensional and strike-slip regimes.

Up to this point, the software has been used to generate generic models (Chapter 3) and to simulate real world examples where the geological control consists of reflection seismic and well data (Chapter 2 & 4). Chapter 3 also highlighted *Onlapse-2D*'s capability to investigate fundamental geological questions, such as if relative sea-level fall really is responsible for the development of offlap in deep-water sedimentary environments. Expanding on this, *Onlapse-2D* could be used to model outcrop examples and ascertain if there are multiple non-unique histories that could produce the stratal geometries seen. For example could the stratal terminations in deep-water turbidite basins that have been described as "sediment input controlled", such as the Gres d'Annot turbidite basin in the southern French Alps be produced in structurally active tectonic settings? Or vice versa, could stratal geometries seen in basin's that have been described as structurally controlled, such as the Gosau formation in the Austrian Alps be produced through varying sediment input rates?

Onlapse-2D has been used within the context of a single isolated basin, moving into modelling multiple, potentially linked basins provides an exciting opportunity to explore the capabilities of the program and the inputs used. For example, how does the Clastic Limiting Surface method for modelling sedimentation input work when modelling linked basins? Furthermore, adding the capability to simulate more geological processes, especially the effect of compaction remains a high priority. Testing to see what effect this has on the stratal geometries produced using a combination of idealized mini-basins and real-world mini-basin would naturally come next. Because of its novel capabilities to simulate the evolution of basin fill architecture incredibly rapidly, *Onlapse-2D* could be a prime candidate to explore the use of machine learning. One potential is to explore the use of optimization algorithms that can automate the program's ability to hunt for a best fit solution through changing the input values used.

The overall aim of further development however, would be to take *Onlapse-2D* develop it into *Onlapse-3D*. This is because as highlighted by Paper 3/Chapter 4, structural growth can be highly three-dimensional, so analysis using 2D lines only may not always be sufficient. While a 2D approach can provide valuable information, it is possible that a 2D approach may underestimate the complexity of the structural history.

Appendix A Chapter 2: A new geometric tool to model tectonostratigraphic evolution of deep-water basins

A.1 Inputs for Hypothetical Basins:

A.1.1 Symmetrical Basin

Basin Length	Matrix Spacing	Simulation Time	Time per step	Total TS	HR
15000	12.5	1000000	10000	100	1200

Figure 5.1 Bounding conditions for Symmetrical Basin

Initial Basin Height	IBH Position	Absolute Structural Growth Rate (mm/y)	SGR Position
150	1	1	1
150	340	1	240
140	600	0	600
150	960	1	960
150	1200	1	1200

Figure 5.2 Initial Basin Height and Position in Matrix, along with Absolute Structural Growth Rate and their position

Structural Growth Amplification Rate	Amplification Position
0.5	1
1	12
0.5	25
0	38
0.5	50
1	63
0.5	75
0	87
0.5	100

Figure 5.3 Structural Growth Amplification Rate initial inputs

Appendix A

Initial Clastic Limiting Surface	Initial CLS Position
140	1
140	1200
CLS Growth Per Time Step (mm/y)	CLS Growth Position
1	1
1	1200

Figure 5.4 Initial Clastic Limiting Surface and Positions in Matrix, along with the growth per time step and its position in matrix

CLS Amplification Rate	CLS Amplification Rate Position
1	1
1	16
0	17
0	32
1	33
1	50
0	51
0	68
1	69
1	84
0	85
0	100

Figure 5.5 Clastic Limiting Surface Amplification Rate Input parameters

Background Sediment Growth Rate (mm/year)	Background Sediment Growth Rate position
0.25	1
0.25	1200
Background Sediment Growth Rate Amp	Background Sediment Amp Position
1	1
1	100

Figure 5.6 Background Sediment input parameters

A.1.2 Asymmetrical Basin

Basin Length	Matrix Spacing	Simulation Time	Time per step	Total TS	HR
15000	12.5	1000000	10000	100	1200

Figure 5.7 Initial Basin bounding conditions

Initial Basin Height	IBH Position
150	1
150	240
50	760
150	920
150	1200

Figure 5.8 Initial Basin Height and Position in matrix

Structural Growth Amplification Rate	Amplification Position
1	1
1	100
Absolute Structural Growth Rate (mm/y)	SGR Position
0.5	1
0.5	240
0	760
0.5	920
0.5	1200

Figure 5.9 Structural Growth input parameters

Initial Clastic Limiting Surface	Initial CLS Position
50	1
50	1200
CLS Growth Per Time Step (mm/y)	CLS Growth Position
1	1
10	1200
CLS Amplification Rate	CLS Amplification Rate Position
1	1
0	16
1	32
0	50
1	68
0	84
1	100

Figure 5.10 Clastic Limiting Surface input parameters

Background Sediment Growth Rate (mm/year)	Background Sediment Growth Rate position
0.25	1
0.25	1200
Background Sediment Growth Rate Amp	Background Sediment Amp Position
1	1
1	100

Figure 5.11 Background Sediment input parameters

A.1.3 Tilted Strata

Basin Length	Matrix Spacing	Simulation Time	Time per step	Total TS	HR
15000	12.5	1000000	10000	50	1200

Figure 5.12 Bounding conditions

Initial Basin Height	IBH Position
0	1
0	1200

Figure 5.13 Input conditions for initial basin structure

Absolute Tilt Rate (mm/y)	Tilt Position
0	1
1.3	1200
Structural Tilt Amplification Rate	Amplification Position
1	1
1	50

Figure 5.14 Structural growth input parameters

Initial Clastic Limiting Surface	Initial CLS Position
0	1
0	1200
CLS Growth Per Time Step (mm/y)	CLS Growth Position
0.75	1
0.75	1200
CLS Amplification Rate	CLS Amplification Rate Position
0	1
0	9
1	10
1	19
0	20
0	29
1	30
1	39
0	40
0	20
3	631

Figure 5.15 Clastic Limiting Surface input parameters

Background Sediment Growth Rate (mm/year)	Background Sediment Growth Rate position
0.25	1
0.25	1200
Background Sediment Growth Rate Amp	Background Sediment Amp Position
1	1
1	100

Figure 5.16 Background Sediment input parameters

A.1.4 Turtle Anticline

Basin Length	Matrix Spacing	Simulation Time	Time per step	Total TS	HR
15750	25	1000000	10000	100	631

Figure 5.17 Bounding Conditions used

Initial Basin Height	IBH Position
0	1
0	631

Figure 5.18 Initial Basin Structure conditions

Profile 1		Profile 1	
Absolute Structural Growth Rate (mm/y)	SGR Position	Structural Growth Amplification Rate	Amplification Position
1.25	1	1	1
1.25	30	1	35
0	316	0	65
1.25	601	0	100
1.25	631		
Profile 2		Profile 2	
Absolute Structural Growth Rate (mm/y)	SGR Position	Structural Growth Amplification Rate	Amplification Position
0.5	1	0	1
0	157	0	35
0.5	316	1	65
0	473	1	100
0.5	631		

Figure 5.19 Structural Growth Profile and Rate input parameters for Profile 1 and Profile 2

Appendix A

Initial Clastic Limiting Surface	Initial CLS Position
0	1
0	631
CLS Growth Per Time Step (mm/y)	CLS Growth Position
3	1
3	631
CLS Amplification Rate	CLS Amplification Rate Position
0.2	1
0.6	30
0.3	50
0.2	70
0.3	90
0.3	100

Figure 5.20 Input Parameters for Clastic Limiting Surface Profile and Rise as well as initial starting positions

Background Sediment Growth Rate (mm/year)	Background Sediment Growth Rate position
0.3	1
0.3	631
Background Sediment Growth Rate Amp	Background Sediment Amp Position
1	1
1	100

Figure 5.21 Input parameters for Background Sedimentation

A.2 Inputs for SymB1

A.2.1 Run 26

Basin Length	Matrix Spacing	Simulation Time	Time per step	Total TS	HR
15750	25	1000000	10000	100	631

Figure 5.22 Bounding Conditions for Run 26 of SymB1

Initial Basin Height	IBH Position
166	1
166	40
166	80
166	120
166	160
166	170
64	200
38	240
0	280
4	320
8	360
32	400
74	440
103	480
166	504
166	520
166	560
166	600
166	631

Figure 5.23 Input parameters for Initial Basin Structure

Absolute Structural Growth Rate (mm/y)	SGR Position	Structural Growth Amplification Rate	Amplification Position
2.44674213	1	1	1
2.209960633	52	1	100
1.999488192	105		
1.604852365	158		
0.999744096	210		
0.447253938	263		
0.05261811	315		
0	336		
0.092061693	368		
0.447253938	420		
1.104980317	473		
1.973179137	525		
2.49936024	578		
2.630905516	631		

Figure 5.24 Input parameters for Structural Growth Profile and Rate

Initial Clastic Limiting Surf.	Initial CLS Position	CLS Growth Per Time Step (mm/y)	CLS Growth Position
0	1	6.5616798	1
0	631	6.5616798	631

Figure 5.25 Input parameters for initial starting height of Clastic Limiting Surface and Growth per Time-Step

Appendix A

CLS Amplification Rate	CLS Amplification Rate Position
0	1
0	18
2.75	19
1	23
0	24
0	29
4	30
2	31
0	32
0	33
2.8	34
0	35
0	38
1.5	39
0.5	44
0	45
0	50
3	51
0	52
0	55
0.9	56
0	57
0	63
5	64
0	65
1	66
0	67
0	75
0.7	76
0.7	81
0	82
0	91
0.8	92
0	96
0	100

Figure 5.26 Input parameters for Clastic Limiting Surface Rise Amplification rate

Background Sediment Growth Rate (mm/year)	Background Sediment Growth Rate position
0.32808399	1
0.32808399	631
Background Sediment Growth Rate Amp	Background Sediment Amp Position
1	1
1	100

Figure 5.27 Input parameters for Background Sedimentation Rate

A.2.2 Run 39

Basin Length	Matrix Spacing	Simulation Time	Time per step	Total TS	HR
15750	25	1000000	10000	100	631

Figure 5.28 Bounding Conditions for Run 39 of Symb1

Initial Basin Height	IBH Position
175	1
175	40
175	80
175	120
175	122
115	160
90	200
70	240
0	280
6	320
12	360
40	400
117	440
175	478
175	480
175	506
175	520
175	560
175	600
175	631

Figure 5.29 Input parameters for Initial Basin Height

Absolute SGR P1 (mm/y)	SGR Position	Absolute SGR P2 (mm/y)	SGR Position
2.300371123	1	2.545278552	1
1.868042574	40	2.362331142	40
1.851720662	80	2.201051057	80
1.607886835	120	2.006547104	120
0.968801817	160	1.755782222	160
0.769214074	200	1.227779905	200
0.625167557	240	0.687140925	240
0.297668837	280	0.230075849	280
0.016799652	320	0	337
0	360	0.060956197	360
0.280081701	400	0.276332835	400
0.643424054	440	0.662822467	440
0.897731413	480	1.264479122	480
1.79191915	520	1.982685355	520
2.439440744	560	2.388941955	560
2.484668557	600	2.671867828	600
2.526654563	631	2.716832863	631

Figure 5.30 Input parameters for Structural Growth Profile 1 and 2

SG Amp P1	Amp Position	SGR Amp P2	Amp Position
1	1	0	1
1	20	0	20
0	30	1	30
0	100	1	100

Figure 5.31 Input parameters for Structural Growth Profile 1 and 2 amplitudes

Initial Clastic Limiting Surf	Initial CLS Position	CLS Growth Per Time Step (mm/y)	CLS Growth Position
0	1	6.5616798	1
0	631	6.5616798	631

Figure 5.32 Input parameters for Clastic Limiting Surface profile and initial height

Appendix A

CLS Amplification Rate	CLS Amplification Rate Position
1.44	1
0.9	4
0	5
0	6
1.6625	7
0	8
0	9
1.1875	10
0	12
0	24
5.13	25
0	26
0	32
1.1	34
0	37
1	38
0.9	43
0	44
0	54
0.9	55
0.5	59
0	60
0	65
5.5	66
0	67
0	72
1.2	73
0	76
0	79
0.7	81
0.4	86
0	87
0.9	88
0	89
0.75	90
0	91
0	100

Figure 5.33 Input parameters for Clastic Limiting Surface rate of rise (amplitude)

Background Sediment Growth Rate (mm/year)	Background Sediment Growth Rate position	k
0.32808399		1
0.32808399		631
Background Sediment Growth Rate Amp	Background Sediment Amp Position	
1		1
1		100

Figure 5.34 Input parameters for Background Sedimentation rate

Appendix B Chapter 3: Conditions favouring Onlap and Offlap: Why are onlaps common, and offlaps rare?

B.1 Input Parameters for Basins

Initial Basin Structure	
Height (m)	Position
150	1
150	80
50	200
150	320
150	400
Initial Basin Inputs	
Total Basin Length (m)	10000
Horizontal Resolution (m)	25
Total Simulation Time (y)	1000000
Time per step (y)	10000
Total Time Steps	100
Number of Columns	400

Figure 5.35 Input parameters for Initial Basin Structure and Bounding conditions

Background Sediment	
Background Sediment GR (mm/year)	Background Sediment GR position
0.25	1
0.25	400
Background Sediment GR Amp	Background Sediment Amp Position
1	1
1	100

Figure 5.36 Input parameters for Background Sedimentation Rate

Structural Growth Rate	
Constant	
Structural Growth Amplification Rate	Amplification Position
1	1
1	100
Sin - Decreasing (On)	
Structural Growth Amplification Rate	Amplification Position
1	1
0	34
1	66
0	100
Sin - Increasing (Off)	
Structural Growth Amplification Rate	Amplification Position
0	1
1	34
0	66
1	100
Lin - Increasing	
Structural Growth Amplification Rate	Amplification Position
0.5	1
1	100

Figure 5.37 Input parameters for Structural Growth Rate Amplitude

Absolute Structural Growth Rate (mm/y)			
Low		SGR Position	
	0.75		1
	0.75		80
	0		200
	0.75		320
	0.75		400
Medium		SGR Position	
	1.5		1
	1.5		80
	0		200
	1.5		320
	1.5		400
High		SGR Position	
	2.25		1
	2.25		80
	0		200
	2.25		320
	2.25		400

Figure 5.38 Input parameters for Structural Growth Profile

Clastic Limiting Surface	
Constant	
CLS Amplification Rate	CLS Amplification Rate Position
1	1
1	100
Binary - On	
CLS Amplification Rate	CLS Amplification Rate Position
1	1
1	33
0	34
0	50
1	51
1	84
0	85
0	100
Binary - Off	
CLS Amplification Rate	CLS Amplification Rate Position
0	1
0	15
1	16
1	49
0	50
0	66
1	67
1	100

Figure 5.39 Input parameters for Clastic Limiting Surface Profile Rise

Sin - On (Decreasing)	
CLS Amplification Rate	CLS Amplification Rate Position
1	1
0	16
1	32
0	50
1	68
0	84
1	100
Sin - Off (Increasing)	
CLS Amplification Rate	CLS Amplification Rate Position
0	1
1	16
0	32
1	50
0	68
1	84
0	100

Figure 5.40 Input parameters for Clastic Limiting Surface Profile Rise continued

CLS Growth Rates (mm/y)	
Low	CLS Growth Rate Position
0.55	1
0.55	400
Medium	CLS Growth Rate Position
0.65	1
0.65	400
High	CLS Growth Rate Position
0.8	1
0.8	400

Figure 5.41 Input parameters for Low, Medium, High Clastic Limiting Surface Profiles

B.2 Horizontal Resolution Increase Inputs

Initial Basin Inputs - HR Inc	
Total Basin Length (m)	10000
Horizontal Resolution (m)	10
Total Simulation Time (y)	1000000
Time per step (y)	10000
Total Time Steps	100
Number of Columns	1000
Initial Basin Structure HR	
Height (m)	Position
150	1
150	200
50	500
150	800
150	1000

Figure 5.42 Input parameters for Initial Basin Structure and Bounding Conditions

Absolute Structural Growth Rate (mm/y) - HR	
Low	SGR Position
0.75	1
0.75	200
0	500
0.75	800
0.75	1000
Medium	SGR Position
1.5	1
1.5	200
0	500
1.5	800
1.5	1000
High	SGR Position
2.25	1
2.25	200
0	500
2.25	800
2.25	1000

Figure 5.43 Input Parameters for Structural Growth Profile HR increase

B.3 Time-Step Increase Inputs

Initial Basin Structure	
Height (m)	Position
150	1
150	80
50	200
150	320
150	400
Initial Basin Inputs	
Total Basin Length (m)	10000
Horizontal Resolution (m)	25
Total Simulation Time (y)	1000000
Time per step (y)	5000
Total Time Steps	200
Number of Columns	400

Figure 5.44 Input parameters for Initial Basin Structure and Bounding Conditions

Clastic Limiting Surface	
Constant	
CLS Amplification Rate	CLS Amplification Rate Position
1	1
1	200
Binary - On	
CLS Amplification Rate	CLS Amplification Rate Position
1	1
1	66
0	67
0	100
1	101
1	168
0	169
0	200
Binary - Off	
CLS Amplification Rate	CLS Amplification Rate Position
0	1
0	30
1	31
1	99
0	100
0	132
1	133
1	200

Figure 5.45 Input parameters for Clastic Limiting Surface Profile Rise

Sin - On (Decreasing)	
CLS Amplification Rate	CLS Amplification Rate Position
1	1
0	32
1	64
0	100
1	136
0	168
1	200
Sin - Off (Increasing)	
CLS Amplification Rate	CLS Amplification Rate Position
0	1
1	32
0	64
1	100
0	136
1	168
0	200

Figure 5.46 Input parameters for Clastic Limiting Surface Profile Rise continued

CLS Growth Rates (mm/y)	
Low	CLS Growth Rate Position
0.55	1
0.55	400
Medium	CLS Growth Rate Position
0.65	1
0.65	400
High	CLS Growth Rate Position
0.8	1
0.8	400

Figure 5.47 Input Parameters for Clastic Limiting Surface Profile

B.3.1 Total Number of Beds Raw Numbers

Appendix B

Total Number of Beds

	A	B	C	D	E	F	G	H	I	J	K	L
1	99	99	99	99	99	99	99	99	99	99	99	99
2	35	35	35	35	35	35	35	35	35	35	35	35
3	51	51	51	51	51	51	51	51	51	51	51	51
4	60	60	60	60	60	60	60	60	60	60	60	60
5	54	54	54	54	54	54	54	54	54	54	54	54
6	99	99	99	99	99	99	99	99	99	99	99	99
7	26	26	26	26	26	26	26	26	26	26	26	26
8	42	42	42	42	42	42	42	42	42	42	42	42
9	57	57	57	57	57	57	57	57	57	57	57	57
10	48	48	48	48	48	48	48	48	48	48	48	48
11	99	99	99	99	99	99	99	99	99	99	99	99
12	16	16	16	16	16	16	16	16	16	16	16	16
13	31	31	31	31	31	31	31	31	31	31	31	31
14	53	53	53	53	53	53	53	53	53	53	53	53
15	41	41	41	41	41	41	41	41	41	41	41	41

Table 5 Total number of Gravity Flow deposits

Total Number of Offlapping Surfaces

	A	B	C	D	E	F	G	H	I	J	K	L
1	0	10	4	11	0	15	15	9	0	15	20	9
2	5	5	3	5	6	5	4	5	6	6	4	7
3	8	7	6	9	9	8	8	9	9	8	9	10
4	0	0	0	0	0	0	7	0	0	0	11	0
5	0	0	0	0	0	0	0	0	0	0	0	0
6	0	13	7	7	0	13	14	8	0	15	17	7
7	3	4	1	2	3	4	2	3	4	4	2	3
8	5	3	5	6	5	5	6	7	5	6	6	7
9	0	0	0	0	0	0	6	0	0	0	8	0
10	0	0	0	0	0	0	0	0	0	0	0	0
11	0	13	7	5	0	12	13	6	0	13	15	6
12	0	0	0	0	1	1	0	0	1	2	0	1
13	3	2	3	2	3	2	4	4	3	2	4	3
14	0	0	0	0	0	0	5	0	0	0	7	0
15	0	0	0	0	0	0	0	0	0	0	0	0

Table 6 Total Number of Gravity Flow Deposits that terminate in Offlap

Total Number of Static Pinchout Surfaces

	A	B	C	D	E	F	G	H	I	J	K	L
1	63	35	46	45	78	28	45	66	84	33	49	72
2	8	2	7	5	7	6	7	7	8	6	8	5
3	6	5	6	4	8	8	10	7	11	9	11	7
4	9	2	9	3	22	7	14	16	30	10	15	24
5	8	0	6	2	15	3	19	13	19	7	24	17
6	69	23	38	57	80	33	52	69	85	41	56	75
7	5	3	5	5	7	4	6	4	7	5	8	6
8	4	8	5	4	11	8	8	6	11	8	11	7
9	13	3	13	8	24	7	15	19	29	12	17	25
10	8	0	11	4	15	5	21	13	19	9	24	16
11	72	28	50	63	82	40	58	74	87	48	62	78
12	5	5	2	3	4	4	5	4	5	7	5	3
13	6	5	4	5	8	6	6	5	8	7	7	3
14	15	2	15	9	24	7	16	20	30	15	18	26
15	7	0	11	9	12	3	19	11	17	8	21	14

Table 7 Total number of Gravity Flow Deposits that terminate in Static Pinchout

Total Number of Onlapping Surfaces

	A	B	C	D	E	F	G	H	I	J	K	L
1	36	54	49	43	21	56	39	24	15	51	30	18
2	22	28	25	25	22	24	24	23	21	23	23	23
3	37	39	39	38	34	35	33	35	31	34	31	34
4	51	58	51	57	38	53	39	44	30	50	34	36
5	46	54	48	52	39	51	35	41	35	47	30	37
6	30	63	54	35	19	53	33	22	14	43	26	17
7	18	19	20	19	16	18	18	19	15	17	16	17
8	33	31	32	32	26	29	28	29	26	28	25	28
9	44	54	44	49	33	50	36	38	28	45	32	32
10	40	48	37	44	33	43	27	35	29	39	24	32
11	27	58	42	31	17	47	28	19	12	38	22	15
12	11	11	14	13	11	11	11	12	10	7	11	12
13	22	24	24	24	20	23	21	22	20	22	20	25
14	38	51	38	44	29	46	32	33	23	38	28	27
15	34	41	30	32	29	38	22	30	24	33	20	27

Table 8 Total number of Gravity Flow Deposits that terminate in Onlap

Horizontal Resolution				
	Total Beds	Onlap	Offlap	Static Pinchout
C2	35	29	3	3
B7	26	22	2	2
B11	99	71	14	14
H11	99	22	15	62
G13	31	24	4	3
K4	60	40	15	5
L1	99	25	22	52

Table 9 Total Number of Gravity Flow Deposits, and number that end in Onlap, Offlap, and Static Pinchout

Time-Step				
	Total Beds	Onlap	Offlap	Static Pinchout
C2	32	20	2	10
B7	51	33	4	14
B11	199	101	22	76
H11	199	29	7	163
G13	83	41	13	29
K4	119	55	11	53
L1	199	26	9	164

Table 10 Total number of Gravity flow Deposits, and number that end in Onlap, Offlap, and Static Pinchout

Appendix C Chapter 4 : Forward Stratigraphic Modelling with *Onlapse-2D* for Reservoir Prediction: Offshore Sureste Basin, Mexico

C.1 Input Parameters Line 1

Basin Length	Horizontal Resolution	Simulation Time	Time per step	Total TS	HR
8550	25	12200000	500000	244	342

Figure 5.48 Bounding Conditions

Initial Basin Height	IBH Position
12.6	1
0	40
0.6	80
37.8	120
130	160
160.44	200
172.8	218
185	240
140.7	280
123.06	320
117.18	342

Figure 5.49 Input parameters for Initial Basin Structure

Absolute Structural Growth Rate (mm/y)	SGR Position
0.001983443	1
0	40
0.003622951	80
0.017092623	120
0.060767294	160
0.104658248	200
0.106010492	218
0.10535628	240
0.0825782	280
0.069052311	320
0.059869363	342
Amplification Rate SGR	Amp SGR Position
1	1
1	244

Figure 5.50 Input parameters for Structural Growth Profile and Rise

Initial Clastic Limiting Surface	Initial CLS Position
80	1
80	342
CLS Growth Per Time Step (mm/y)	CLS Growth Position
0.16	1
0.16	342

Figure 5.51 Input parameters for Clastic Limiting Surface

CLS Amplification Rate	CLS Amplification Rate Position
0	1
0	4
8	5
0	6
0	14
8	15
0	16
0	29
6.8	30
0	31
0	33
5	34
0	35
0	37
5	38
0	39
0	40
5	41
0	42
2.5	43
0	44
6.7	45
1	46
0	47
0	50
0	51
0	53
6.5	54
5	55
0	56
0	57
5	58
6	59
0	60

Figure 5.52 Input parameters for Clastic Limiting Surface continued

CLS Amplification Rate	CLS Amplification Rate Position
0	64
6	65
4	69
3	70
2.1	71
0	72
0	88
5	89
5	92
0	94
2	95
0	97
0	109
4	110
2.5	111
0	112
0	114
4	115
0	116
0	122
4.8	124
4	125
1.2	126
0	127
0	134
5	135
0	136
0	138

Figure 5.53 Input parameters for Clastic Limiting Surface continued

CLS Amplification Rate	CLS Amplification Rate Position
0	144
0	145
7	146
0	147
0	148
0	151
6.5	152
0	153
0	159
5.5	160
0	162
0	163
4.2	164
0	165
0	169
4.2	170
0	172
0	174
4.2	175
0	177
0	180
4.2	181
0	185
0	186
12	187
0	188
0	190
5	191
2	193
2	195
0	196
0	198
4	199
0	201
0	202
0	203
7.5	204
0	205
0	206
4	207
3	209
0	210
0	212
15	213
0	214
0	215
3	216
3	226
0	227
0	231
10	232
0	233
5	234
3	236
1.25	237
3	238
3	240
6	241
3	242
3	244

Figure 5.54 Input parameters for Clastic Limiting Surface continued

Background Sediment Growth Rate (mm/year)		Background Sediment Growth Rate position	
	0.022		1
	0.022		342
Background Sediment Growth Rate Amp		Background Sediment Amp Position	
1	1		1
2	1		80
	2.127		88
	2.127		128
	2.6		138
	2.6		204
	5		244

Figure 5.55 Input parameters for Background Sedimentation

C.2 Input Parameters Line 2

Basin Length	Horizontal Resolution	Simulation Time	Time per step	Total TS	HR
10875	25	12200000	500000	244	435

Figure 5.56 Bounding Conditions Line 2

Initial Basin Height	IBH Position
180	1
90	40
70	80
65	120
80	160
110	200
120	242
150	280
170	320
172.8	367
190	400
260	435

Figure 5.57 Input Parameters for Initial Basin Structure

Amplification Rate SGR P1	Amp SGR Position P1	Amplification Rate SGR P2	Amp SGR Position P2
0.5	1	0.2	1
0.8	20	0.4	35
1	40	0.65	40
1.5	42	0.7	50
1.7	50	0.8	85
1.7	55	0.85	100
1.7	59	0.9	120
0	65	1.5	150
0	80	2.15	244
2.6	88		
1.2	120		
1	175		
0.3	200		
0	244		

Figure 5.58 Input parameters for Line 2 Structural Growth Profile amplitudes

Absolute SGR (mm/y) P1	SGR Position
0.041909582	1
0.034620641	40
0.02755519	80
0.024348328	120
0.029043611	160
0.042985909	200
0.0495	220
0.055380437	242
0.074885028	280
0.085974269	320
0.088701935	367
0.084266641	400
0.067409414	435
Absolute SGR (mm/y) P2	SGR Position
0.135944205	1
0.089580908	40
0.071299055	80
0.055222008	120
0.04576734	160
0.03806044	200
0.033330818	242
0.02814113	280
0.027202796	320
0.023462687	367
0.022698085	400
0.048871825	435

Figure 5.59 Input parameters for Line 2 Structural Growth Profiles

CLS Amplification Rate	CLS Amplification Rate Position
0	1
0	4
8	5
0	6
0	14
8	15
0	16
0	29
6.8	30
0	31
0	33
5.5	34
0	35
0	37
5	38
0	39
0	40
4.5	41
0	42
2.5	43
0	46
5	47
0	48
2.5	49
0	50
0	51
0	53
0	54
0	55
0	58
5	60
3.75	61
2	62
0	63

Figure 5.60 Input parameters for Clastic Limiting Surface Profile rate of rise

CLS Amplification Rate	CLS Amplification Rate Position
2	64
4	65
1	68
0	72
0	73
1.5	74
1	76
0	77
0	86
1.3	87
1.3	88
10	89
1.3	90
1.3	110
1.3	111
1.3	112
1.3	114
1.3	115
1.3	116
1.3	122
1.3	124
1.3	125
1.3	126
1.3	129
5	130
1.3	131
1.3	136
1.3	138

Figure 5.61 Input parameters for Clastic Limiting Surface Profile rate of rise continued

CLS Amplification Rate	CLS Amplification Rate Position
0	144
0	145
7	146
0	147
0	148
0	151
6.5	152
0	153
0	159
5.5	160
0	162
0	163
4.2	164
0	165
0	169
4.2	170
0	172
0	174
4.2	175
0	177
0	180
4.2	181
0	185
0	186
8.7	187
0.25	188
0.25	190
5	191
2	193
2	195
0.25	196
0.25	198
4	199
0.25	201
0.25	202
0.5	203
7.5	204
1	205
1	206
4	207
3	209
1	210
1	212
14	213
1	214
1	215
3	216
3	226
1	227
1	231
8	232
1	233
5	234
3	236
1.25	237
3	238
3	240
6	241
3	242
3	244

Figure 5.62 Input parameters for Clastic Limiting Surface Profile rate of rise continued

Background Sediment Growth Rate (mm/year)	Background Sediment Growth Rate position
0.022	1
0.022	435
Background Sediment Growth Rate Amp	Background Sediment Amp Position
1	1
1	80
2.127	88
2.127	128
2.6	138
2.6	204
5	244

Figure 5.63 Input parameters for Background Sedimentation Rate

Bibliography

- Allan, J. R., Sun, S. Q. & Trice, R., 2006. The deliberate search for stratigraphic and subtle combination traps: where are we now?. *Geological Society, London, Special Publications*, 1 January, Volume 254, pp. 57 - 103.
- Allen, P. A. & Allen, J. R., 2013. *Basin Analysis: Principles and Application to Petroleum Play Assessment, 3rd Edition*. s.l.:Wiley-Blackwell.
- Amy, L. A., 2019. A review of producing fields inferred to have upslope stratigraphically trapped turbidite reservoirs: trapping styles (pure and combined), pinchout formation and depositional setting. *AAPG Bulletin*, December, 103(12), pp. 2860 - 2889.
- Amy, L. A., Mccaffrey, W. D. & Kneller, B. C., 2004. The influence of a lateral basin-slope on the depositional patterns of natural and experimental turbidity currents. *Geological Society Special Publication*, Volume 221, pp. 311-330.
- Baas, J. H., 2004. Conditions of formation of massive turbiditic sandstones by primary depositional processes. *Sedimentary Geology*, Volume 166, pp. 293 - 310.
- Bakke, K. et al., 2013. Seismic modelling in the analysis of deep-water sandstone termination styles. *AAPG Bulletin*, 97(9).
- Barrett, B. J., Hodgson, D. M., Collier, R. E. & Dorrell, R. M., 2018. Novel 3D sequence stratigraphic numerical model for syn-rift basins: Analysing architectural responses to eustasy, sedimentation, and tectonics. *Marine and Petroleum Geology*, Volume 92, pp. 270 - 284.
- Basani, R. et al., 2014. MassFLOW-3DTM as a simulation tool for turbidity currents: some preliminary results. In: A. W. Martinus, et al. eds. *Depositional Systems to Sedimentary Successions on the Norwegian Continental Margin*. s.l.:International Association of Sedimentologists, pp. 587 - 608.
- Behera, L., 2006. *Sub-basalt imaging using converted waves: A numerical approach*. s.l., SEG, pp. 2318 - 2322.
- Bouma, A. H., 2004. Key controls on the characteristics of turbidite systems. *Geological Society, London, Special Publications*, Volume 222, pp. 9 - 22.
- Bourget, J., Ainsworth, R. B. & Thompson, S., 2014. Seismic stratigraphy and geomorphology of a tide or wave dominated shelf-edge delta (NW Australia): Process-based classification from 3D

Bibliography

seismic attributes and implications for the prediction of deep-water sands. *Marine and Petroleum Geology*, Volume 57, pp. 359-384.

Brunt, R. L., McCaffrey, W. D. & Kneller, B. C., 2004. Experimental modeling of the spatial distribution of grain size developed in a fill-and-spill mini-basin setting. *Journal of Sedimentary Research*, 74(3), pp. 348 - 446.

Burgess, P. M., 2012. A brief review of developments in stratigraphic forward modelling, 2000 - 2009. In: *Principles of Geologic Analysis*. s.l.:Elsevier B.V., pp. 379 - 404.

Burgess, P. M., 2012. A brief review of developments in stratigraphic forward modelling, 2000 - 2009. *Regional Geology and Tectonics*, pp. 378 - 404.

Burgess, P. M., Masiero, I., Toby, S. C. & Duller, R. A., 2019. A Big Fan of Signals? Exploring Autogenic and Allogenic Porcess and Product in a Numerical Stratigraphic Forward Model of Submarine-Fan Development. *Journal of Sedimentary Research*, Volume 89, pp. 1 -12.

Burgess, P. M., Masiero, I., Toby, S. C. & Duller, R. A., 2019. A big fan of signals? Exploring autogenic and allogenic process and product in a numerical stratigraphic forward model of submarine-fan development. *Journal of Sedimentary Research*, Volume 89, pp. 1-12.

Burgess, P. M., Masiero, I., Toby, S. C. & Duller, R. A., 2019. A Big Fan of Signals? Exploring Autogenic and Allogenic Process and Product in a Numerical Stratigraphic Forward Model of Submarine-Fan Development. *Journal of Sedimentary Research*, Volume 89, pp. 1 - 12.

Cartigny, M. J., Eggenhuisen, J. T., Hansen, E. W. M. & Postma, G., 2013. Concentration-Dependent Flow Stratification in Experimental High-Density Turbidity Currents and their Relevance to Turbidite Facies Models. *Journal of Sedimentary Research*, Volume 83, pp. 1047 - 1065.

Cartwright, J. A., Haddock, R. C. & Pinheiro, L. M., 1993. The lateral extent of sequence boundaries. *Geological Society Special Publications*, Volume 71, pp. 15 - 34.

Carvajal, C., Steel, R. & Petter, A., 2009. Sediment supply: The main driver of shelf-margin growth. *Earth-Science Reviews*, Volume 96, pp. 221 - 248.

Catuneanu, O., 2006. *Principles of sequence stratigraphy*. Amsterdam: Elsevier.

Catuneanu, O., 2019. Model-independent sequeunce stratigraphy. *Earth-Science Reviews*, Issue 188, pp. 312-388.

- Catuneanu, O., 2020. Sequence stratigraphy of deep-water systems. *Marine and Petroleum Geology*, Volume 114, p. 104238.
- Catuneanu, O. et al., 2009. Towards the standardization of sequence stratigraphy. *Earth-Science Reviews*, Volume 92, pp. 1 - 33.
- Catuneanu, O. et al., 2011. Sequence Stratigraphy: Methodology and Nomenclature. *Newsletters on Stratigraphy*, 44(3), pp. 173 - 245.
- Christie-Blick, N., 1991. Onlap, offlap, and the origin of unconformity-bounded depositional sequences. *Marine Geology*, pp. 35-56.
- Christie, D. N. et al., 2021. Onlapse-2D: A new geometric tool to model the tectonostratigraphic evolution of deep-water basins.. *Basin Research*.
- Clevis, Q., Be Doer, P. L. & Nijman, W., 2004. Differentiating the effect of episodic tectonism and eustatic sea-level fluctuations in foreland basins filled by alluvial fans and axial deltaic systems: insights from a three-dimensional stratigraphic forward model. *Sedimentology*, 51(2004), pp. 809 - 835.
- Clevis, Q., de Jager, G., Nijman, W. & de Boer, P., 2004. Stratigraphic signatures of translation of thrust-sheet top basins over low-angle detachment faults. *Basin Research*, Volume 16, pp. 145 - 163.
- Corredor, F., Shaw, J. H. & Bilotti, F., 2005. Structural styles in the deep-water fold and thrust belts of the Niger Delta. *AAPG Bulletin*, June, 89(6), pp. 753 - 780.
- Covault, J. A. & Graham, S. A., 2010. Submarine fans at all sea-level stands: Tectonomorphologic and climatic controls on terrigenous sediment delivery to the deep sea. *Geology*, 38(10), pp. 939 - 942.
- Cunha, R. S., Tinterri, R. & Magalhaes, P. M., 2017. Annot Sandstone in the Peira Cava basin: An example of an asymmetric facies distribution in a confined turbidite system (SE France). *Marine and Petroleum Geology*, Volume 87, pp. 60 - 79.
- Dade, W. B. & Huppert, H. E., 1994. Predicting the geometry of channelized deep-sea turbidites. *Geology*, Volume 22, pp. 645-648.
- Davison, I., 2020. Salt tectonics in the Sureste Basin, SE Mexico: some implications for hydrocarbon exploration. *Geological Society, London, Special Publications*, pp. 147 - 165.

Bibliography

- Davison, I., Pindell, J. & Hull, J., 2021. The basins, orogens and evolution of the southern Gulf of Mexico and Northern Caribbean. *Geological Society, London, Special Publications*, pp. 1 - 27.
- Dixon, J. F., Steel, R. J. & Olariu, C., 2012. Shelf-Edge Delta Regime as a Predictor of Deep-Water Deposition. *Journal of Sedimentary Research*, Volume 82, pp. 681 - 687.
- Duffy, O. B. et al., 2019. Obstructed minibasins on a salt-detached slope: An example from above the Sigsbee canopy, northern Gulf of Mexico. *Basin Research*, pp. 1 - 20.
- Falivene, O. et al., 2014. Automatic calibration of stratigraphic forward models for predicting reservoir presence in exploration. *AAPG Bulletin*, 98(9), pp. 1811 - 1835.
- Fossen, H., 2010. *Structural Geology*. Cambridge: Cambridge University Press.
- Gervais, V., Ducros, M. & Granjeon, D., 2018. Probability maps of reservoir presence and sensitivity analysis in stratigraphic forward modelling. *AAPG Bulletin*, 102(4), pp. 613 - 628.
- Gómez-Cabrera, P. T. & Jackson, M. P. A., 2009. Neogene Stratigraphy and Salt Tectonics of the Santa Ana Area, Offshore Salina del Istmo Basin, Southeastern Mexico. In: *Petroleum Systems in the Southern Gulf of Mexico*. s.l.:AAPG, pp. 237 - 255.
- Granjeon, D., 2014. 3D forward modelling of the impact of sediment transport and base level cycles on continental margins and incised valleys. In: *From Depositional Systems to Sedimentary Successions on the Norwegian Continental Margin*. s.l.:International Association of Sedimentologists, pp. 453 - 472.
- Groenenberg, R. M. et al., 2010. Flow–Deposit Interaction in Submarine Lobes: Insights from Outcrop Observations and Realizations of a Process-Based Numerical Model. *Journal of Sedimentary Research*, 80(3), pp. 252 - 267.
- Hage, S. et al., 2018. How to recognize crescentric bedforms formed by supercritical turbidity currents in the geologic record: Insights from active submarine channels. *Geology*, Volume 46, pp. 563 - 566.
- Hage, S. et al., 2019. Direct Monitoring Reveals Initiation of Turbidity Currents from Extremely Dilute River Plumes. *Geophysical Research Letters*, Volume 46, pp. 11310 - 11320.
- Harris, A. D., Baumgardner, S. E., Sun, T. & Granjeon, D., 2018. A Poor Relationship Between Sea Level and Deep-Water Sand Delivery. *Sedimentary Geology*, Volume 370, pp. 42 - 51.
- Haughton, P. D. W., 2000. Evolving turbidite systems on a deforming basin floor, Tabernas, SE Spain. *Sedimentology*, Volume 47, pp. 497 - 518.

- Hawie, N., Covault, J. A., Dunlap, D. & Sylvester, Z., 2018. Slope-fan depositional architecture from high-resolution forward stratigraphic models. *Marine and Petroleum Geology*, Volume 91, pp. 576-585.
- Heijnen, M. S. et al., 2020. Rapidly-migrating and internally-generated knickpoints can control submarine channel evolution. *Nature Communications*, June, pp. 1 - 15.
- Helland-Hansen, W. & Hampson, G. J., 2009. Trajectory analysis: concepts and applications. *Basin Research*, pp. 454 - 483.
- Hodgson, D. M. & Haughton, P. D. W., 2004. Impact of syndepositional faulting on gravity current behaviour and deep-water stratigraphy: Tabernas-Sorbas Basin, SE Spain. *Geological Society, London, Special Publications*, Volume 222, pp. 135- -158.
- Howlett, D. M. et al., 2019. Response of unconfined turbidity current to deep-water fold and thrust belt topography: Orthogonal incidence on solitary and segmented folds. *Sedimentology*, Volume 66, pp. 2425 - 2454.
- Huang, X., Griffiths, C. M. & Liu, J., 2015. Recent development in the stratigraphic forward modelling and its application in petroleum exploration. *Australian Journal of Earth Sciences*, Volume 62, pp. 903-919.
- Hudec, M. R. & Norton, I. O., 2019. Upper Jurassic structure and evolution of the Yucatan and Campeche subbasins, southern Gulf of Mexico. *AAPG Bulletin*, 103(5), pp. 1133 - 1151.
- Hutton, E. W. & Syvitski, J. P., 2008. Sedflux 2.0: An advanced process-response model that generates three-dimensional stratigraphy. *Computers and Geoscience*, Volume 34, pp. 1319 - 1337.
- Imran, J., Harff, P. & Parker, G., 2001. A numerical model of submarine debris flow with graphical user interface. *Computers and Geosciences*, Volume 27, pp. 717 - 729.
- Jackson, C. A.-L., Barber, G. P. & Martinsen, O. J., 2008. Submarine slope morphology as a control on the development of sand-rich turbidite depositional systems: 3D seismic analysis of the Kyrre Fm (Upper Cretaceous), Måløy Slope, offshore Norway. *Marine and Petroleum Geology*, Volume 25, pp. 663 - 680.
- Jackson, M. & Hudec, M., 2017. *Salt Tectonics: Principles and Practice*. Cambridge: Cambridge University Press.

Bibliography

- Jackson, M. P. A. & Hudec, M. R., 2017. *Salt Tectonics Principles and Practice*. Cambridge: Cambridge University Press.
- Jerolmack, D. J. & Paola, C., 2007. Complexity in a cellular model of river avulsion. *Geomorphology*, Volume 91, pp. 259 - 270.
- Jerolmack, D. & Paola, C., 2010. Shredding of environmental signals by sediment transport. *Geophysical Research Letters*, Volume 37.
- Kane, I. A. et al., 2017. The stratigraphic record and processes of turbidity current transformation accross deep-marine lobes. *Sedimentology*, Volume 64, pp. 1236 - 1273.
- Kilhams, B., Hartley, A., Huuse, M. & Davis, C., 2012. Characterizing the Paleocene turbidites of the North Sea: the Mey Sandstone Member, Lista Formation, UK Central Graben. *Petroleum Geoscience*, Volume 18, pp. 337 - 354.
- Kneller, B., 2003. The influence of flow parameters on turbidite slope channel architecture. *Marine and Petroleum Geology*, March, Volume 20, pp. 901-910.
- Kneller, B. C. & Branney, M. J., 1995. Sustained high-density turbidity currents and the deposition of thick massive sands. *Sedimentology*, Volume 42, pp. 607 - 616.
- Kneller, B., Edwards, D., McCaffrey, W. & Moore, R. M., 1991. Oblique reflection of turbidity currents. *Geology*, Volume 14, pp. 250 - 252.
- Kneller, B. & McCaffrey, W., 1999. Depositional Effects of Flow Nonuniformity and Stratification within Turbidity Currents Approaching a Bounding Slope: Deflection, Reflection, and Facies Variation. *Journal of Sedimentary Research*, 69(5), pp. 980-991.
- Leveille, J. P. et al., 2011. Subsalt imaging for exploration, production, and development: A review. *Geophysics*, September - October, 76(5), pp. WB3 - WB20.
- Liu, X., Rendle-Bühning, R. & Henrich, R., 2016. Climate and sea-level controls on turbidity current activity on the Tanzanian upper slope during the last deglaciation and the Holocene. *Quaternary Science Reviews*, pp. 15 - 27.
- Lovely, H. R., 1948. Discussion, "Overlap and Strike-Overlap". *AAPG Bulletin*, December, 32(12), pp. 2295 - 2297.
- Lowe, D. R., 1982. Sediment Gravity Flows: II. Depositional Models with Special Reference to the Deposits of High-Density Turbidity Currents. *Journal of Sedimentary Petrology*, 52(1), pp. 279 - 297.

- Magoon, L. B. & Dow, W. G., 1994. The Petroleum System. In: *The Petroleum System - from source to trap*. s.l.:American Association of Petroleum Geologists.
- Mandujano-Velazquez, J. J. & Keppie, J. D., 2009. Middle Miocene Chiapas fold and thrust belt of Mexico: a result of collision of the Tehuantepec Transform/Ridge with the Middle America Trench. *Geological Society, London, Publications*, Volume 327, pp. 55- 69.
- Mayall, M., Jones, E. & Casey, M., 2006. Turbidite channel reservoirs - Key elements in facies prediction and effective development. *Marine and Petroleum Geology*, Volume 23, pp. 821 - 841.
- Meiburg, E. & Kneller, B., 2010. Turbidity Currents and Their Deposits. *Annual Review of Fluid Mechanics*, pp. 135-156.
- Melton, F. A., 1947. Onlap and Strike-Overlap. *AAPG Bulletin*, October, 31(10), pp. 1868 - 1878.
- Mitchum, R. M., 1977. Seismic Stratigraphy and Global Changes of Sea Level, Part 11: Glossary of Terms used in Seismic Stratigraphy. In: *Seismic Stratigraphy - applications to hydrocarbon exploration*. s.l.:s.n., pp. 205 - 212.
- Mitchum, R. M., Vail, P. R. & Sangree, J. B., 1977. Seismic Stratigraphy and Global Changes of Sea Level: Part 6. Stratigraphic Interpretation of Seismic Reflection Patterns in Depositional Sequences: Section 2. Application of Seismic Reflection Configuration to Stratigraphic Interpretation. In: *Seismic Stratigraphy--Applications to Hydrocarbon Exploration*. AAPG: s.n., pp. 117 - 133.
- Moscardelli, L., Wood, L. & Mann, P., 2006. Mass-transport complexes and associated processes in the offshore area of Trinidad and Venezuela. *AAPG Bulletin*, July, 90(7), pp. 1059 - 1088.
- Padilla y Sánchez, R. J., 2007. Evolución geológica del sureste mexicano desde el Mesozoico al presente en el contexto regional del Golfo de México. *Boletín de la Sociedad Geológica Mexicana*, pp. 19 - 42.
- Paola, C., 2000. Quantitative models of sedimentary basin filling. *Sedimentology*, 47(1), pp. 121-178.
- Paull, C. K. et al., 2018. Powerful turbidity currents driven by dense basal layers. *Nature Communications*, pp. 1 - 9.
- Peel, F., 2014. How do salt withdrawal minibasins form? Insights from forward modelling, and implications for hydrocarbon migration. *Tectonophysics*, 630(C), pp. 222-235.

Bibliography

- Pettingill, H. S. & Weimer, P., 2002. Worldwide deepwater exploration and production: Past, present, and future. *The Leading Edge*, April, pp. 371-376.
- Pichel, L. M., Peel, F. J., Jackson, C. A.-L. & Huuse, M., 2018. Geometry and kinematics of salt-detached ramp syncline basins. *Journal of Structural Geology*, October, Volume 115, pp. 208 - 230.
- Pindell, J. et al., 2019. *Strontium isotope dating of evaporites and the breakup of the Gulf of Mexico and proto-Caribbean seaway (abs.)*. San Antonio, AAPG.
- Pomar, L. & Ward, W. C., 1994. Response of a late Miocene Mediterranean reef platform to high-frequency eustasy. *Geology*, 22(2), pp. 131 - 134.
- Prather, B. E., 2003. Controls on reservoir distribution, architecture and stratigraphic trapping in slope settings. *Marine and Petroleum Geology*, pp. 529-545.
- Prather, B. E., Booth, J. R., Steffens, G. S. & Craig, P. A., 1998. Classification, lithologic calibration, and stratigraphic succession of seismic facies of intraslope basins, deep-water Gulf of Mexico. *AAPG Bulletin*, Volume 82, pp. 701-728.
- Prélat, A., Hodgson, D. M. & Flint, S. S., 2009. Evolution, architecture and hierarchy of distributary deep-water deposits: a high-resolution outcrop investigation from the Permian Karoo Basin, South Africa. *Sedimentology*, Volume 56, pp. 2132 - 2154.
- Ritchie, B. D., Gawthorpe, R. L. & Hardy, S., 2004. Three-Dimensional Numerical Modelling of Deltaic Depositional Sequences 2: Influence of Local Controls. *Journal of Sedimentary Research*, 74(2), pp. 221 - 238.
- Rivenaes, J. C., 1992. Application of dual lithology, depth dependent diffusion equation in stratigraphic simulation. *Basin Research*, Volume 4, pp. 133-146.
- Romans, B. W. et al., 2016. Environmental signal propagation in sedimentary systems across timescales. *Earth Science Reviews*, pp. 7 - 29.
- Ross, A. N., Linden, P. F. & Dalziel, S. B., 2002. A study of three-dimensional gravity currents on a uniform slope. *Journal of Fluid Mechanics*, Volume 453, pp. 239 - 261.
- Salvador, A., 1987. Late-Triassic-Jurassic Paleogeography and Origin of Gulf of Mexico Basin. *AAPG Bulletin*, 71(4), pp. 419-451.
- Sanford, O. G., Hobbs, R. W., Schofield, N. & Brown, R. ., 2018. *Understanding the challenges of sub-sill seismic imaging using full-waveform seismic modelling*. Anaheim, SEG, pp. 3858 - 3862.

- Shann, M. V., Vazquez-Reyes, K., Ali, H. M. & Horbury, A. D., 2020. The Sureste Super Basin of southern Mexico. *AAPG Bulletin*, 104(12), pp. 2643 - 2700.
- Sharman, G. R., Sylvester, Z. & Covault, J. A., 2019. Conversion of tectonic and climat forcings into records of sediment supply and provenance. *Scientific Reports*, pp. 1 - 7.
- Smith, R. & Joseph, P., 2004. Onlap stratal architectures in the Grès d'Annot: Geometric models and controlling factors. *Geological Society Special Publication*, Volume 221, pp. 389-399.
- Soutter, E. L. et al., 2019. The stratigraphic evolution of Onlap in siliciclastic deep-water systems: Autogenic modulation of allogenic signals. *Journal of Sedimentary Research*, Volume 89, pp. 890 - 917.
- Spychala, Y. T. et al., 2017. Frontal and Lateral Submarine Lobe Fringes: Comparing Sedimentary Facies, Architecture and Flow Processes. *Journal of Sedimentary Research*, Volume 87, pp. 75 - 96.
- Stanbrook, D. A. et al., 2020. *Onshore Structural Movement Revealed Through the Presence of Volcanoclastic Deposition Offshore. Cholula-1EXP, Miocene Salinas del Istmo Basin, Mexico*. Houston, Texas, AAPG, p. 18.
- Stanbrook, S., 2003. *The Geology of Grand Coyer, Southeast France. Relationships between Basin-Floor Topography and the Deposition of the Grès d'Annot and the Marnes Brunes Inférieures (PhD)*. Edinburgh: Institute of Petroleum Engineering: Heriot-Watt University.
- Stern, R. J. & Dickinson, W. R., 2010. The Gulf of Mexico is a Jurassic backarc basin. *Geosphere*, 6(6), pp. 739 - 754.
- Stirling, E. J., Fugelli, E. M. G. & Thompson, M., 2018. The edges of the wedges: a systematic approach to trap definition and risking for stratigraphic, combination, and sub-unconformity traps. *Petroleum Geology of NW Europe: 50 Years of Learning – Proceedings of the 8th Petroleum Geology Conference*, pp. 273 - 286.
- Stow, D. A. V. & Mayall, M., 2008. Deep-water sedimentary systems: New models for the 21st century. *Marine and Petroleum Geology*, pp. 125 - 135.
- Suppe, J., Chou, G. T. & Hook, S. C., 1992. Rates of folding and faulting determined from growth strata. In: *Thrust Tectonics*. Dordrecht: Springer.
- Swain, F. M., 1949. Onlap, Offlap, Overstep, and Overlap. *AAPG Bulletin*, April, 33(4), pp. 634 - 636.

Bibliography

Sylvester, Z., Cantelli, A. & Pirmez, C., 2015. Stratigraphic evolution of intraslope minibasins: Insights from surface-based mode. *AAPG Bulletin*, 99(6), pp. 1099 - 1129.

Symons, W. O. et al., 2017. A new model for turbidity current behavior based on integration of flow monitor and precision coring in a submarine canyon. *Geology*, Volume 45, pp. 367 - 370.

Syvitski, J. P. et al., 2007. Prediction of margin stratigraphy. In: C. A. Nittrouer, et al. eds. *Continental Margin Sedimentation: From Sediment Transport to Sequence Stratigraphy*. s.l.:International Association of Sedimentologists, pp. 459 - 529.

Szulczewski, M. L., Hesse, M. A. & Juanes, R., 2013. Carbon dioxide dissolution in structural and stratigraphic traps. *Journal of Fluid Mechanics*, Volume 736, pp. 287 - 315.

Talling, P. J., 2014. On the triggers, resulting flow types and frequencies of subaqueous sediment density flows in different settings. *Marine Geology*, Volume 352, pp. 155 - 182.

Talling, P. J., Amy, L. A. & Wynn, R. B., 2007. New insight into the evolution of large-volume turbidity currents: comparison of turbidite shape and previous modelling results. *Sedimentology*, Volume 54, pp. 737 - 769.

Talling, P. J. et al., 2007. Onset of submarine debris flow deposition far from original giant landslide. *Nature Letters*, Volume 450, pp. 451 - 544.

Teles, V. et al., 2016. CATS – A process-based model for turbulent turbidite systems at the reservoir scale. *Comptes Rendus Geoscience*, pp. 489-498.

Tofelde, S., Bernhardt, A. & Romans, B. W., 2021. Times associated with source-to-sink propagation of environmental signals during landscape transience. *Frontiers in Earth Science*, Volume 9.

Trusheim, F., 1960. Mechanism of Salt Migration in Northern Germany. *AAPG Bulletin*, 44(9), pp. 1519 - 1540.

Twichell, D. C. et al., 2005. Seismic Architecture and Lithofacies of Turbidites in Lake Mead (Arizona and Nevada, U.S.A), an Analogue for Topographically Complex Basins. *Journal of Sedimentary Research*, 75(1), pp. 134 - 148.

Vail, P. R., Mitchum, R. M. & Thompson, S., 1977. Seismic Stratigraphy and Global Changes of Sea Level: Part 4. Global Cycles of Relative Changes of Sea Level.: Section 2. Application of Seismic Reflection Configuration to Stratigraphic Interpretation. In: *Seismic Stratigraphy - Applications to Hydrocarbon Exploration*. s.l.:American Association of Petroleum Geologists, pp. 83 - 97.

- Waltham, D., Jaffey, N., Maclean, S. & Zampetti, V., 2008. Stratigraphic modelling of turbidite prospects to reduce exploration risk. *Petroleum Geoscience*, Volume 14, pp. 273 - 280.
- Wang, X. et al., 2017. Turbidite stacking patterns in salt-controlled mini-basins: Insights from integrated analogue models and numerical fluid flow simulations. *Sedimentology*, 20 July, 64(2), pp. 530-552.
- Warren, J. K., 2006. *Evaporites: Sediments, resources and hydrocarbons*. Berlin: Springer Berlin Heidelberg.
- Wynn, R. B., Weaver, P. P. E., Masson, D. G. & Stow, D. A. V., 2002. Turbidite depositional architecture across three interconnected deep-water depositional basins on the north-west African margin. *Sedimentology*, Volume 49, pp. 669 - 695.
- Xu, J., 2011. Measuring currents in submarine canyons: Technological and scientific progress in the past 30 years. *Geosphere*, Volume 7, pp. 868 - 876.
- Yu, X. et al., 2021. Recognition and application of offlap in endorheic basins: new insights into plateau growth. *International Geology Review*.
- Zhang, J., Burgess, P. M., Granjeon, D. & Steel, R., 2018. Can sediment supply variations create sequences? Insights from stratigraphic forward modelling. *Basin Research*, pp. 1 - 16.